FINAL REPORT
STUDY OF DUAL-CHANNEL INFRARED SPECTRORADIOMETER SYSTEMS

(JUNE 1967 THROUGH FEBRUARY 1973)

BY

J. A. WRUBEL

ROCKETDYNE DIVISION/ROCKWELL INTERNATIONAL
6633 CANOGA AVENUE
CANOGA PARK, CALIFORNIA 91304

MARCH 1973

CONTRACT NAS8-21144

PREPARED FOR

GEORGE C. MARSHALL SPACE FLIGHT CENTER
MARSHALL SPACE FLIGHT CENTER
ALABAMA 35812

N73-21387

(NASA-CR-124207) STUDY OF DUAL-CHANNEL INFRARED SPECTRORADIOMETER SYSTEMS Final Report, Jun. 1967 - Feb. 1973 (Rocketdyne) 123 p HC $8.25 CSCL 14B G3/14 Unclas 17565

FINAL REPORT

STUDY OF DUAL-CHANNEL INFRARED SPECTRORADIOMETER SYSTEMS

(June 1967 through February 1973)

by

J. A. Wrubel

Rocketdyne Division/Rockwell International
6633 Canoga Avenue
Canoga Park, California 91304

March 1973

Contract NAS8-21144

Prepared For

George C. Marshall Space Flight Center
Marshall Space Flight Center
Alabama 35812

FOREWORD

This report was prepared by the Rocketdyne Division/Rockwell International under Contract Number NAS8-21144, "Study of Dual-Channel Infrared Spectroradiometer Systems," for the George C. Marshall Space Flight Center of the National Aeronautics and Space Administration. The work was administered under technical direction of the Aero-Astrodynamics Laboratory of the George C. Marshall Space Flight Center.

This final report covers the work performed from June 1967 through February 1973 in five phases: Phase I, June 1967 through November 1967; Phase II, December 1967 to December 1968; Phase III, December 1968 through May 1970; Phase IV, June 1970 to December 1971; and Phase V, December 1971 through February 1973. The contract monitor for Phases I, II, IV, and V was Dr. Terry Greenwood. Mr. David Seymour was the contract monitor for Phase III.

This report has been assigned the Rocketdyne Report Number R-9183.

ABSTRACT

A dual-channel infrared spectroradiometer system was designed, fabricated, and utilized. The system includes an internal blackbody intensity calibration source, external radiation sources for absorption measurements, spatial and spectral scanning mechanisms, power supplies, and recording apparatus. It was designed to provide radiometry measurements at discrete locations for absorption and emission determinations of temperature and partial pressure distributions of species within the exhaust of large rocket engines. The dual-channel spectroradiometer system was installed at the Nevada Field Laboratory high-altitude facility where spectral data were obtained from F_2/H_2, FLOX/CH_4, FLOX/B_2H_6, OF_2/CH_4, and OF_2/B_2H_6 propellant combinations. Simultaneous emission and absorption data were not obtained and, therefore, the plume property calculations could not be made. However, basic feasibility was demonstrated. A good HF emission spectra was obtained for tests with the OF_2/B_2H_6 propellant combination. Subsequently, the system was installed at the Santa Susana Field Laboratory high-altitude facility (cell 29, CTL-4) where data were obtained on the LOX/GH_2 propellant combination at sea level and altitude conditions (4:1 and 25:1 nozzle expansion ratios, respectively). The data obtained were inconsistent because the calculation of plume properties led to physically unrealistic results. The inconsistencies resulted from measurement accuracy not being within the narrow limits required by the data reduction scheme. Although the anticipated program results were not obtained, the data gathered will be useful for guiding future experimental efforts and formulations of less sensitive analytical models.

ACKNOWLEDGMENT

The contributions of Dr. W. F. Herget, Mr. R. L. Proffit, Mr. R. K. Hales, Mr. B. T. McDunn, and Mr. J. A. Daugherty for Phase I; Dr. W. F. Herget and Mr. T. L. Nielsen for Phase II; Dr. L. J. Zajac and Mr. R. Badger for Phase IV; and Dr. L. J. Zajac and Dr. C. L. Oberg for Phase V are gratefully acknowledged. A special acknowledgment is extended to Mr. E. A. Rojec for his indispensible assistance during the Phase IV and V efforts.

CONTENTS

ILLUSTRATIONS

TABLES

INTRODUCTION AND SUMMARY

Zone radiometry of rocket engine exhaust plumes involves measurement of spectral absorption and emission at a fixed wavelength and along a set of predetermined lines of sight in a plane through the exhaust. From the resultant data, the temperature and partial pressure profiles for certain species in the exhaust may be calculated. Knowledge of these properties is required to minimize performance losses and to predict the influence of the plume on adjacent portions of the vehicle. By comparing experimentally determined profiles with corresponding analytical predictions, the accuracy of analytical exhaust plume models may be evaluated and improved.

Zone radiometry overcomes the common disadvantage of probe-type instrumentation systems which, in the past, have been the primary measurement method. This disadvantage is the disruption of the flowfield in the vicinity of the measurement station which introduces an inherent uncertainty in the results. Optical techniques to measure plume characteristics (except velocity) without disturbing the flowfield have been used at Rocketdyne for a number of years.

The dual-channel spectroradiometer designed, fabricated, and utilized under this contract has one channel with a low spectral resolution and one channel with a moderately high resolution afforded by a quarter-meter grating monochromator. It is equipped to operate in the 0.8- to 3.5 x 10^{-6}-meter (0.8- to 3.5-micron) infrared spectral range. However, the wavelength was normally a fixed setting of 2.5 x 10^{-6} meter (2.5 microns) because it was characteristic of the exhaust species of interest. Nontheless, gratings and detectors could be used to extend the spectral range of the instrument through the visible and ultraviolet to 0.3 x 10^{-6} meter (0.3 micron) or to longer wavelengths (infrared), if required.

This contractual effort was performed in five distinct phases, as follows. Under Phase I (June through November 1967), a dual-channel spectroradiometer (DCS) system for zone radiometry measurements was designed and fabricated. This system, which consists of a set of continuum radiation sources for absorption measurements, a device for optically scanning the desired lines of sight through the exhaust, a

grating monochromator and detectors, and associated amplification and recording apparatus, is described in Ref. 1.

Under Phase II (December 1967 to November 1968), the DCS system was installed in the B-3 altitude chamber at the Rocketdyne Nevada Field Laboratory (NFL). The system was set up to monitor the rocket engine test firings, carried out under Contract NASw-2119. Installation at this locality required some modifications to the DCS system, which are described in Ref. 2.

The number of test firings available for optical measurements during Phase II were: (1) considerably less than originally anticipated, (2) made with a wide variety of propellants, and (3) of very short duration. These three factors severely compromised the quality and quantity of the optical data obtained.

Under Phase III (December 1968 to May 1970), measurements were to be made on rocket engine firings being carried out under Contract NASw-2119. In addition, modifications were to be made to the spectroradiometer to increase its response and the response of the data recording system. Tests under NASw-2119 were never made and this program was reoriented to NAS3-12051, which was being conducted at Rocketdyne's Propulsion Research Area at the Santa Susana Field Laboratory (SSFL). However, a series of malfunctions on the latter test program prevented acquisition of optical data.

Under Phase IV (June 1970 to December 1971), the program was redirected to monitor H_2/O_2 test firings being conducted under still another contract, NASw-2106, "Experimental Investigation of Combustor Effects on Rocket Thrust Chamber Performance." These tests were conducted at cell 29, CTL-4, located at SSFL. The DCS system was installed at this facility and limited optical data were gathered. A description of the Phase III and Phase IV effort is given in Ref. 3.

During the final phase (Phase V, December 1971 through February 1973), continued use of the existing zone radiometry equipment was made to measure the plume flowfield properties of an experimental H_2/O_2 rocket engine being tested under Contract

NASw-2106. Additionally, improvements to the basic procedures were sought and the measurement technique was evaluated.

Emission and absorption data were obtained at sea level and at altitude conditions (4:1 and 25:1 expansion ratios, respectively). However, the data obtained were found to be inconsistent because calculations of plume properties led to physically unrealistic results. The inconsistencies resulted from measurements not being within the narrow limits required by the data reduction scheme. Although the anticipated program results were not obtained, the data gathered will be extremely helpful in guiding future experimental efforts and formulating less sensitive analytical models.

This is the final report on the subject contract and all phases are described herein. The Phase V efforts which have not been previously reported are described in somewhat more detail.

PHASE I

SYNOPSIS

Phase I, conducted during June 1967 through November 1967, was directed toward the design and fabrication of a spectroscopic instrumentation system to perform zone radiometry on "large" rocket engine plumes. The design was based upon technology developed under Contract NAS8-11261 (Ref. 4), and used under Contract NASw-16 (Ref. 5) to study the exhausts of small rocket engines [4448 newtons (1000 pounds thrust, 10.18- to 20.36-cm (4- to 8-inch) nozzle exit diameters] firing liquid propellants such as LO_2/RP-1 and LO_2/C_2H_5OH. In these studies temperature profiles and concentration profiles for the species CO_2 and carbon particles were determined experimentally. In conjunction with theoretical analyses, mixture ratio profiles within the rocket nozzle were deduced from the experimental data.

The fabricated instrumentation system consisted of an internal blackbody calibration source, external radiation sources for absorption measurements, spectral and spatial scanning mechanisms, power supplies, and recording equipment. All components used during engine firings, with the exception of the power supplies and recording equipment, could be operated in a vacuum environment. Thus, the exhausts of engines operated in altitude simulation facilities could be studied.

The spectroradiometer was equipped to operate in the 0.8×10^{-6} to 3.5×10^{-6} meter (0.8- to 3.5-micron) spectral range with one channel of low spectral resolution and one channel having the moderately high resolution afforded by a quarter-meter grating monochromator, hence, the name dual-channel spectroradiometer (DCS). Additional gratings and detectors can be used to extend the spectral range of the instrument through the visible and ultraviolet to 0.3×10^{-6} meter (0.3 micron) or, further into the infrared, if required.

The DCS system was designed for use in both the J-4 test cell at the Arnold Engineering Development Center (AEDC), Tullahoma, Tennessee, and the B-3 test cell at NFL.

DESIGN CRITERIA

The basic requirement for the spectroradiometer system was the ability to perform zone radiometry experiments on large engine exhausts. The principles of zone radiometry are described in considerable detail in Ref. 4 and 5 and, therefore, are reviewed only briefly here.

For a conventional bell nozzle, it is often reasonable to assume circumferential symmetry. Therefore, if the plume is divided into a series of concentric zones (Fig. 1), the partial pressure and temperature, and therefore the spectral radiance and spectral emissivity, of a particular species may be assumed constant in each zone. The line-of-sight values of spectral radiance and spectral emissivity may be expressed in terms of the zonal values by equations of radiative transfer that take into account the absorptance of each zone. The principal equations are listed in Fig. 1.

If the line-of-sight spectral radiance and spectral emissivity are each measured along N lines of sight and the plume is divided into N zones, then the corresponding 2N equations of radiative transfer may be solved for the zonal values of spectral radiance and spectral emissivity. The zonal values of temperature and species partial pressure may be calculated there from. A computer program to carry out the necessary calculations is available at Rocketdyne (Ref. 4, 5, and 6).

For meaningful zone radiometry measurements pertaining to concentrations, the spectral band pass of the instrument must be small enough to ensure that fluctuations of spectral emissivity are negligible within the wavelength region encompassed by the band pass.

The practical implications of the necessity for a narrow band pass are as follows: If the radiation being measured is primarily continuum in nature, such as is found with incandescent carbon particles or in the central region of the 4.3×10^{-6} meter (4.3-micron) CO_2 band, then the spectral band pass, 5.0×10^{-8} meter (0.05 micron), furnished by a narrow band interference filter is sufficient for meaningful

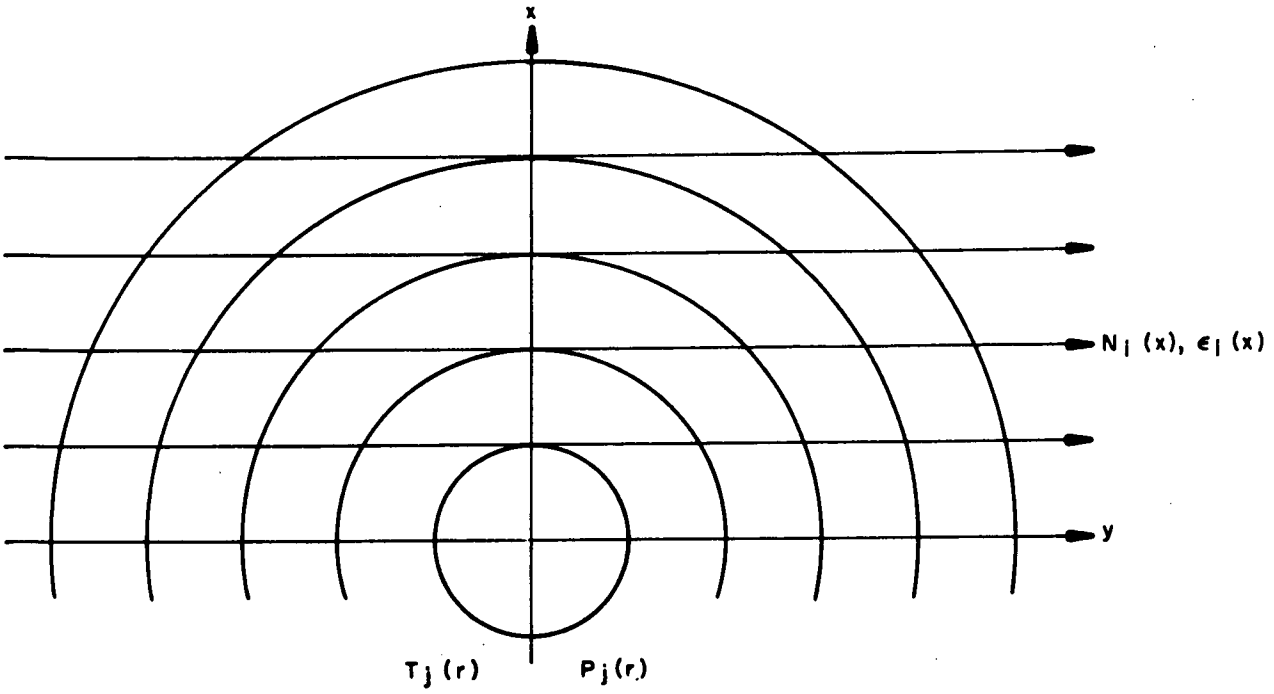

$$N(x) = \int_{-y_o}^{y_o} N(r) \exp \left[- \int_{y}^{y_o} K(r)\, P(r)\, dy \right] dy$$

$$1 - \epsilon(x) = \exp \left[- \int_{-y_o}^{y_o} K(r)\, P(r) \right] dy$$

Where

$P_j(r)$ = partial pressure of a particular species in the j^{th} zone
$T_j(r)$ = temperature in the j^{th} zone
$K_j(r)$ = spectral absorption coefficient of a particular species in the j^{th} zone
$N_j(r)$ = spectral radiance per unit path length in the j^{th} zone
$\epsilon_j(r)$ = spectral emissivity in the j^{th} zone
$N_i(x)$ = measured spectral radiance along i^{th} line of sight
$\epsilon_i(x)$ = measured spectral emissivity along i^{th} line of sight

Figure 1. Division of Plume Cross-Section into annular Zones of Uniform Temperature and Species Partial Pressure; Basic Equations for Radiative Transfer of Energy Through the Plume

concentration determinations. Also, relative concentration distributions for such species as OH and CH may be determined under low spectral resolution. However, if radiating species possessing spectral fine structure (e.g., H_2O, CO, HF, etc.) are being studied, higher spectral resolution such as that afforded by a grating monochromator 2.5×10^{-10} meter (0.00025 micron) is required. The grating monochromator is also suitable for making spectral scans of exhaust radiation along a fixed line of sight for species identifications.

These general considerations indicate that a zone radiometry system must provide for absorption and emission measurements along a series of lines of sight lying in a single plane, and for maximum data collection, with channels of high and low spectral resolution. An additional particular requirement for this instrument is that it be suitable for studying rocket engines being operated in altitude simulation facilities.

The zone radiometry system developed to study small engine exhausts (Ref. 4) utilized a spatial scanning device that traversed an image of the plume at the monochromator entrance slit. This technique is impractical for large engine exhausts. Therefore, the major difference between the Ref. 4 instrumentation system and the system required to study large exhaust plumes is in the method of achieving spatial scanning (variation of line of sight).

ZONE RADIOMETRY SYSTEM

Two altitude simulation facilities were considered in the design of the system: (1) the J-4 test cell at AEDC, Tullahoma, Tennessee, where test durations could be several hundred seconds and all spectroscopic components are inside the test cell; and (2) the B-3 test cell at the NFL where the test duration is 2 to 3 seconds and part of the spectroscopic apparatus could be located outside the test cell.

The placement of the major system components for the two engine test facilities considered is shown schematically in Fig. 2. The location of the spectroradiometer with respect to the test cell is dictated primarily by spatial considerations.

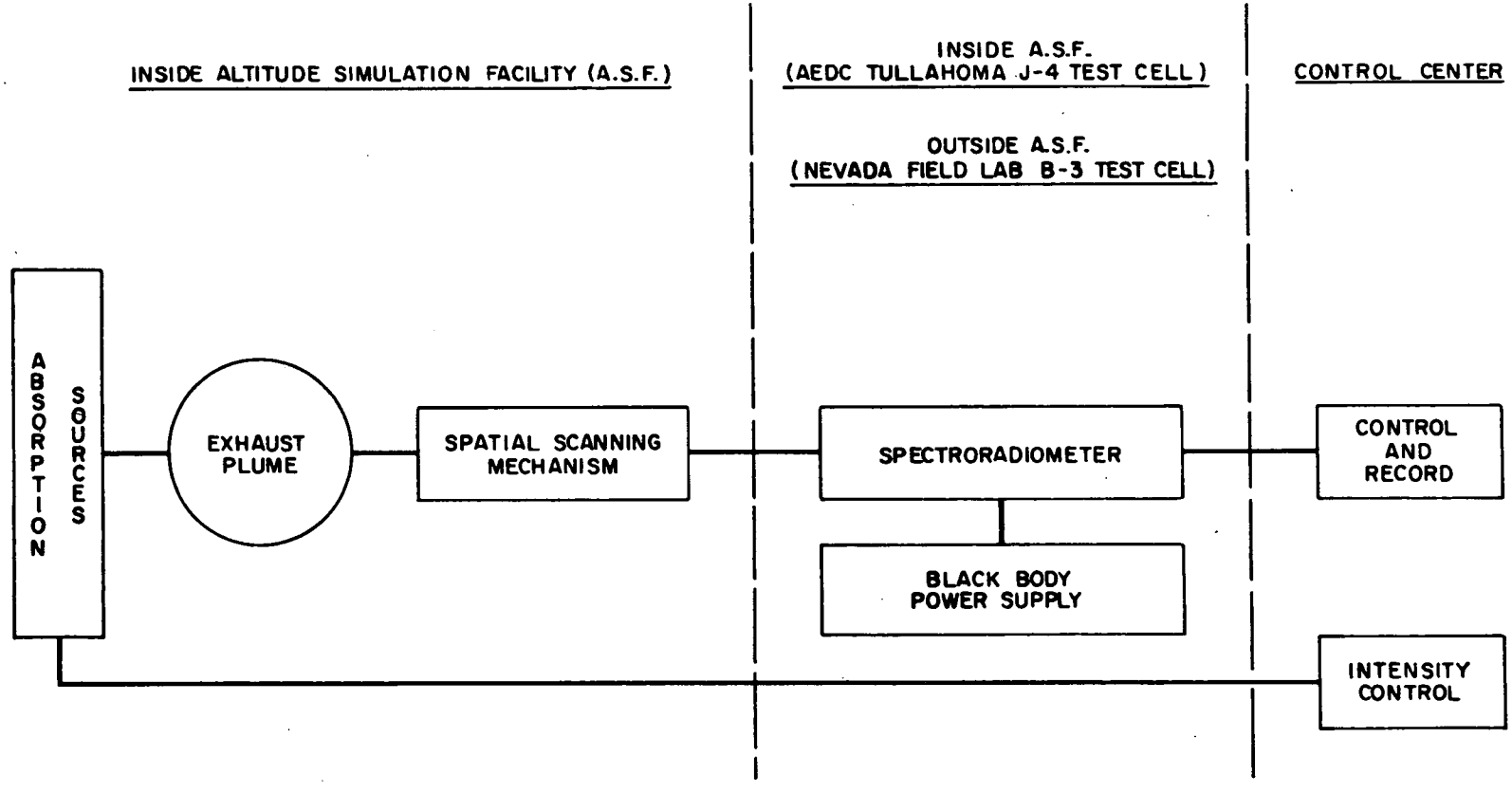

Figure 2. Block Diagram of Dual-Channel Infrared Spectroradiometer System

SPECTRORADIOMETER

An optical diagram of the spectroradiometer is shown in Fig. 3. Radiation from the exhaust and/or absorption sources is directed by the tracking flat mirror, M_1, to an 0.314-radian (18-degree) off-axis parabolic mirror, M_2. Flat mirror, M_3, directs the converging light rays from the parabola to a focus on the monochromator entrance slit. The monochromator is a Perkin-Elmer Model 98-G equipped with a 240 grooves/mm grating and a PbS detector. A wide-band germanium filter, F_1, is used to filter out unwanted short wavelength radiation. An optical chopper with reflective surfaces allows radiation to be time shared between the monochromator (high-resolution channel) and a low-resolution channel. In the low-resolution channel, radiation transmitted by an aperture, A, and narrow band interference filter, F_2, is focused onto a PbS detector by elliptical mirror, M_4. Blackbody radiation is brought into the two channels for an intensity calibration by mirrors M_3' and M_2'; M_1 is moved to position M_1' during the calibration. All mirrors are first surface, aluminized, and overcoated with silicon monoxide. Figure 4 is a photograph of the spectroradiometer and the major recording and control consoles.

During zone radiometry experiments, the monochromator transmits a fixed wavelength to the detector. If desired, spectral scans of the exhaust plume emission or transmittance may also be made. The maximum resolution of the monochromator is approximately 0.3 cm^{-1} at 2.5 x 10^{-6} meter (2.5 microns). However, the brightness temperature of exhaust plumes at simulated altitudes is probably not sufficient to allow use of slits narrow enough to achieve 0.3 cm^{-1} resolution and maintain a good signal-to-noise ratio. Therefore, an estimated working resolution of about 1 cm^{-1} for the DCS system is used.

The PbS detector allows the high-resolution channel coverage of the approximate spectral range from 0.8 x 10^{-6} to 3.5 x 10^{-6} meter (0.8 to 3.5 microns). Sufficient space was allowed for addition of a photomultiplier to extend coverage down to 3.0 x 10^{-7} meter (3000 Angstroms) or a liquid nitrogen-cooled PbSe detector to extend coverage up to 7.5 x 10^{-6} meter (7.5 microns).

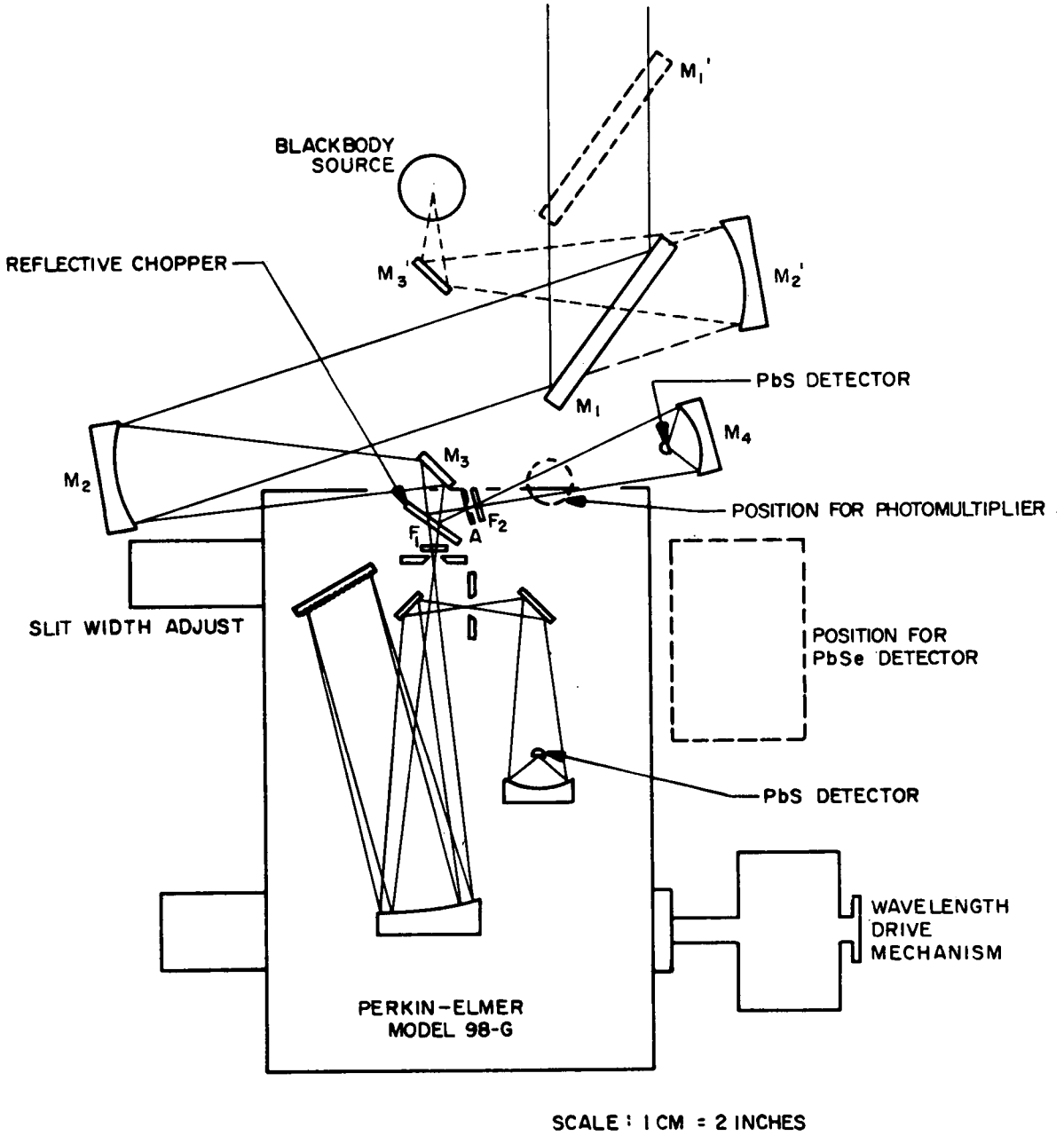

Figure 3. Optical Diagram of the Spectroradiometer

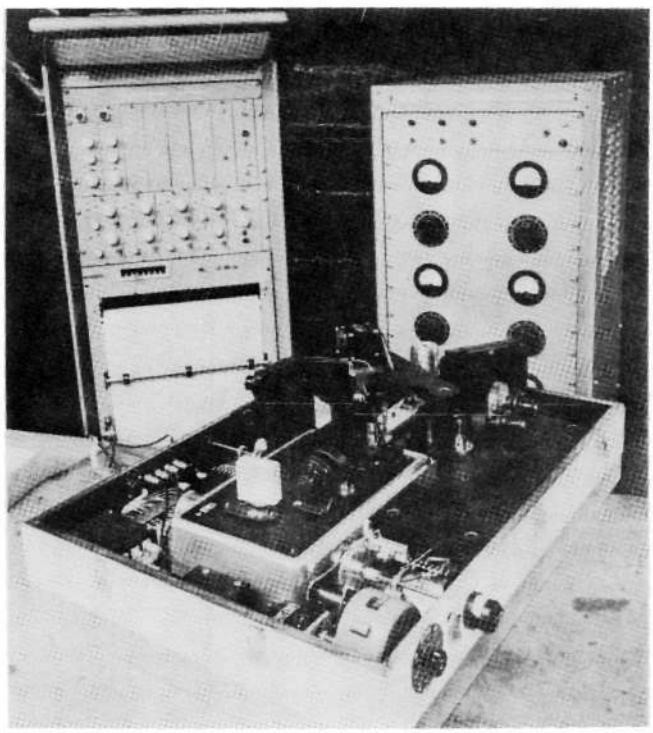

Figure 4. Photograph of the Spectroradiometer and Recording and Control Consoles

The spectroradiometer was assembled on a 71.1 by 96.5 cm (28- by 38-inch) ribbed aluminum baseplate. The instrument was designed so that the internal pressure is equal to ambient pressure--working range from 1.013×10^5 newton/meter^2 (1 atmosphere) to 1.333×10^2 newton/meter^2 (1 millimeter of mercury). For operation at atmospheric pressure, the instrument is purged with dry nitrogen to eliminate the effects of atmospheric water vapor absorption in the 2.5×10^{-6} meter (2.5-micron) spectral region (where the exhaust species HF and H_2O radiate). Also electrical power, cooling water, and an argon purge are connected to the blackbody through the baseplate. All other electrical and mechanical connections are made through an apron attached to the baseplate. The tracking flat can be moved manually with access provided through a port in the removable spectroradiometer cover.

SPATIAL SCANNING AND ABSORPTION SOURCE SYSTEM

The spatial scanning and absorption source system was designed for both rocket engine test facilities: the J-4 test cell at AEDC (a J-2 engine facility) and the B-3 test cell at NFL (an experimental engine facility). The J-4 facility can accommodate nozzle exit diameters of 203.5 cm (80 inches) and test durations up to 150 seconds (with the engine fired vertically). The B-3 facility can accommodate nozzles exit diameters up to 101.8 cm (40 inches) and test durations between 3 and 4 seconds (horizontal test facility). In spite of these differences, the system is equally adaptable to either facility.

The arrangement of the spatial scanning and absorption source system for NFL is shown schematically in Fig. 5. The 10 absorption sources consist of individually housed tungsten ribbon filament lamps. For either test site, the lamps are equally spaced across the primary scan angle which encompasses lines of sight from the plume center to the plume edge. The scanning mirror S_1, is different for each test facility, but the same scanning mirror motor and mount, relay mirror, and housing may be utilized.

Each absorption source package consists of a tungsten lamp and transformer housed in a vacuum tight cylinder. A lens, mounted in the wall of the cylinder, provides optical access.

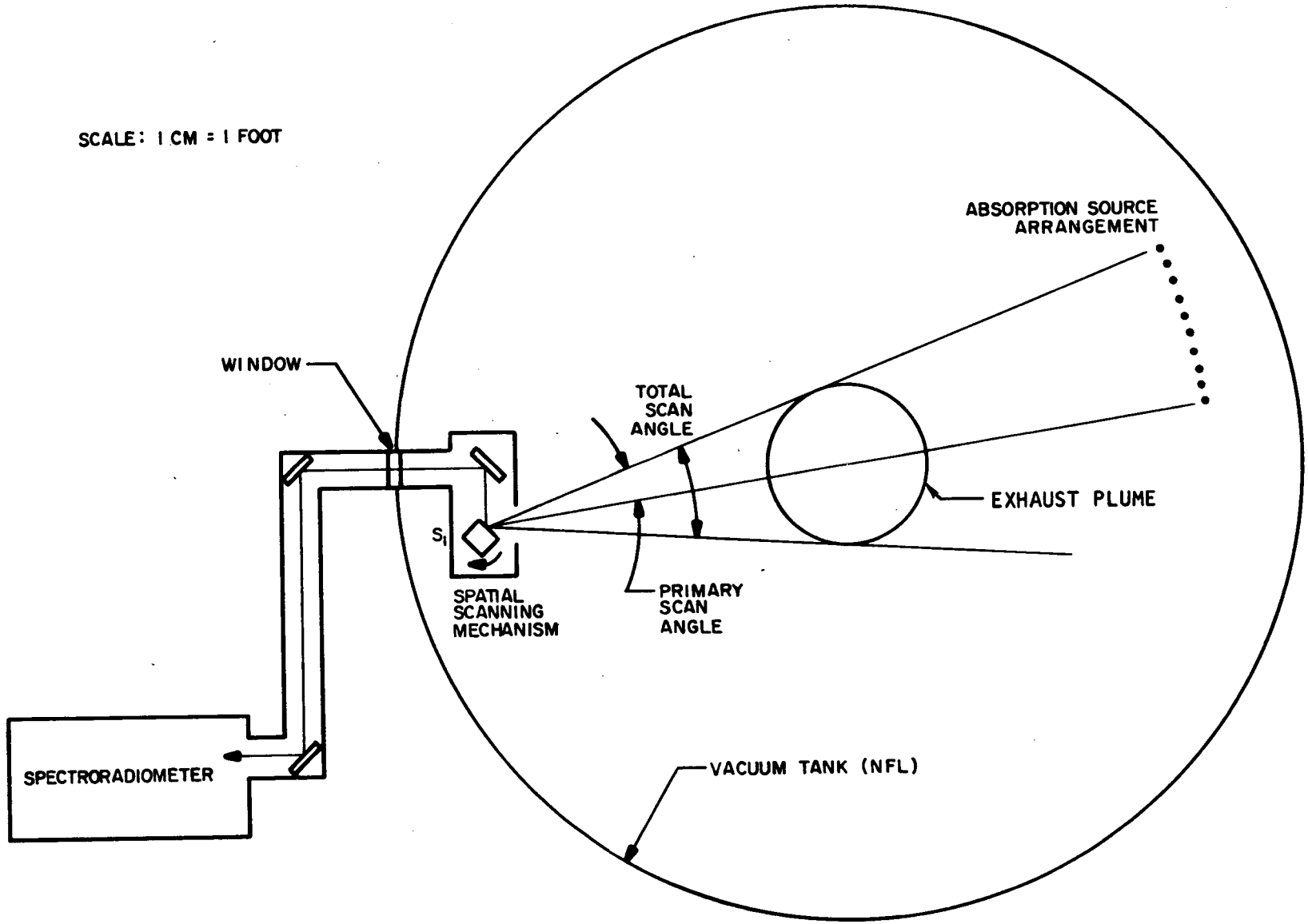

Figure 5. Arrangement of Spatial Scanning Mechanism and Absorption Sources at Nevada Field Laboratory

Tungsten lamps with glass, rather than quartz, envelopes were selected for the absorption sources. The glass envelope transmits a minimum of 50 percent of the filament radiation over the wavelenth range from 0.31×10^{-6} to 3.4×10^{-6} meter (0.31 to 3.4 microns). Lamps with quartz windows transmit over a somewhat wider wavelength range, but are significantly more expensive. A glass lens is used with each lamp to form an image (five times enlarged) of the lamp filament in the exhaust plume. At NFL, a thin sapphire window was mounted in front of each lens to prevent exposure of the lens to hydrogen fluoride or other corrosive exhaust products.

The intensity of each lamp is individually adjustable to ensure the most advantageous conditions (see Data Reduction portion of this section) for the absorption-emission measurements. The lamps operate at 3.5 volts and 30 amperes maximum; a transformer mounted in each lamp housing converts 110 volts at 1 ampere (maximum) to the desired values. Lamp intensity is adjustable remotely. The lamp housings are vacuum tight with atmospheric pressure being maintained in the housings at all times. The lamp windows can be purged with nitrogen and covered by shutters during ignition and shutdown of rocket engines containing corrosive exhaust products. A single lamp, housing, and control circuit are shown schematically in Fig. 6a.

The spatial scanning mechanism varies the line of sight as needed for the zone radiometry measurements. The instrument is shown schematically in Fig. 6b. The design of the spatial scanning mechanism was based on three primary considerations: test duration, scan angle, and width of the light beam at the scan mirror. The scan mirror for NFL (S_1, Fig. 6b) was fabricated from a 5.1 cm (2-inch) Pyrex cube with four reflective surfaces; either four or eight scans of the plume can be made in 1 second. Conversely, the J-2 scan mirror had two reflective surfaces 12.7 by 7.6 cm (5 by 3 inches) and could scan the plume at rates of one per second or one per 4 seconds. As shown in Fig. 5, the primary scan angle covers one-half of the exhaust plume (i.e., from a diametrical line of sight out to the plume edge). Across this primary scan angle, both emission and absorption measurements are made (see Data Reduction section). The remaining half of the plume is scanned in emission only. Comparison of the line-of-sight radiance profiles of the two halves of the exhaust plume serves as a check on the circumferential symmetry of the plume.

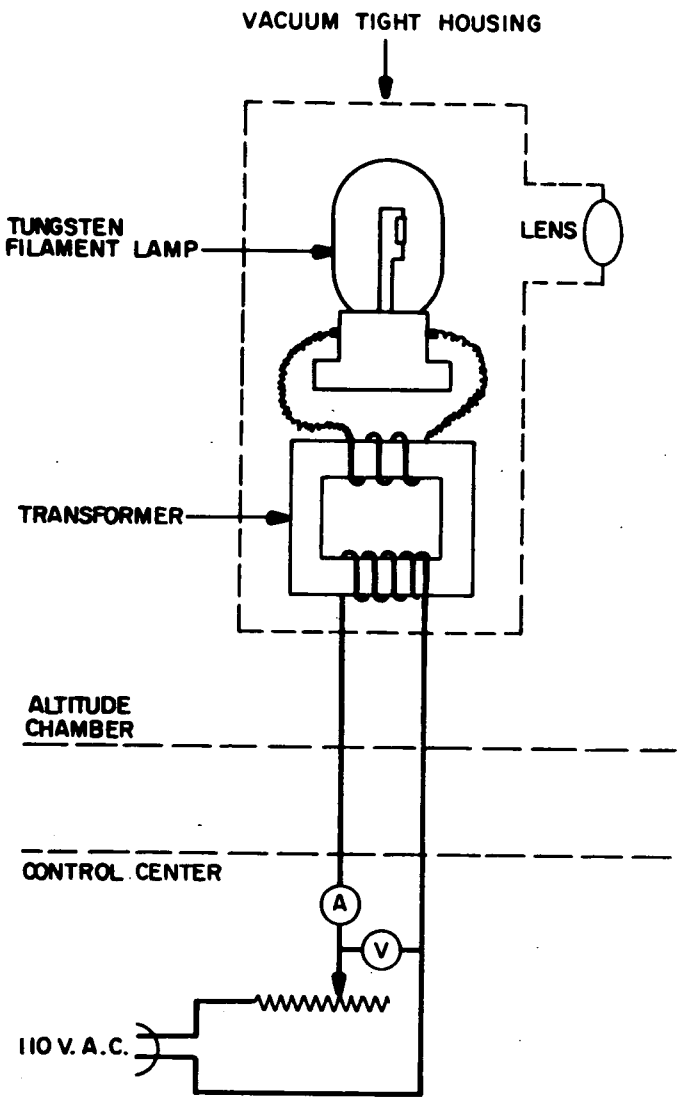

Figure 6a. Absorption Source Housing and Control Circuit

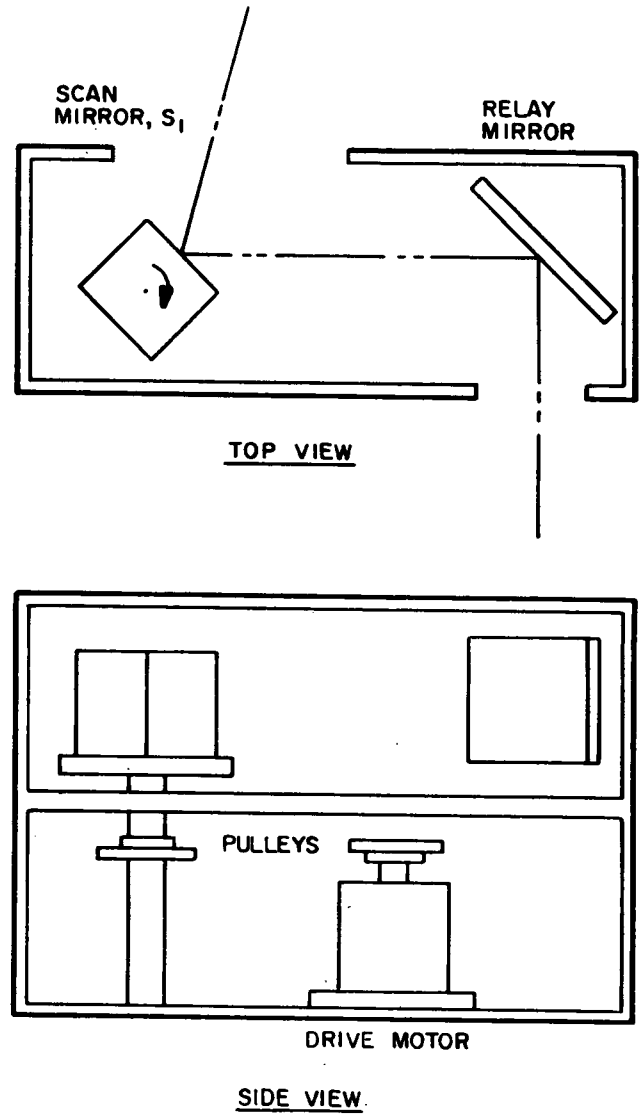

Figure 6b. Spatial Scanning Mechanism

The scan mirror is driven by a 3000 Hz (50 rpm) synchronous motor through pulleys and a drive belt. Scan speeds other than those indicated above can be obtained by substituting various pulley combinations. A coded wheel mounted on the scan mirror drive shaft produces a signal at the recorder for positive identification of scan angle. The spatial scanning mechanism is housed as indicated in Fig. 6b. The opening in the side of the housing through which the plume is scanned can be covered by a remotely operated shutter during motor ignition and shutdowns for experiments with plumes containing corrosive exhaust products.

ELECTRONIC, RECORDING, AND CONTROL SYSTEMS

The electronic and recording system assembled for the spectroradiometer is basically identical with that used in previous zone radiometry programs. Data are recorded on an eight-channel strip chart recorder. Six channels are used to record detector output (three channels at different amplifications for each detector). One channel records a timing signal from the spatial scan system to indicate the scan angle accurately. The remaining channel records a wavelength calibration signal during spectral scans. Provision was made to operate the entire spectroradiometer system either at the recorder location or at a remote location if the recorder is not located in the test site control center. All signal processing and recording electronics are mounted in a single relay rack. The power supplies for the 10 absorption sources, the power switch for the spatial scan mechanism, and the shutter controls for the above are mounted in a separate relay rack. These two consoles were shown in Fig. 4.

A third console houses the blackbody power supplies and controls. These controls include two flow-sensing switches installed in the argon purge line and the water cooling line, respectively. If the argon or water flowrates drop to levels that could possibly damage the blackbody, power is automatically shut down. Shown schematically in Fig. 7 are the recording and control systems and their relationship to other system components.

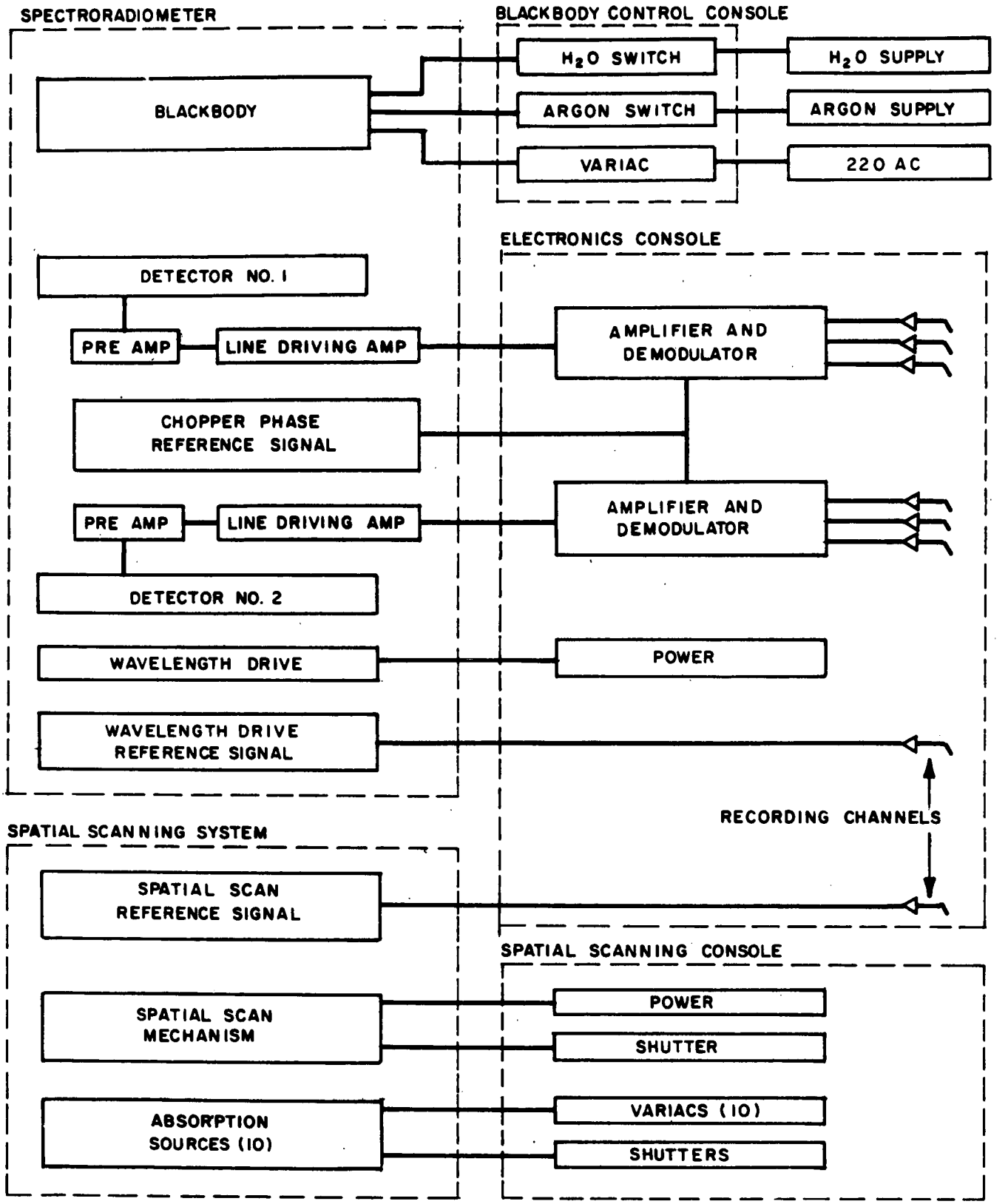

Figure 7. Schematic of Electronic, Recording, and Control Systems

DATA REDUCTION

In previously developed zone radiometry systems, two optical choppers have been used, one located between the absorption source and the exhaust plume and the other between the plume and the detector. Emission and absorption were measured on successive scans of the plume with only the appropriate chopper being activated for each scan. With this double-chopper method, plume spectral radiance and spectral emissivity are measured independently. However, the double-chopper method is not suitable for use with the DCS system because multiple absorption sources are employed. Additionally, at NFL, test durations were relatively short and time sharing incoming radiation with two detectors would become impractical. A single optical chopper is used with the DCS system that permitted emission and absorption measurements during a single scan when the absorption sources are designed to illuminate only discrete portions of the plume. With this arrangement, as the scanning mirror rotates through the primary scan angle during a firing, the recorder pen deflections alternately corresponding to first line-of-sight (LOS) plume spectral radiance and then LOS plume spectral radiance plus the absorption source radiation transmitted along that LOS. A conceptual recorder trace is shown in Fig. 8. Note that to obtain D_n and $D_{n+\tau}$ for identical lines of sight, a value of D_n must be interpolated from values obtained for adjacent lines of sight and conversely. Because pen deflections are proportional to spectral radiance, the above deflections are converted to radiance values by comparison with pen deflections produced by a blackbody calibration source at known temperature. The LOS spectral emissivity is obtained from the following equation relating D_n, $D_{n+\tau}$, and D_τ (the pen deflection produced by scanning the absorption sources when unattenuated by plume radiation), i.e., $D_{n+\tau} = D_n + D_\tau (1-\varepsilon_{LOS})$ or, after rearrangement

$$\varepsilon_{LOS} = 1 - \frac{D_{n+\tau} - D_n}{D_\tau}$$

if $D_n >> D_\tau$ or $D_\tau >> D_n$, then this expression becomes inaccurate; therefore, a provision was included in the DCS system to adjust the intensity of the various absorption sources in a predetermined manner prior to a run so that the brightness temperature would be on the same order of magnitude as the corresponding LOS radiance.

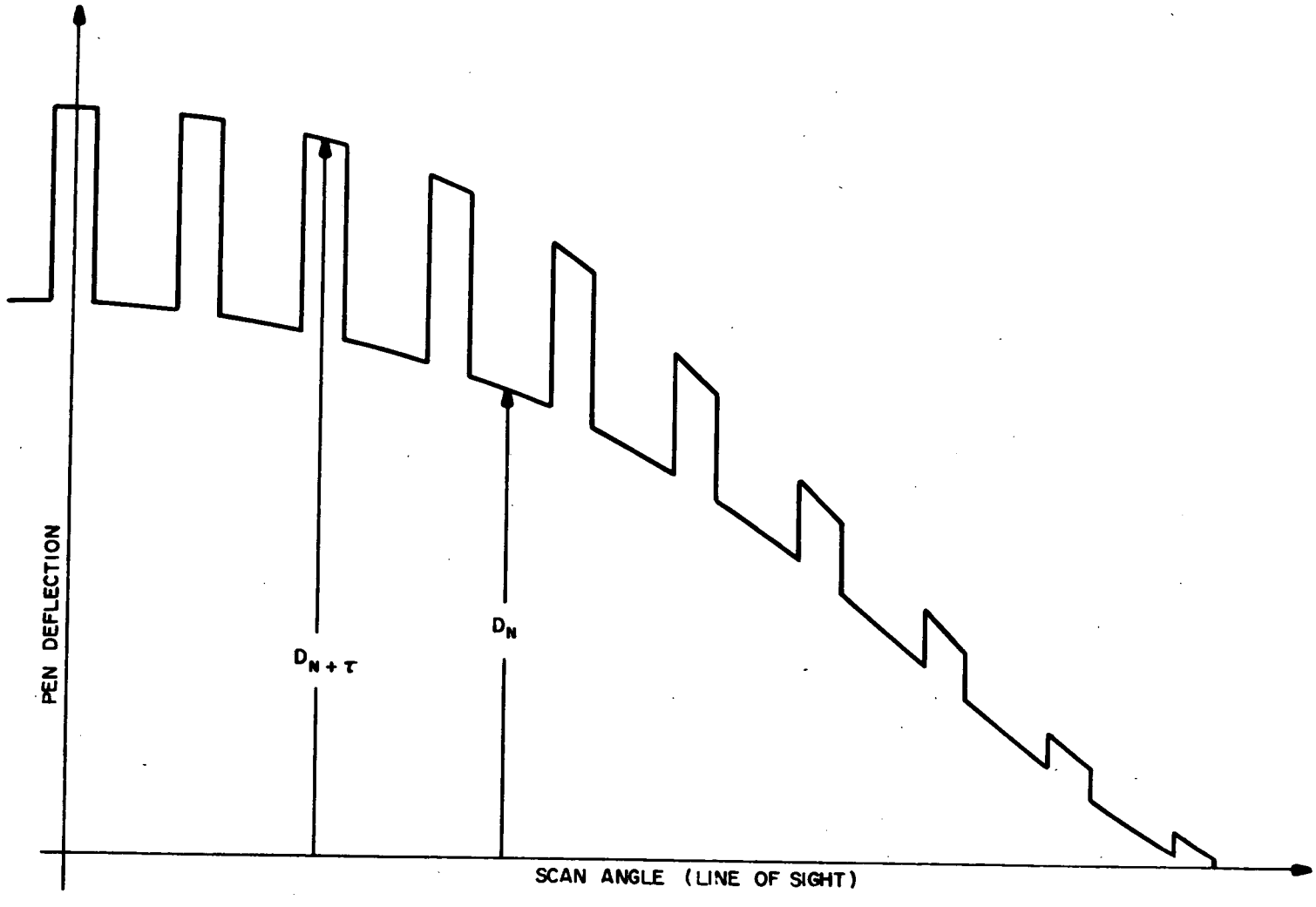

Figure 8. Idealized Recorder Trace During Zone Radiometry Measurement

Operation in the prescribed manner (line-of-sight values of plume spectral radiance) allows subsequent computer calculation of the radial distribution of temperature and selected specie partial pressure. A computer program is available at Rocketdyne and has recently been revised to allow the use of band model parameters, if desired (Ref. 4, 5, and 6).

CHECKOUT AND EVALUATION

Checkout and evaluation of the spectroradiometer included a determination of the following:

1. Stray light level
2. Wavelength calibration
3. Spectral resolution

The spectroradiometer was used to measure the well-known atmospheric absorption lines of H_2O and to determine therefrom stray light levels, wavelength calibration, and spectral resolution. The spectrum recorded is shown in Fig. 9. This spectrum is a portion of the 2.7×10^{-6} meter (2.7 microns) absorption band of atmospheric H_2O recorded with a slit width of 0.05 mm. The internal blackbody source operated at a temperature of 1800 degrees Kelvin and the path length was 2.2 meters.

Stray light results as radiation of unwanted wavelengths reaching the detector simultaneously with desired radiation. The principal effect of stray light is to cause erroneous transmittance measurements. The stronger absorption lines in the 2.7×10^{-6} meter (2.7 microns) atmospheric H_2O band absorb essentially 100 percent at their line centers with a path length of 2 meters. Thus, any difference between pen deflection at the center of these lines when compared with the pen deflection obtained when an opaque card is inserted in the light beam indicates the presence of stray light. Figure 9a indicates that essentially no stray light is present.

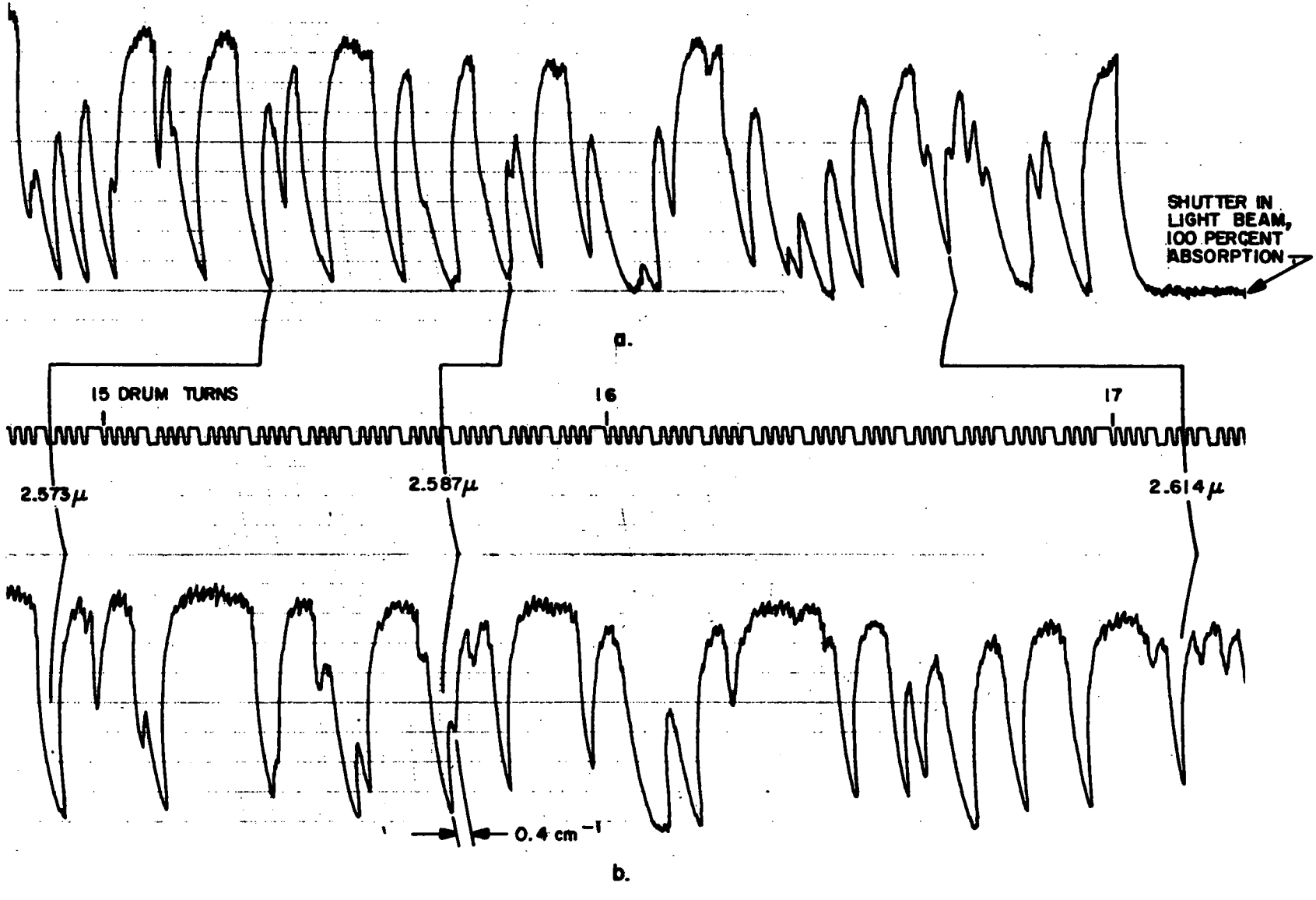

Figure 9. Atmospheric H_2O Absorption: a. Humid Air Recorded to Show Maximum Absorption
b. Dry Air Recorded to Show Maximum Resolution

Wavelength calibration was obtained by comparison of known spectral line positions for atmospheric H_2O with the drum turn calibration signal shown in Fig. 9b. The wavelength drive is linear in drum turns and meters (microns); therefore, these data are sufficient for generation of a wavelength calibration curve.

The spectral resolution (0.4 cm^{-1}) of the spectroradiometer was determined by measuring the separation of the spectral lines at 2.58×10^{-6} meter (2.58 microns). This resolution, obtained at a signal-to-noise ratio of approximately 13, is consistent with that stated by the manufacturer of the monochromator.

PHASE II

SYNOPSIS

Phase II of the contract, conducted from December 1967 through November 1968, was directed toward investigating the dependence of the exhaust plume on injector design and the effects of the injector design and propellant type on propulsion performance.

The B-3 altitude chamber at NFL was selected for installation of the DCS system. The rocket engine test firings were conducted under Contract NASw-2119. The installation required some modifications to the DCS system, which are described in subsequent sections.

The number of test firings available for data collection during Phase II was considerably less than originally anticipated. The total number of tests on Contract NASw-2119 was less than anticipated and a large majority of those tests were made with a conical nozzle. The conical nozzle extended into the facility diffuser and prevented optical access to the exhaust. Five altitude simulations were conducted with a bell nozzle and the DCS system was used on all of these tests. Data acquisition was made difficult because each of the five altitude simulation tests was made with a different propellant combination. Normally, a minimum of two tests per propellant combination is required for zone radiometry to establish proper instrument settings.

Primarily because of the large number of propellant combinations employed and the reduction of run duration to approximately 1 second, the quality of the data obtained during Phase II was considerably below that obtained during previous zone radiometry programs (Ref. 4 and 5). However, the DCS system was thoroughly checked out, and all components of the system performed as designed. The absorption source lamps operated without problems. (The durability of these lamps was a potential problem.)

The results of the five-test series (altitude simulations) monitored during Phase II are summarized in Table 1. A test series consisted of a number of runs with a given experimental arrangement while a simulated altitude was maintained. Upon initiation of a test series, no further adjustments to the DCS system could be made; therefore, as far as the DCS system is concerned, a test series corresponded to only one DCS test.

TABLE 1. SUMMARY OF PHASE II TESTS MONITORED

Date, 1968	Test Series 377-	Propellant	Data Type*	Remarks
6-21	028 through 032	F_2/H_2	ZR	Absorption only; no emission measured
8-5	055 through 060	$FLOX/CH_4$	SS	Data no good; mirrors contaminated during pretest facility activities
10-11	093 through 100	$FLOX/B_2H_6$	ZR	Emission only; no absorption measured
10-28	101 through 108	OF_2/B_2H_6	SS	Good HF emission spectra obtained
10-29	109 through 120	OF_2/CH_4	ZR	Very weak emission; no absorption; therefore not reduced

*ZR = Zone Radiometry
SS = Spectral Scan

The difficulties encountered during Phase II suggested the need for several improvements to the DCS system, namely, (1) a detector with a faster response and greater sensitivity than the existing PbS detector, (2) recording data on magnetic tape, and (3) facility modifications to permit optical access when conical nozzles are utilized.

EXPERIMENT DETAILS

SPECTRORADIOMETER SYSTEM

The major components of the dual-channel spectroradiometer system are shown schematically in Fig. 10. This arrangement is somewhat different from that shown in Fig. 5. The engine plume diameter selected for study was smaller than planned. The 10 absorption sources were distributed over the entire plume. The location of the optical components of the system with respect to the B-3 test cell are shown schematically in Fig. 11. Figure 12 shows the absorption sources and rocket engine, and Fig. 13 is an overall view of the inside of the B-3 test cell. The 10 absorption sources were mounted on an aluminum plate that was bolted to a cast iron plate. The cast iron plate was welded to the test cell wall. The spatial scan mechanism was similarly mounted. This arrangement was designed for precise alignment of the sources and scan mechanism with respect to the rocket nozzle exit plane. Individually adjustable flat relay mirrors R_1, R_2, R_3, and R_4 (Fig. 11) directed radiation from the spatial scan mechanism to the spectroradiometer. Mirror R_3 deflected radiation downward and R_4 deflected radiation horizontally into the spectroradiometer.

The spectroradiometer was secured to a platform at the side of the test cell. The absorption source scan mirror control console and the power supply for the blackbody calibration source were located on a concrete pad underneath the spectroradiometer.

The spectroradiometer with its cover installed and the optical tunnel holding relay mirrors R_3 and R_4 in place are shown in Fig. 14, and Fig. 15 and 16 show the instrument with the cover removed. Figure 17 shows the absorption source and spatial scanning mirror control console and spectroradiometer located outside the test cell. The control console contains individual intensity controls for the 10 tungsten lamp absorption sources, the scan mirror drive switch, and switches for the absorption sources shutters and the scan mirror shutter. These shutters can be operated from the control center, either manually or automatically in sequence with the test firing.

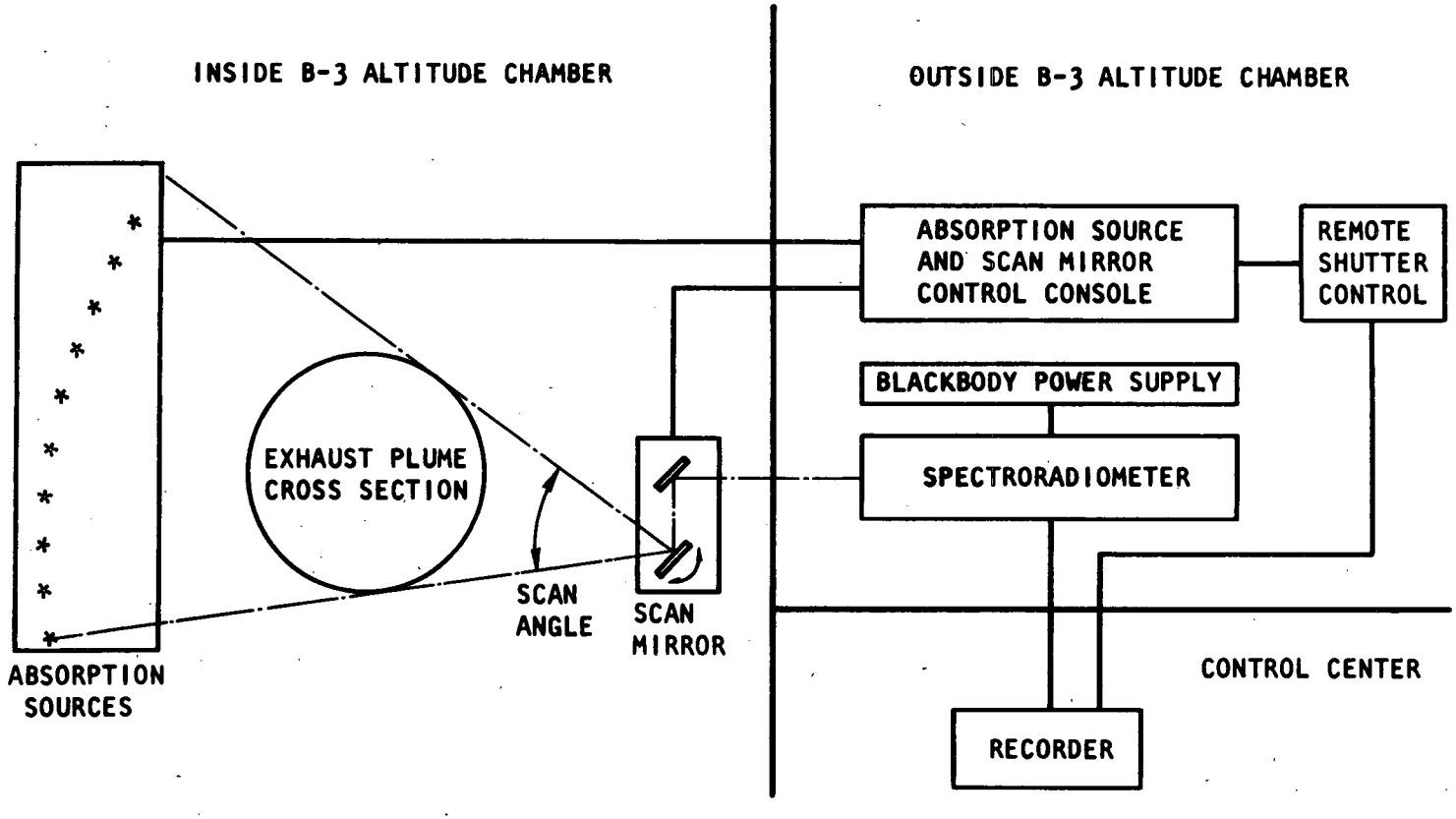

Figure 10. Dual-Channel Spectroradiometer System

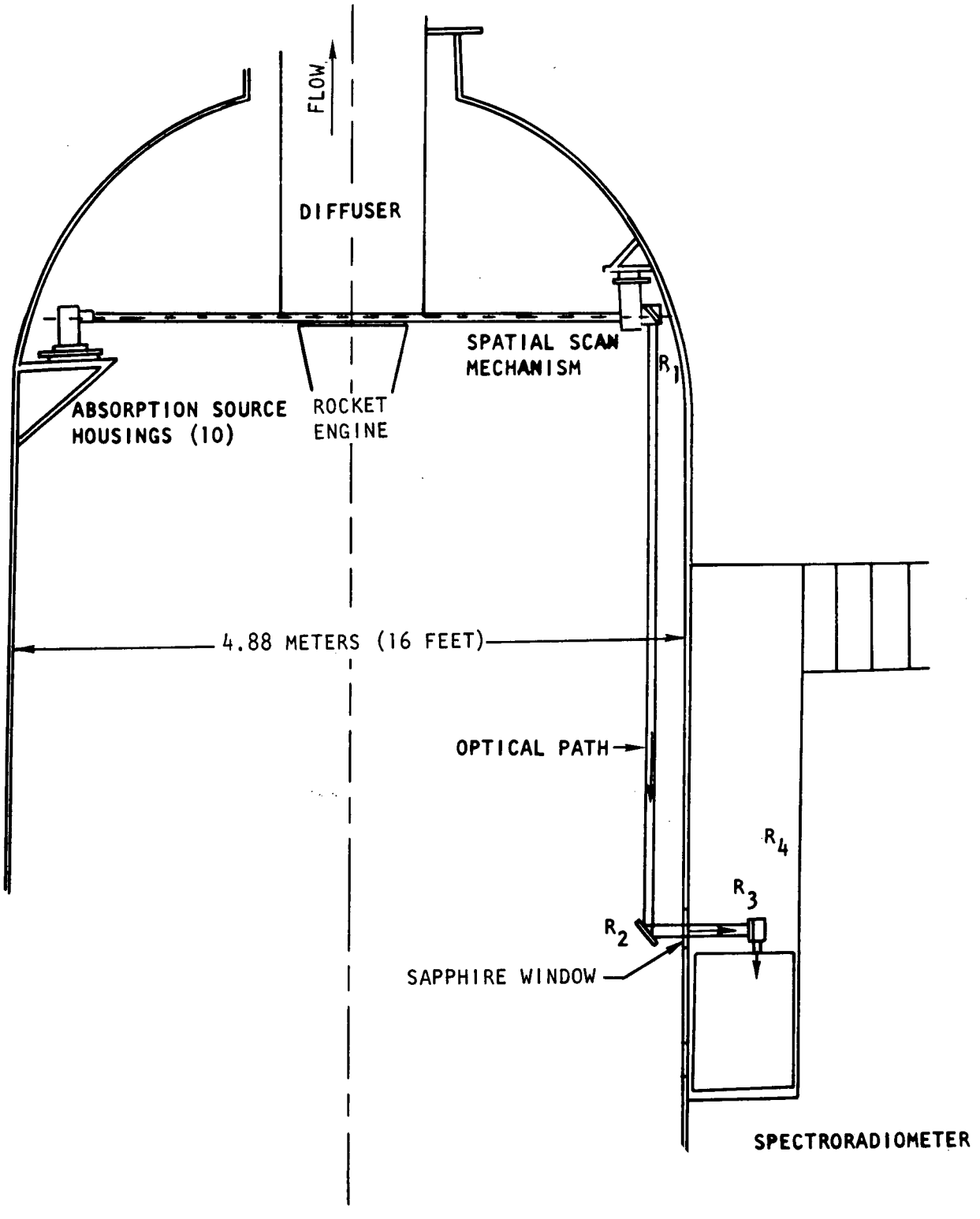

Figure 11. Location of Major System Optical Components With Respect to B-3 Test Cell

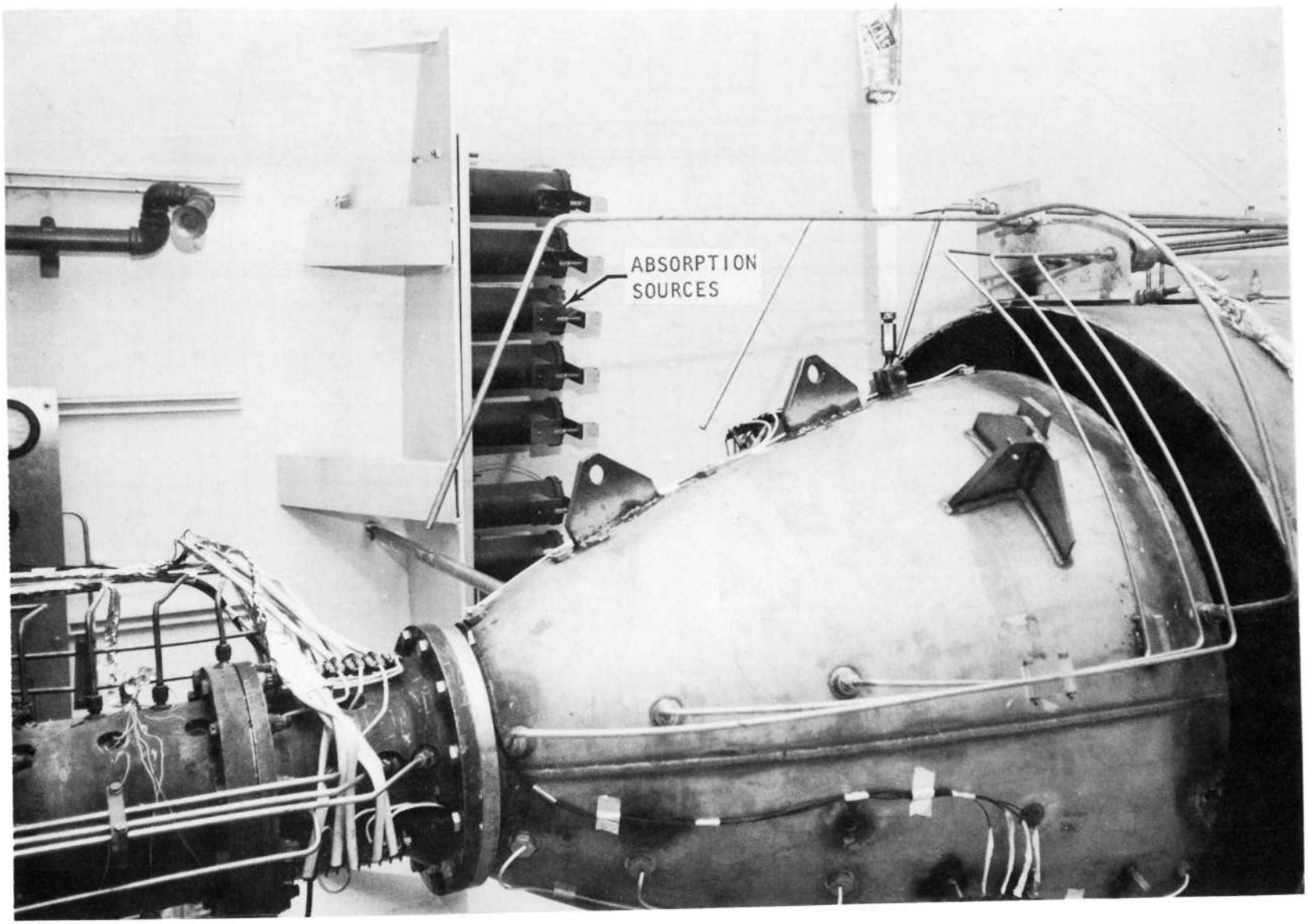

6RE35-8/5/68-R1A

Figure 12. Absorption Sources and Rocket Engine

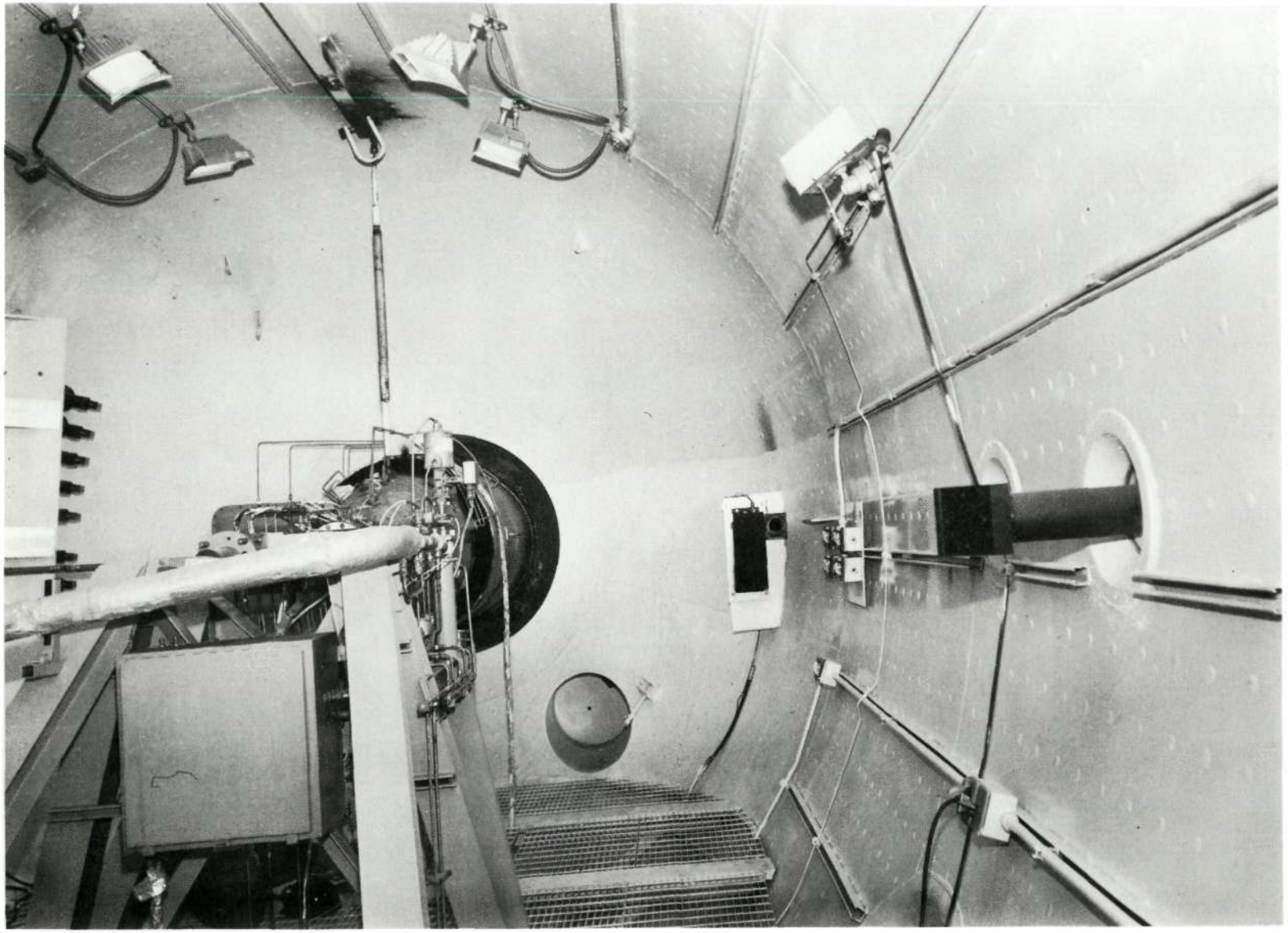

6RE35-8/5/68-R1C

Figure 13. Interior of B-3 Test Cell

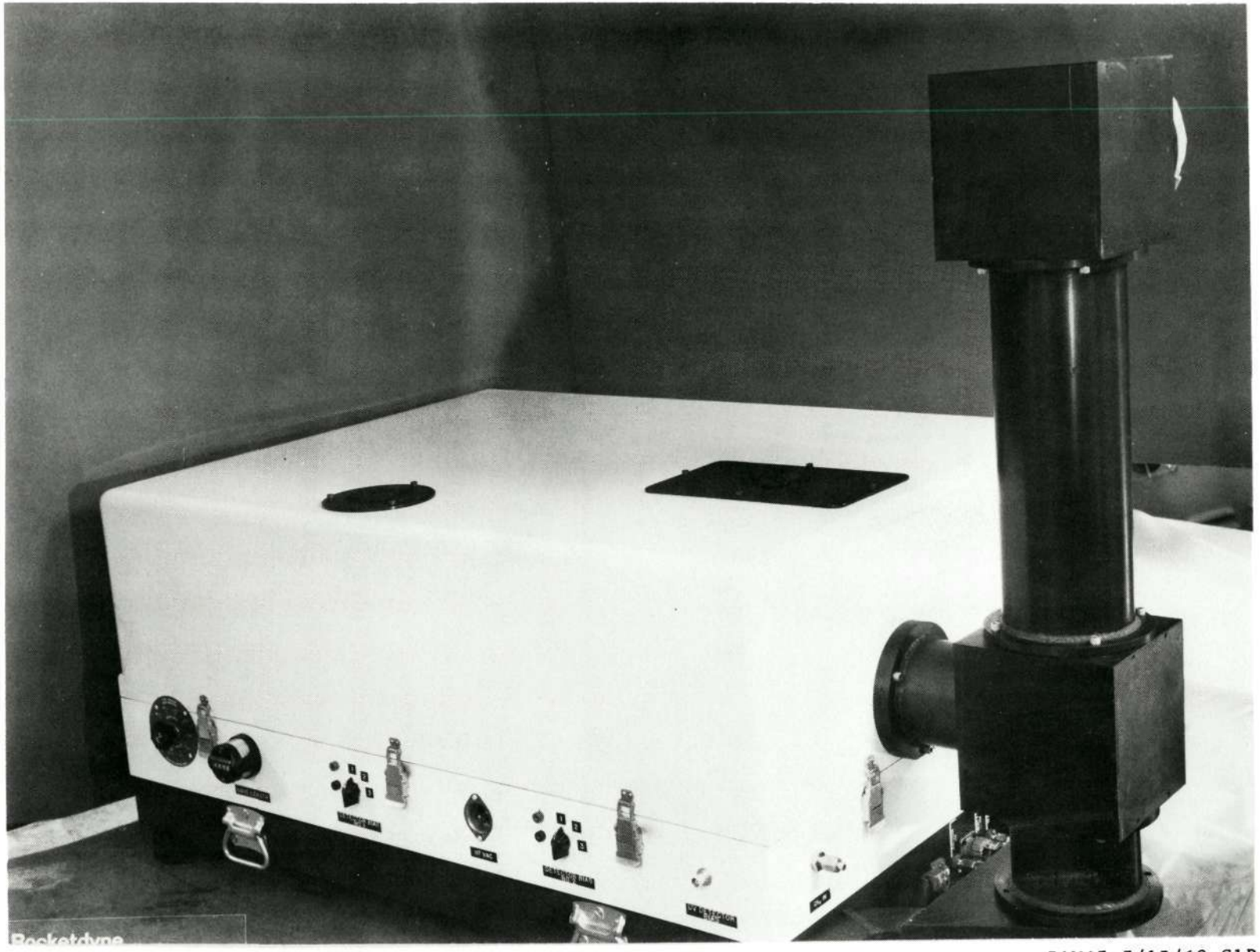

5AH63-3/15/68-S1B

Figure 14. Spectroradiometer With Cover Installed

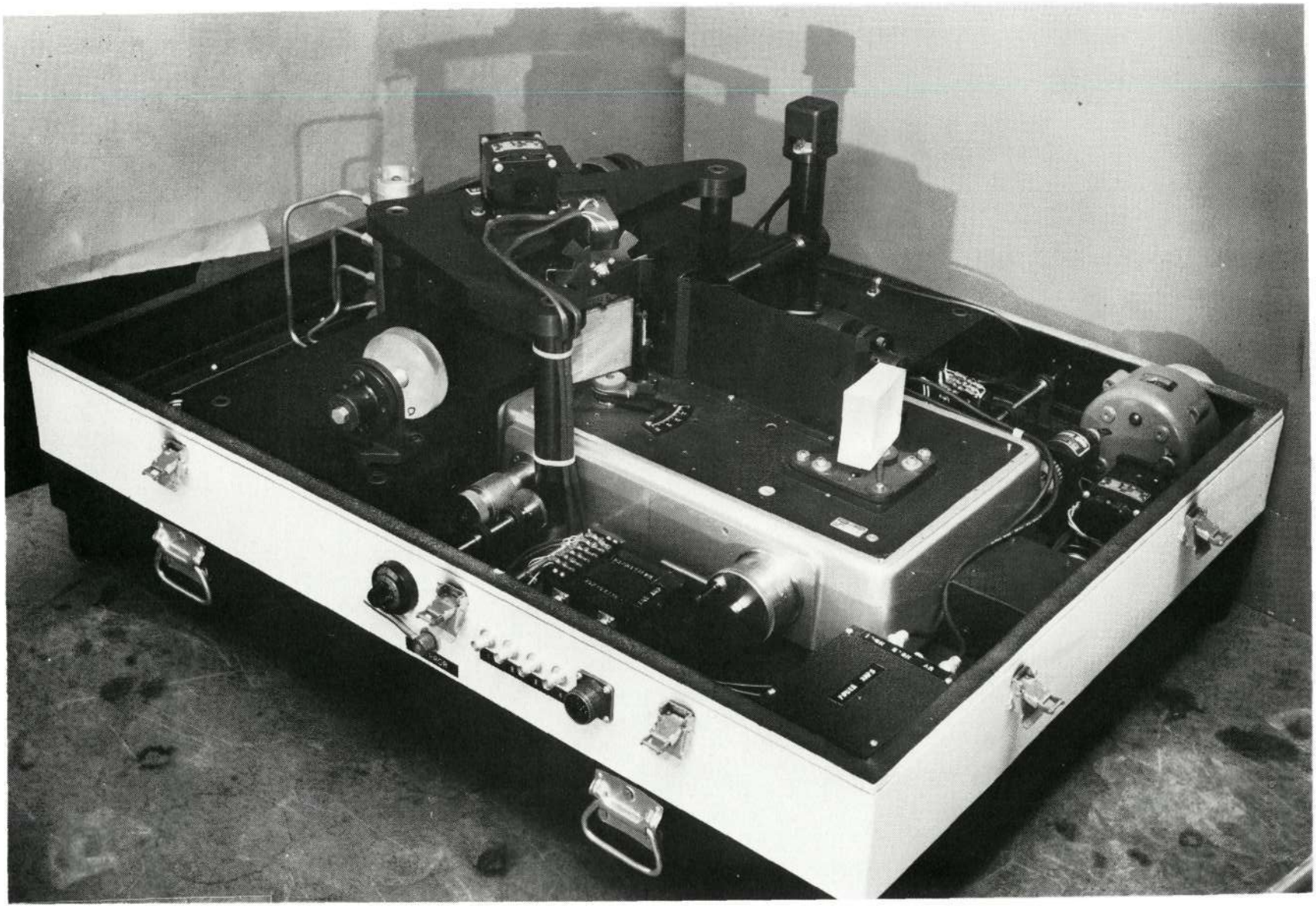

5AH63-3/15/68-S1C

Figure 15. Rear View of Spectroradiometer

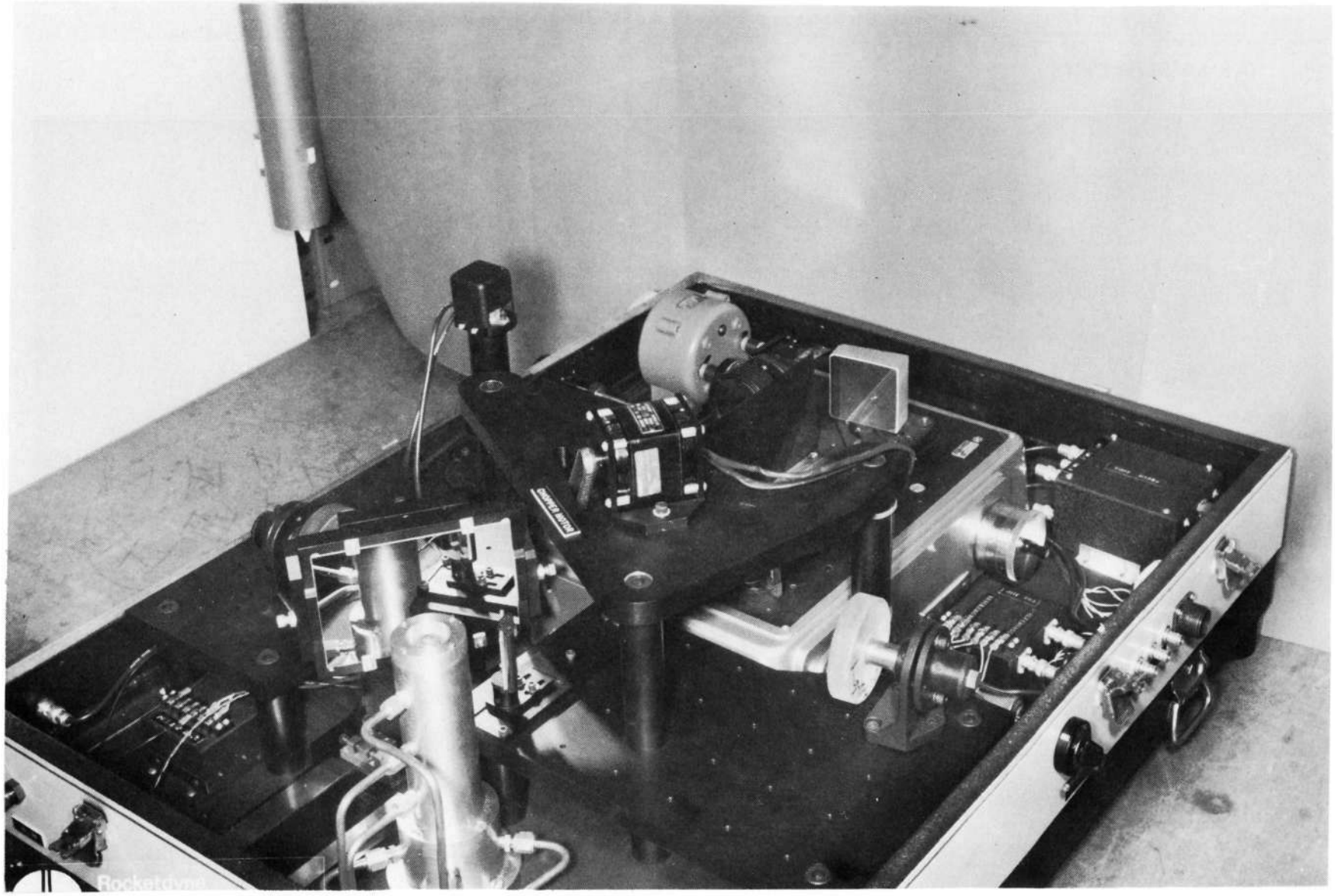

5AH63-3/15/68-S1D

Figure 16. Front View of Spectroradiometer

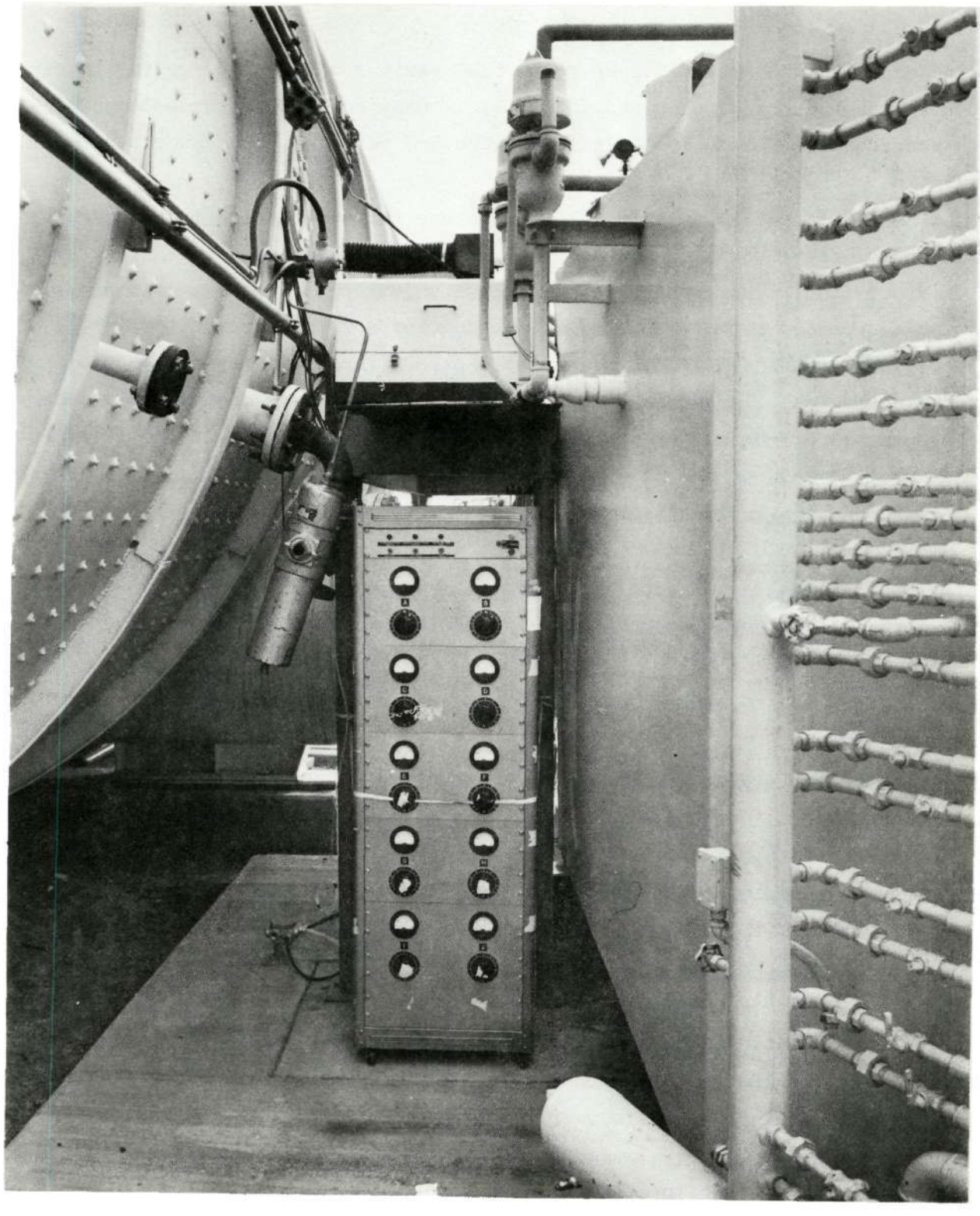

6RE35-8/5/68-R1D

Figure 17. Spectroradiometer and Control Console Outside B-3 Cell

The individual components referred to in the previous paragraphs are fully described in the Phase I section and in Ref. 1 . Only changes to these components that were required due to installation at the B-3 test cell are described below.

The B-3 test cell installation resulted in a one-third reduction in the angular separation of the absorption sources, as measured from the scan mirror, over the design separation. Thus, the scan mirror, which was designed as a continuously rotating four-sided mirror, scanned the absorption sources three times faster than originally intended. This scan rate exceeded the frequency response of the system electronics. Therefore, the scan drive mechanism was changed to reduce the scanning rate from a continuous rotation to a cam-driven oscillation through approximately 0.2095 radian (12 degrees). The cam rotated at 1 Hz (1 revolution per second) and the entire plume was scanned twice per second.

The test site installation also required the addition of relay mirrors R_1 and R_2 to the optical transfer system, as well as additional optical tunnel assemblies.

ROCKET ENGINE

The rocket engine, associated hardware, and testing procedures are described in Ref. 7 , 8, and 9 , and therefore are discussed only briefly here. The engine with the 70-percent bell nozzle is shown in Fig. 12. This nozzle provided an area expansion ratio of 60:1 and had an exit diameter of 82.6 cm (32.5 inches). The engine was operated at a nominal chamber pressure of 5.85×10^5 newtons/m^2 (85 psi) and developed a nominal 11,100 newtons (2500 pounds) of thrust.

The altitude simulation system maintained an altitude in excess of 30,480 meters (100,000 feet) for 150 seconds. During this period of operation, a series of individual engine firings at various mixture ratios was made. The first run of the series was approximately 2 seconds in duration, which was followed by as many as 12 1-second runs. The interval between each run of the series was approximately 10 seconds. The multiplicity of runs during a given test series (altitude simulation) did not improve the probability of obtaining suitable results from

the DCS system because once a test series was initiated, no further adjustments to the DCS system could be made. For purposes of zone radiometry, therefore, a test series was simply one test with multiple parts.

DATA COLLECTION

All of the data obtained are summarized in Table 1. For selected tests, spectral scans of exhaust radiation were conducted along a fixed diametrical line of sight through the exhaust by fixing the spatial scan mirror. The spectral scans were used for species identification and for determination of optimum wavelength and electronic amplification settings for subsequent zone radiometry. Since the entire wavelength region of interest could not be scanned during the 1-second test duration, the wavelength scan mechanism was activated manually for each test during a test series, with a different portion of the region scanned on each individual test.

When zone radiometry measurements were taken, the absorption sources were set to the desired intensity and allowed to stabilize for 3600 seconds before the test series. The spatial scan mirror was subsequently activated and instrument controls were set at desired values. Several seconds before the first test of a series, the absorption source and scan mirror shutters were opened and the recorder paper drive was activated. The emission from the absorption sources was scanned and recorded continuously throughout the test series. During each individual test of a series, the attenuated emission from the sources and exhaust emission were scanned (spatially) and recorded (see Phase I Data Reduction section).

Wavelength calibration was verified by recording the absorption spectra of atmospheric water vapor. The emission from the absorption source lamps, which was recorded between individual tests of a series, served as the background measurement for absorption determination. The absorption sources were also used for intensity calibration and each tungsten lamp was calibrated with an optical pyrometer. Because of the large number of reflections in the optical path from the exhaust to the spectroradiometer, it was not practical to use the internal blackbody calibration source for intensity calibration.

RESULTS

TEST SERIES 377-028 THROUGH 377-032 (F_2/H_2)

This was the first test series where the DCS system was used and the only test series utilizing the F_2/H_2 propellant combination. Therefore, it was decided to attempt zone radiometry rather than scan spectrally. All components of the DCS system performed as scheduled. The absorption source lamps were attenuated by the exhaust plume, but no emission from the plume was measured. The lack of measurable emission resulted from the exhaust being considerably cooler than anticipated and too low a setting for the electronic amplification of the detector signal.

The line-of-sight absorption data for tests 377-028 and -029 with a mixture ratio of 12 were reduced. The results are shown in Fig. 18 as KP_{HF} (product of spectral absorption coefficient and HF partial pressure) versus nozzle exit radius. Since no emission data were obtained, temperatures could not be calculated and, therefore, K could not be determined. However, since K is a slowly varying function of temperature, the curve in Fig. 18 is indicative of the relative variation of hydrogen fluoride partial pressure with nozzle exit radius.

TEST SERIES 377-055 THROUGH 377-060 (FLOX/CH_4)

A spectral scan of exhaust plume emission along a fixed line of sight was attempted for this test series. The data obtained (weak emission) were invalid. Posttest inspection revealed that the mirrors inside the vacuum chamber were covered with water and other contaminants. The contaminants were apparently deposited during pretest facility operations when the vacuum system failed, permitting excessive moisture to enter the B-3 test cell.

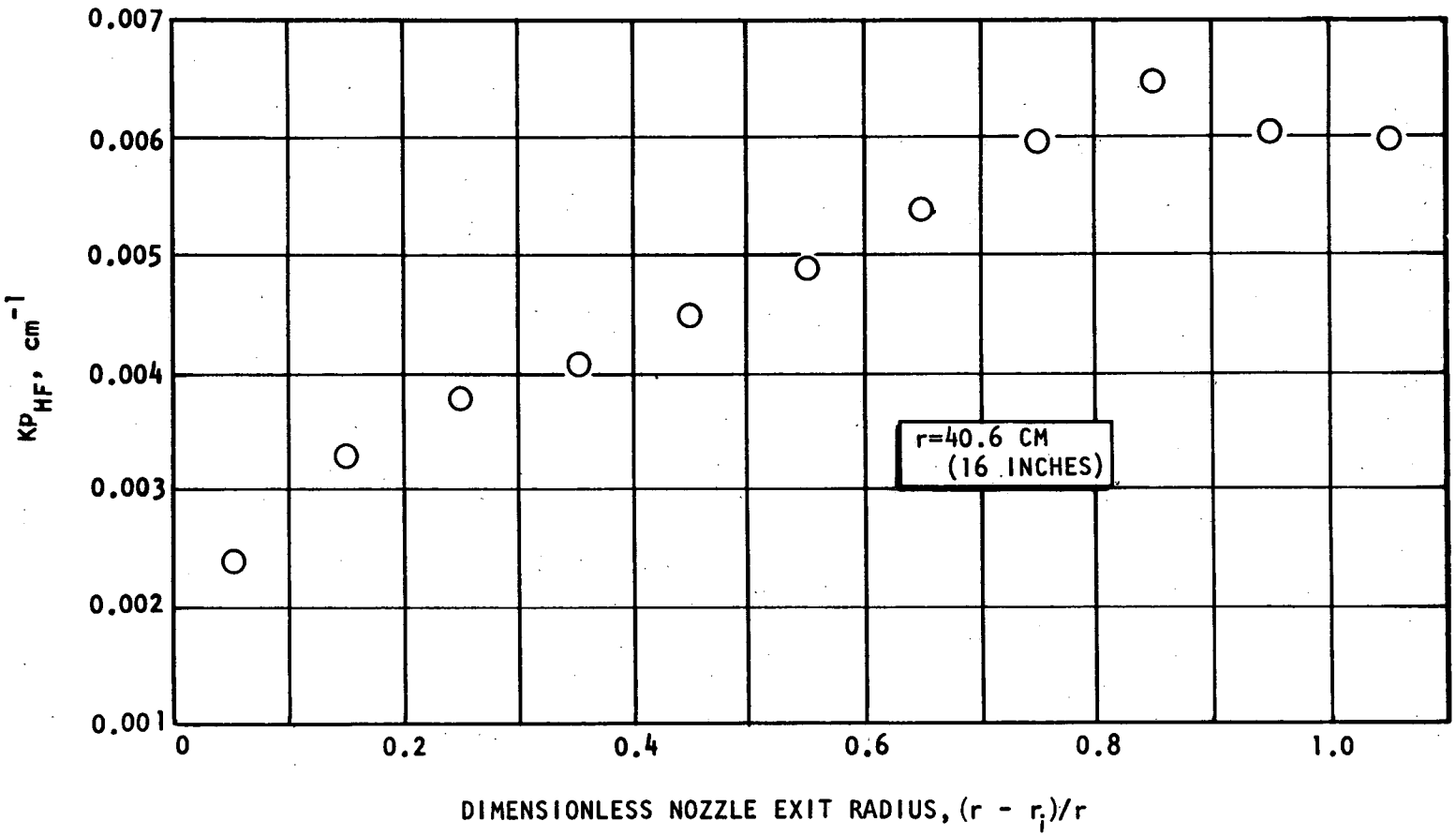

Figure 18. Measured Variation of KP_{HF} With Nozzle Exit Radius, Tests 377-028 and 029

TEST SERIES 377-093 THROUGH 377-100 (FLOX/B_2H_6)

This test series was to be the last series planned with the bell nozzle. Therefore, zone radiometry was attempted, although no spectral scan data were available. The data record for test 377-100 is shown in Fig. 19. Emission from the exhaust plume during the test was readily apparent. However, comparison of the individual absorption source intensities for identical lamps before and during the test indicated little or no plume absorption. This phenomenon, emission without absorption, is indicative of continued reactions in the exhaust, but without spectral scan data this hypothesis cannot be verified. Since radial distributions of brightness are of no particular value unless the corresponding absorption data are available, further data reduction was not attempted.

TEST SERIES 037-101 THROUGH 037-108 (OF_2/B_2H_6)

Spectral scans were taken during this series of tests. Spectral data between 2.39×10^{-6} to 2.28×10^{-6} meter (2.39 to 2.28 microns) are shown in Fig. 20 (test 037-102). Three individual hydrogen fluoride lines in emission were detectable. The maximum brightness temperature of these lines was approximately 1000 K. Figure 21 shows the data obtained during test 037-104, where the spectral scan mechanism was activated from 2.02×10^{-6} to 1.90×10^{-6} meter (2.02 to 1.90 microns). Hydrogen fluoride was not expected to emit in this spectral region; however, very weak continuum radiation was evident. This observation may possibly be attributed to boron particles in the exhaust. This test series demonstrated the workability of all components in the DCS system except for the scanning technique.

TEST SERIES 109 THROUGH 120 (OF_2/CH_4)

The spectral scan data from the previous test series were assumed directly applicable and zone radiometry was attempted on these tests. (The same electronic amplification and slit width settings were used for both test series.) However, the CH_4-fueled exhaust was much cooler than the B_2H_6-fueled exhaust and only very weak emission was observed in the zone radiometry traces. No measurable absorption was recorded.

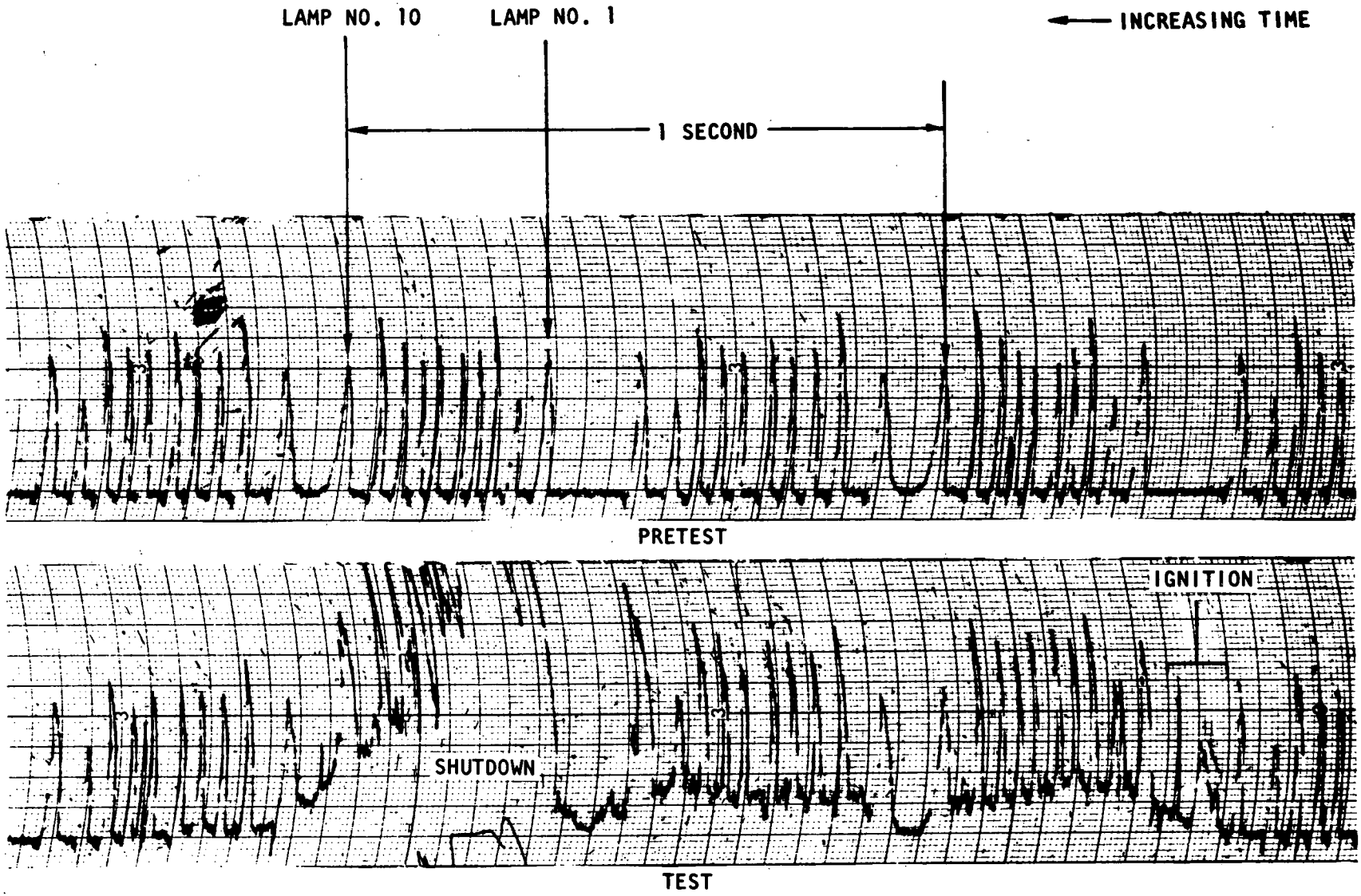

Figure 19. Zone Radiometry Data Obtained for Run 377-100

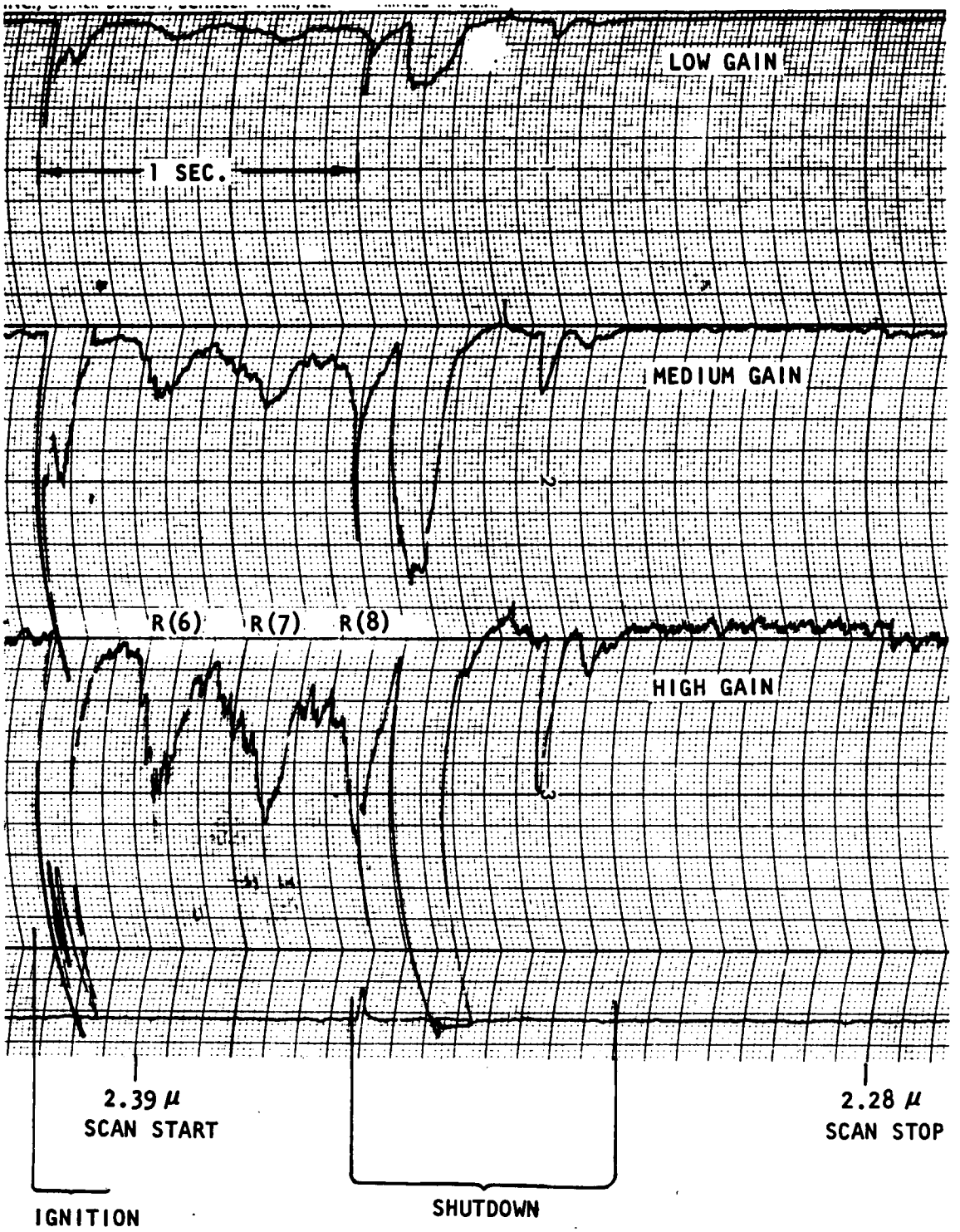

Figure 20. Spectral Scan Data Obtained for Run 377-102

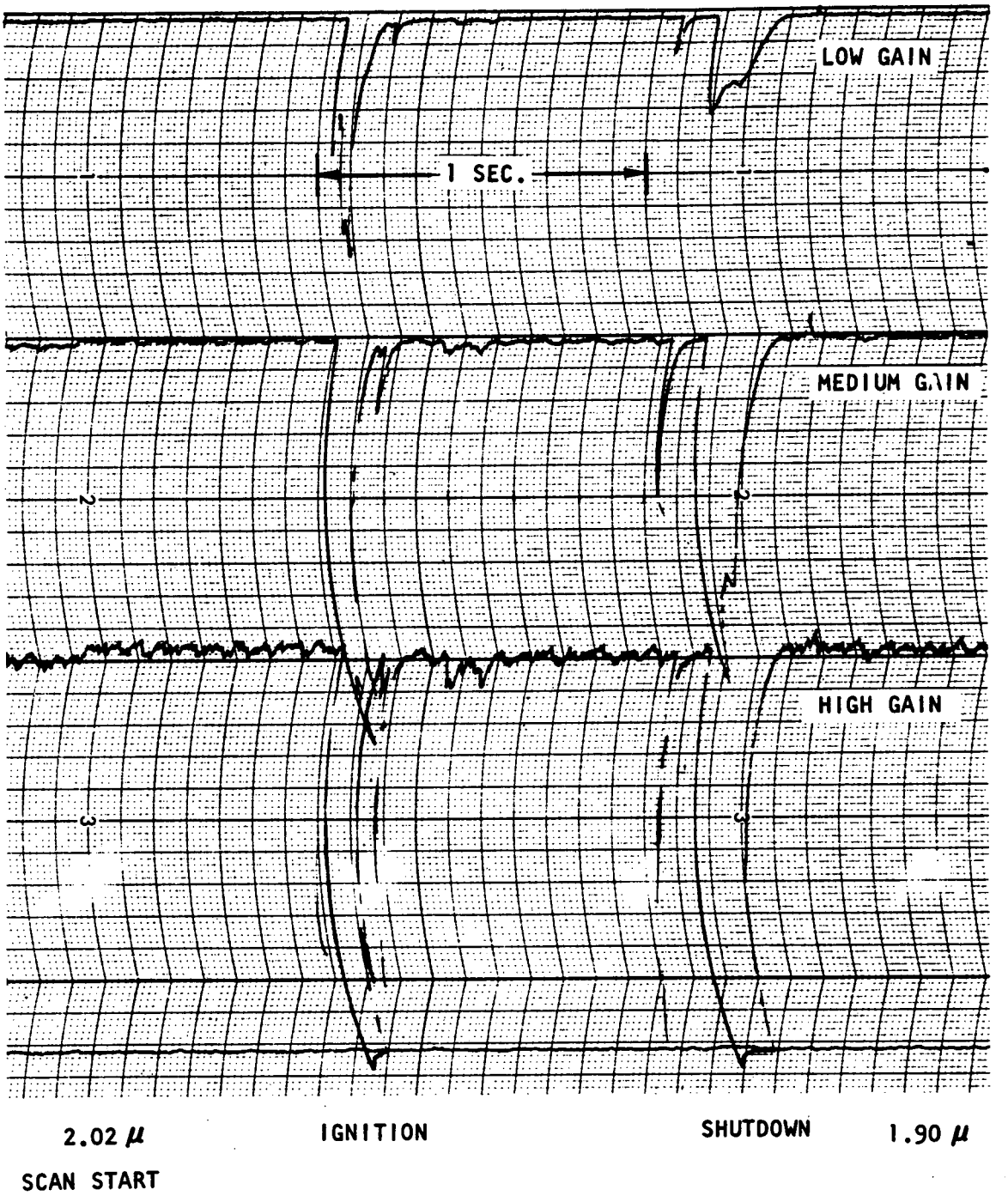

Figure 21. Spectral Scan Data Obtained for Run 377-104

PHASE III

SYNOPSIS

Phase III, conducted from December 1968 to May 1970, was directed toward the improvement of the DCS system and the continued use of the system in obtaining partial pressure and temperature profiles of the exhausts of engines scheduled to be tested in the B-3 cell (NFL) using space-storable propellants.

The specific improvements planned for the DCS system included:

1. Changing from an uncooled PbS detector to an LN_2-cooled, photovoltaic indium arsenide detector
2. Increasing the optical chopping speed from 400 to 2000 Hz, so that the optical scan speed could be increased
3. Assembling appropriate preamplifiers and amplifiers to minimize losses of the detector output signal
4. Recording the output signal on FM magnetic tape
5. Demodulating the 2000-Hz signal and recording the output on existing strip-chart recorders to obtain visual evidence of proper system operation
6. Scanning the entire plume four times per second rather than twice

The requirement for these improvements resulted from Phase II experimental evidence. The sensitivity, both with respect to response time and with respect to signal-to-noise ratio, of the PbS detector and associated electronics was not sufficient for obtaining good zone radiometry data on the cool, highly expanded gases from the space-storable engine tests conducted previously.

These modifications were initiated early in the Phase III program. To facilitate these changes, the spectroradiometer, its control console, and the special scanning mechanism were shipped from NFL to SSFL. A new detector was ordered from the Santa Barbara Research Center. This detector, indium arsenide, has an operating temperature of 77 K and approximately 10 times the sensitivity of PbS. During

the 6-month delivery period of the detector, a number of the mirrors used in the DCS system were realuminized, modification of the system electronics was initiated, and a high-resolution spectrometer (a special laboratory instrument) was prepared for HF absorption coefficient measurements.

Prior to delivery of the indium arsenide detector, completion of the DCS system electronics modification, and initiation of the HF absorption measurements, it was determined that the space-storable engine tests planned for the B-3 cell were postponed indefinitely. Therefore, the DCS program was redirected to gather data on NAS3-12051, a FLOX/CH_4 performance evaluation program being conducted at SSFL.

Since the firing duration for the FLOX/CH_4 engine was on the order of 10 seconds, it was not necessary to complete the modifications to increase system response; however, the spatial scan system used in the B-3 cell was not suitable for these tests because the nozzle exit diameter of the engine to be monitored was on the order of 15.25 cm (6 inches). Therefore, the DCS system was fitted with a "zone ranger" spatial scan mechanism similar to that used on NAS8-11261 (Ref. 4). Additional modifications included replacement of the rotating blade chopper with a tuning fork chopper, and assembly of an absorption source and chopper assembly similar to that utilized on NAS8-24568 (Ref. 10).

The DCS system was installed in the Propulsion Research Area (PRA). During checkout of the FLOX/CH_4 engine, as assessment of the effect of engine vibration on the functioning of critical DCS components was attempted. However, an engine failure occurred that caused considerable thrust chamber, injector, and test stand damage, and further testing was suspended. The DCS system was returned to the Optics Laboratory and minor damage sustained during the test stand fire was repaired. All work on the program was stopped and efforts were again redirected.

PHASE IV

SYNOPSIS

Phase IV, conducted from June 1970 to December 1971, was directed toward monitoring the exhaust plume from a H_2/O_2-fueled engine operated under Contract NASw-2106, "Experimental Investigation of Combustor Effects on Rocket Thrust Chamber Performance." This program was designed to experimentally verify a number of assumptions in the ICRPG rocket engine performance model.

A striated flow injector was utilized to impose a number of controlled mixture ratio gradients. Two nozzles were employed, with expansion ratios of 4:1 and 25:1, for comparing performance at sea level and altitude, respectively.

Testing was originally planned for the B-3 cell at NFL; however, early in that program the testing phase was rescheduled to cell 29, CTL-4, SSFL. This change did not alter the intent of the Phase IV contract but did change program emphasis (i.e., significant consideration had to be given to DCS system installation at this "new" facility).

The DCS system that was originally adjusted to monitor HF spectra did not require any major modifications to "optimize" it for recording water vapor spectra. Calculations indicated that the sensitivity of the original DCS system was adequate for the measurement of relatively large water vapor plumes, provided that the detector output was recorded on magnetic tape rather than strip-chart recorders. Therefore, the instrument was returned to that described under Phase I, refurbished, and provision was made for adding an FM tape recorder to the system.

The scanning method utilized during Phase II, was directly applicable to the cell 29 tests. The tungsten ribbon absorption sources were obtained from NFL; however, they required refurbishment and realignment. Gathering absorption and emission data during the same scan requires "dark" zones between the regions of the plume illuminated by adjacent absorption sources. The 25.4-cm (10-inch) diameter and

61.0-cm (24-inch)-diameter exhaust plumes necessitated tuning the absorption sources to a fixed width at the plume. This was accomplished by rotating the light source filaments until the prescribed light beam width was obtained. The scanning mechanism was utilized intact except for changing the cam drive to increase the included angle scanned by the tracking mirror.

The relatively large number of DSC system relocations since the last complete use of the equipment on a test firing suggested that recalibration of critical components was in order. Wavelength calibration was accomplished by making spectral scans of standard light sources and comparing known spectral lines with the instrument wavelength indicator. An additional check was made by recording the atmospheric water vapor absorption spectra and comparing these results with those published in the literature. These data enabled accurate on-site setting of the desired wavelength. Calibration of the absorption sources consisted of measuring the brightness temperature as a function of filament voltage with an optical pyrometer.

Water vapor absorption spectra were also recorded at conditions approximating those anticipated during actual engine firings. The results indicated that the firings should be monitored at a wavelength of 2.5×10^{-6} meter (2.5 microns) rather than the planned 2.7×10^{-6} meter (2.7 microns). At the 2.7×10^{-6} meter (2.7 micron) wavelength, total absorption would occur, which would prevent calculating zonal temperatures and H_2O partial pressures from the data.

Installation of the DCS system at a "new" facility required design and fabrication of new mounting brackets for the absorption sources, scanning mechanism, and spectroradiometer. Two mounting brackets (bolted to the same stringers welded to the altitude capsule test cell wall) for the absorption sources were fabricated (one each for the 25.4-cm (10-inch) and 61.0-cm (24-inch) nominal-diameter exhaust plumes). Similarly, two mounting brackets for the scanning mechanism were fabricated. Thereby, the individual light sources and scanning mechanism could be relocated, depending on the nozzle configuration employed, without changing the primary support structure. The spectroradiometer was located outside the capsule parallel to the normal to the scanning mechanism inclination and in line with the

capsule penetration. This orientation permitted transmission of the tungsten filament emission to the spectroradiometer through a minimum of mirror paths.

Testing during Phase IV was limited to the 61.0-cm (24-inch) -nominal-diameter plume; therefore, only that structure was installed for the tests. Successful engine operation was achieved on two hyperflows (altitude simulation test series) conducted on 3 November 1971 (three and eight hot-firing tests on hyperflows 2 and 3, respectively). Optical data were recorded on the first hot-firing test of each hyperflow. Deposits on the mirrors after engine cutoff and prior to the second run precluded data acquisition after the first test.

The optical data obtained were time reduced. Inspection of the oscillogram revealed that the quality and quantity of the data were insufficient for further meaningful data reduction. Diffuser blowback and a sustained period of relatively high emission saturated the output signal for a large portion of the valid run duration.

An effort was made during Phase IV to improve the data reduction procedure, which was directed primarily toward determining better values of the absorption coefficients for water vapor. Information was gathered from the literature; however, the low level of effort allocated to this task did not permit the generation of working curves and data interpolations. A simplified computer program for rapid data reduction was prepared; however, it required some empirical formulation of the absorption coefficient and was not completed during this phase.

APPARATUS AND FACILITY

SPECTRORADIOMETER SYSTEM

The major components of the DCS system were identical to those previously employed and are shown schematically in Fig. 10. The location of the optical components of the system, with respect to the cell 29 test chamber, is shown schematically in Fig. 22. Figure 23 shows an overall view of the DCS system installation at the facility. Figure 24 depicts the absorption source mounting structure. A side view

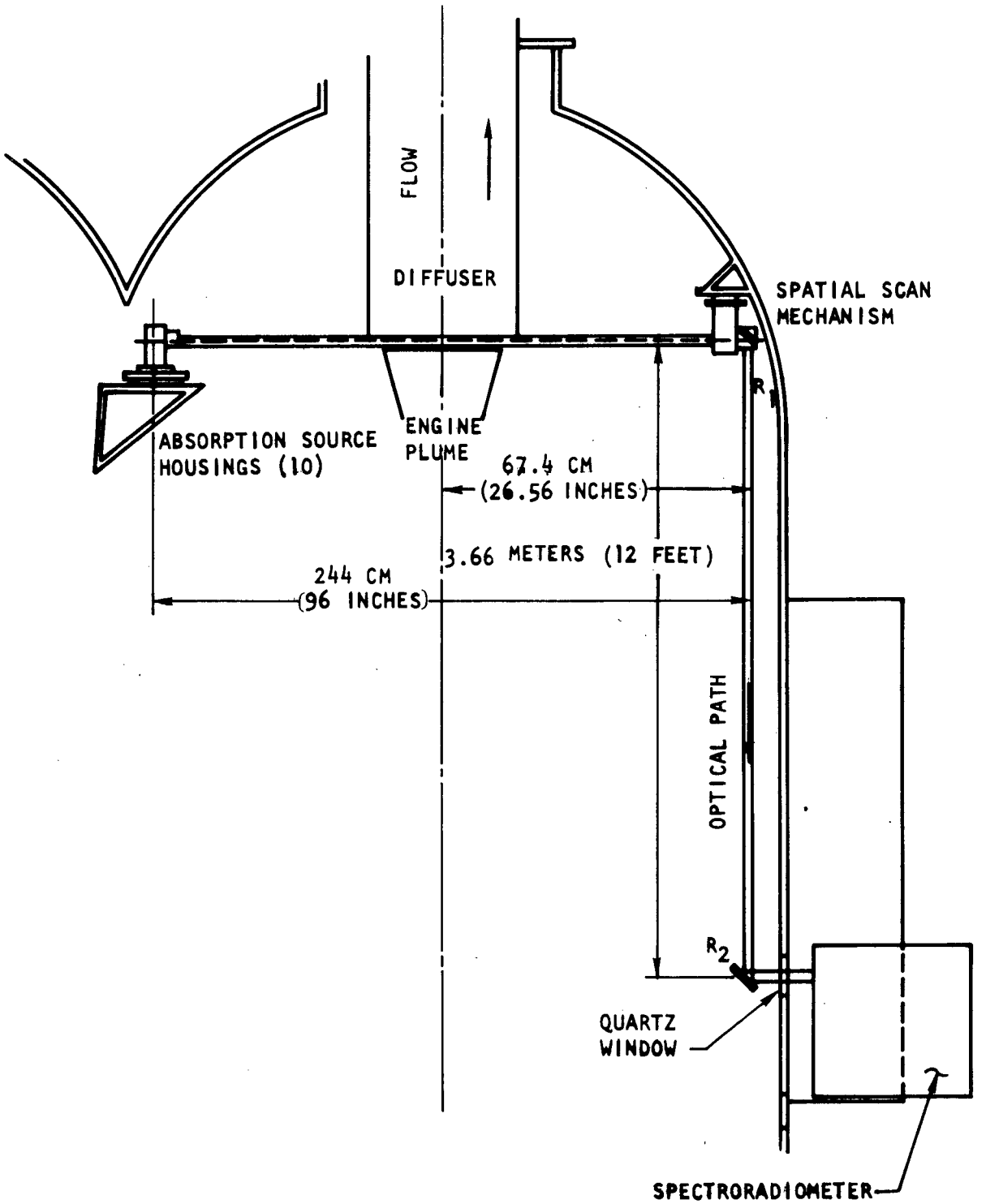

Figure 22. Location of Major System Optical Components With Respect to the Cell 29 Test Chamber

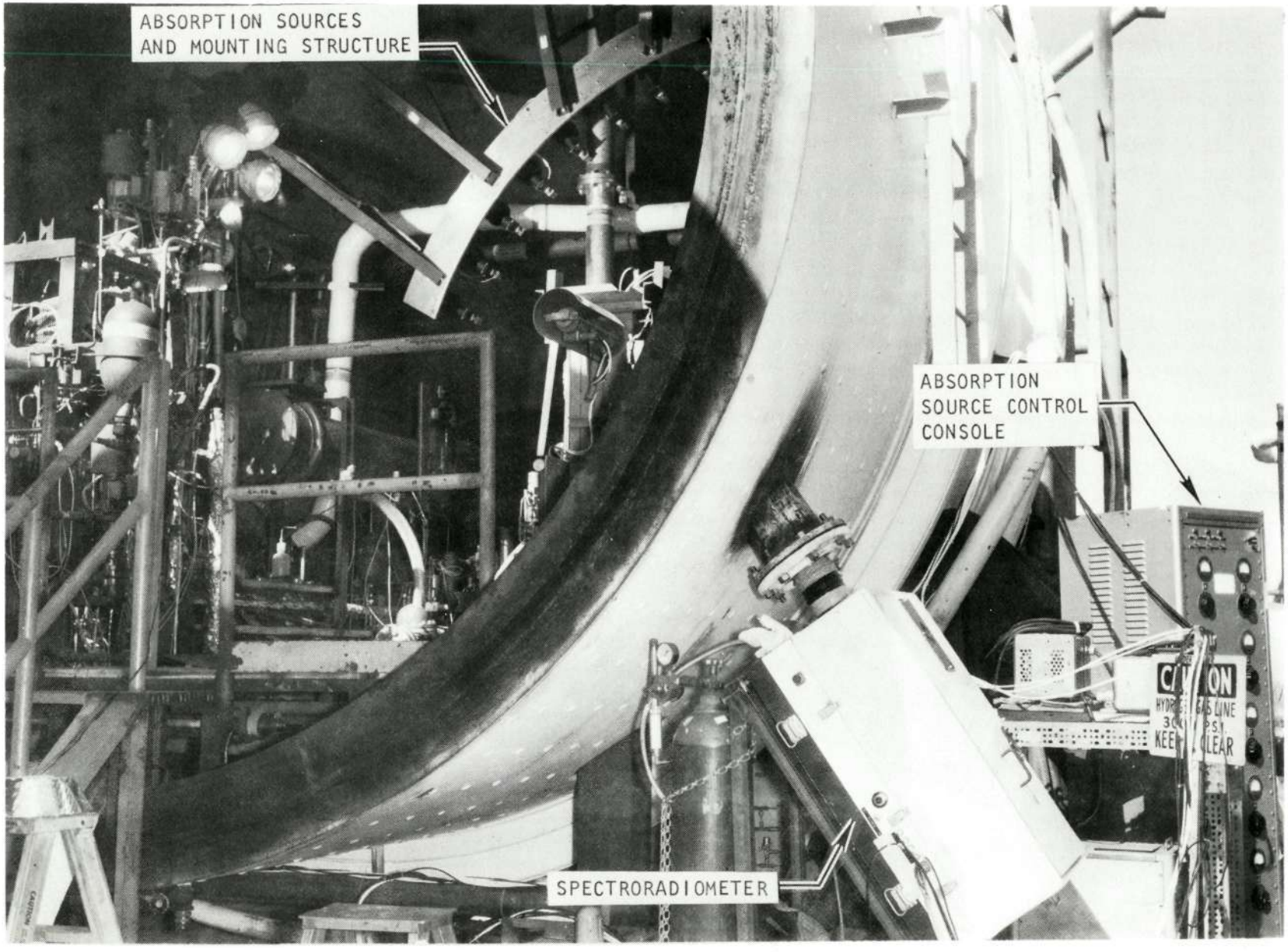

1XX13-10/29/71-S1A

Figure 23. DCS System Installation

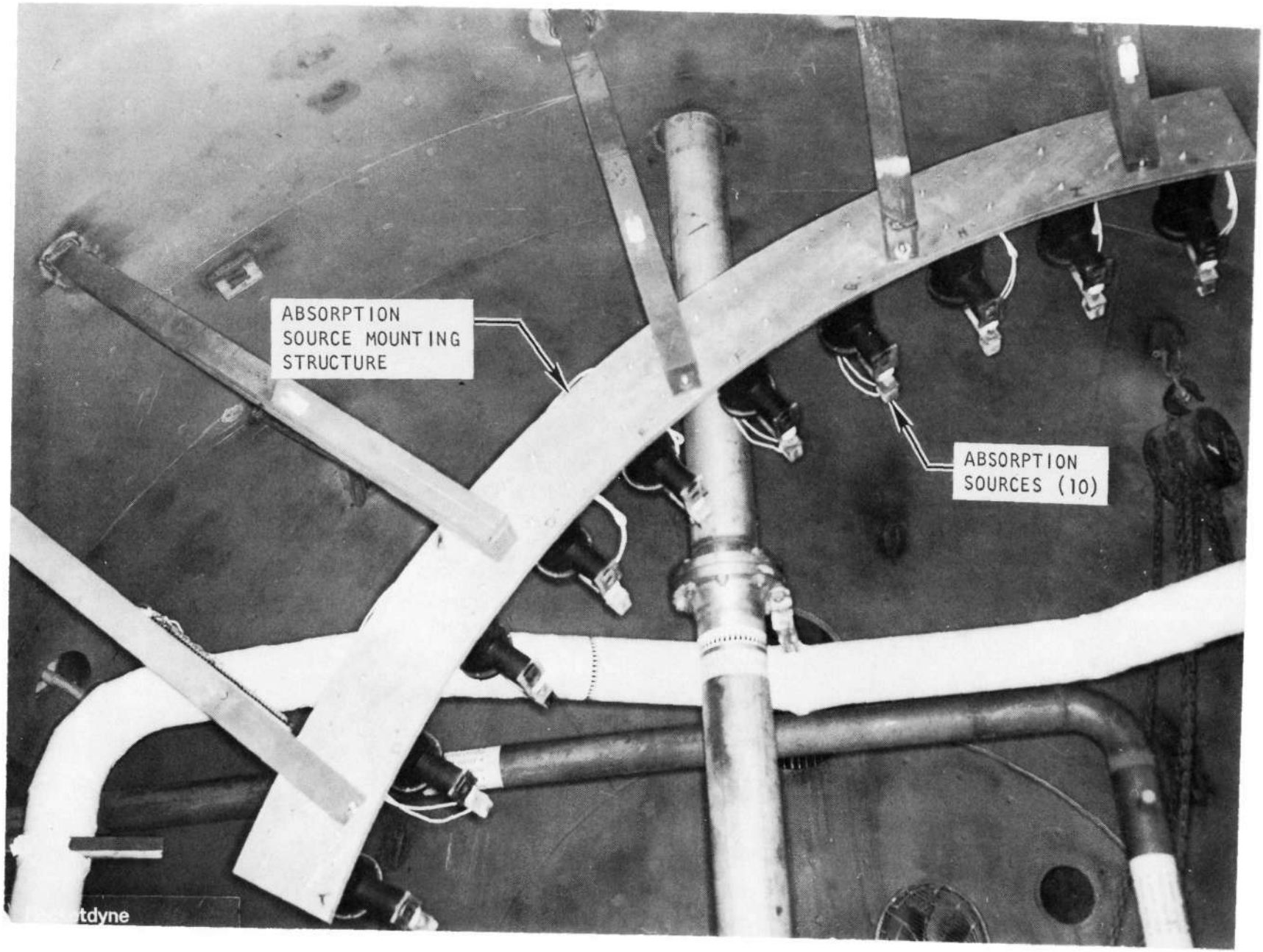

1XX13-10/29/71-S1C

Figure 24. Absorption Source Mounting Structure

of the engine assembly, which also includes the scanning mechanism, is shown in Fig. 25. A view of the engine assembly, which also includes the receiver mirror, is presented in Fig. 26. The external radiometer installation is shown in Fig. 27. Also shown are the spectroradiometer and the absorption source and spatial scanning mechanism control console. The control console contains individual intensity controls for the 10 tungsten lamp absorption sources, the scan mirror drive switch, and switches for the absorption source shutters and the scan mirror shutter. These shutters were operated manually from the control center in sequence with the test firing.

The 10 absorption sources were mounted on an aluminum plate which, in turn, was bolted to steel channel stringers. The stringers were welded to the test cell wall. The spatial scan mechanism was similarily mounted. This bolting arrangement permited precise alignment of the sources and scan mechanism with respect to the rocket nozzle exit plane. Individually adjustable flat relay mirrors R_1 and R_2 (Fig. 22) direct radiation from the spatial scan mechanism to the spectroradiometer.

The spectroradiometer was secured to a rigid platform at the side of the test cell. The absorption source and scan mirror control console and the power supply for the blackbody calibration source were located alongside the spectroradiometer. Figure 3 is a schematic of the spectroradiometer, and Fig. 15 and 16 show the instrument with the cover removed.

The individual components referred to in the previous photographs were described in detail in the Phase I section, and modifications to the scanning mechanism were described in the Phase II section. The DCS system utilized in the Phase IV tests was as described previously and in Ref. 1 and 2.

ROCKET ENGINE AND ALTITUDE FACILITY

The rocket engine and associated hardware are described in Ref. 11 and are, therefore, discussed only briefly here. The engine, with a 0.262-radian (15-degree) conical nozzle, is shown in Fig. 25 and 26. This nozzle provided an expansion ratio of 25:1 and had an exit diameter of 60.7 cm (23.911 inches). The engine was

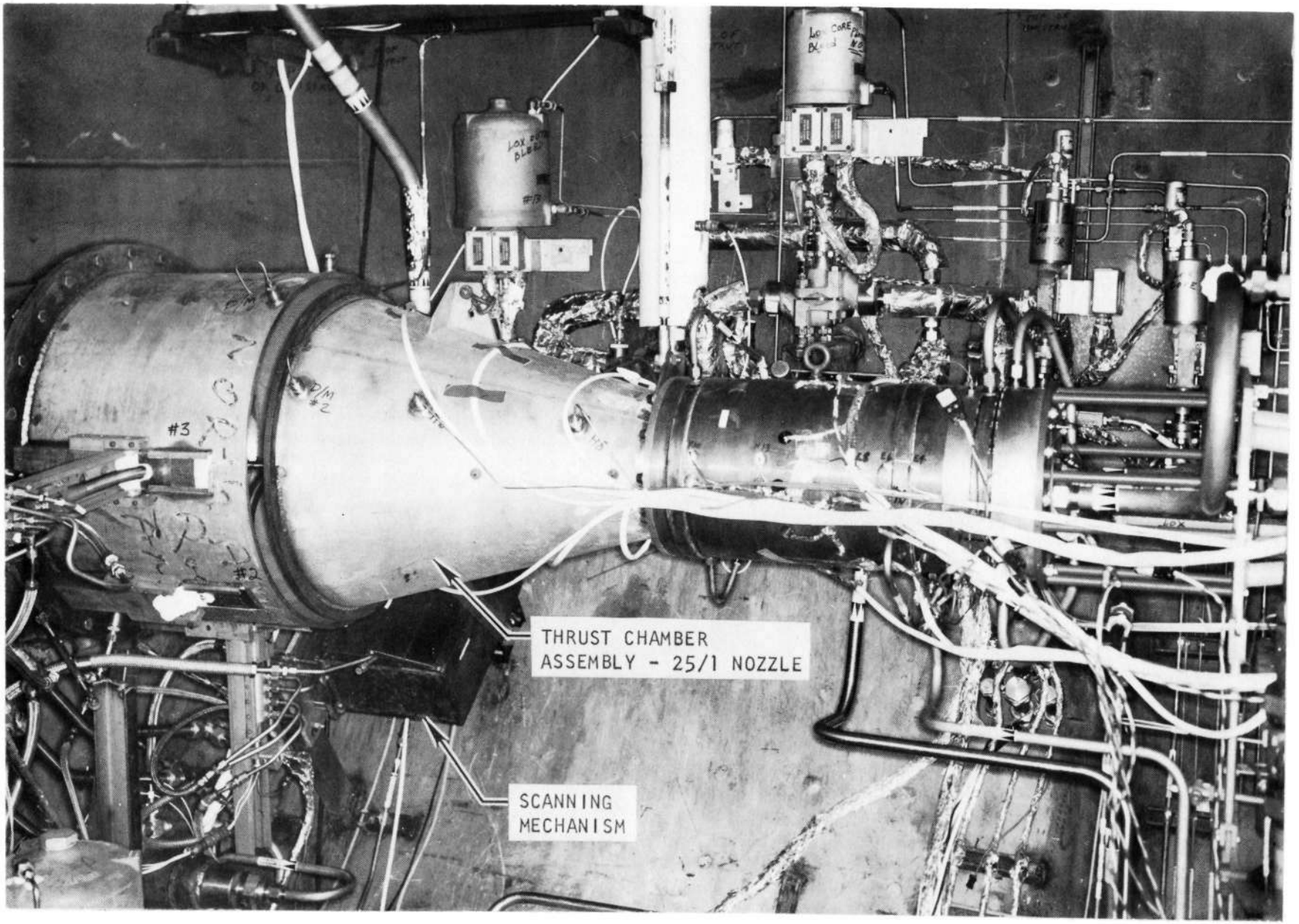

1XX13-10/29/71-S1D

Figure 25. View of Engine Showing Scanning Mechanism

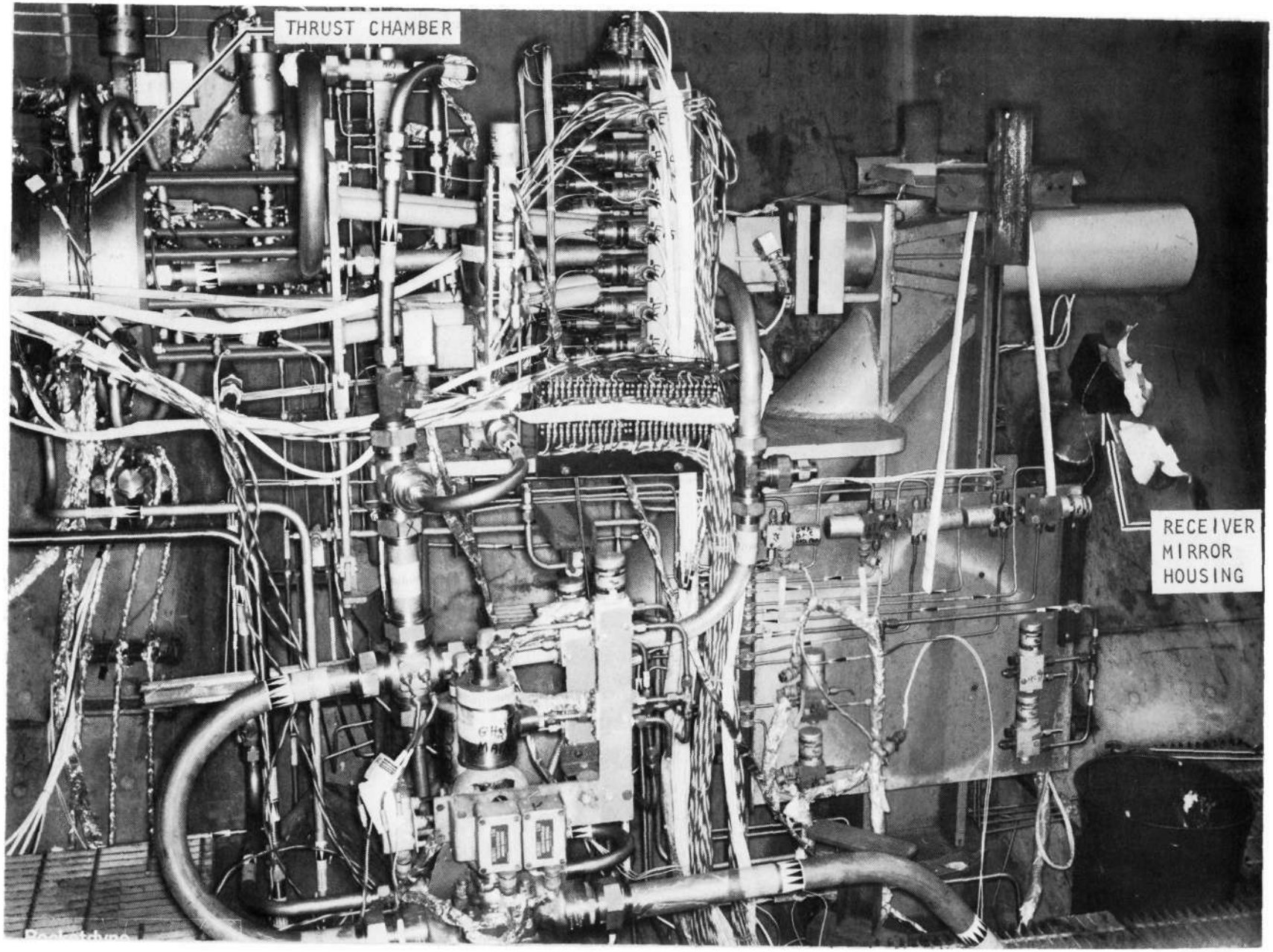

1XX13-10/29/71-S1E

Figure 26. View of Engine Showing Receiver Mirror Housing

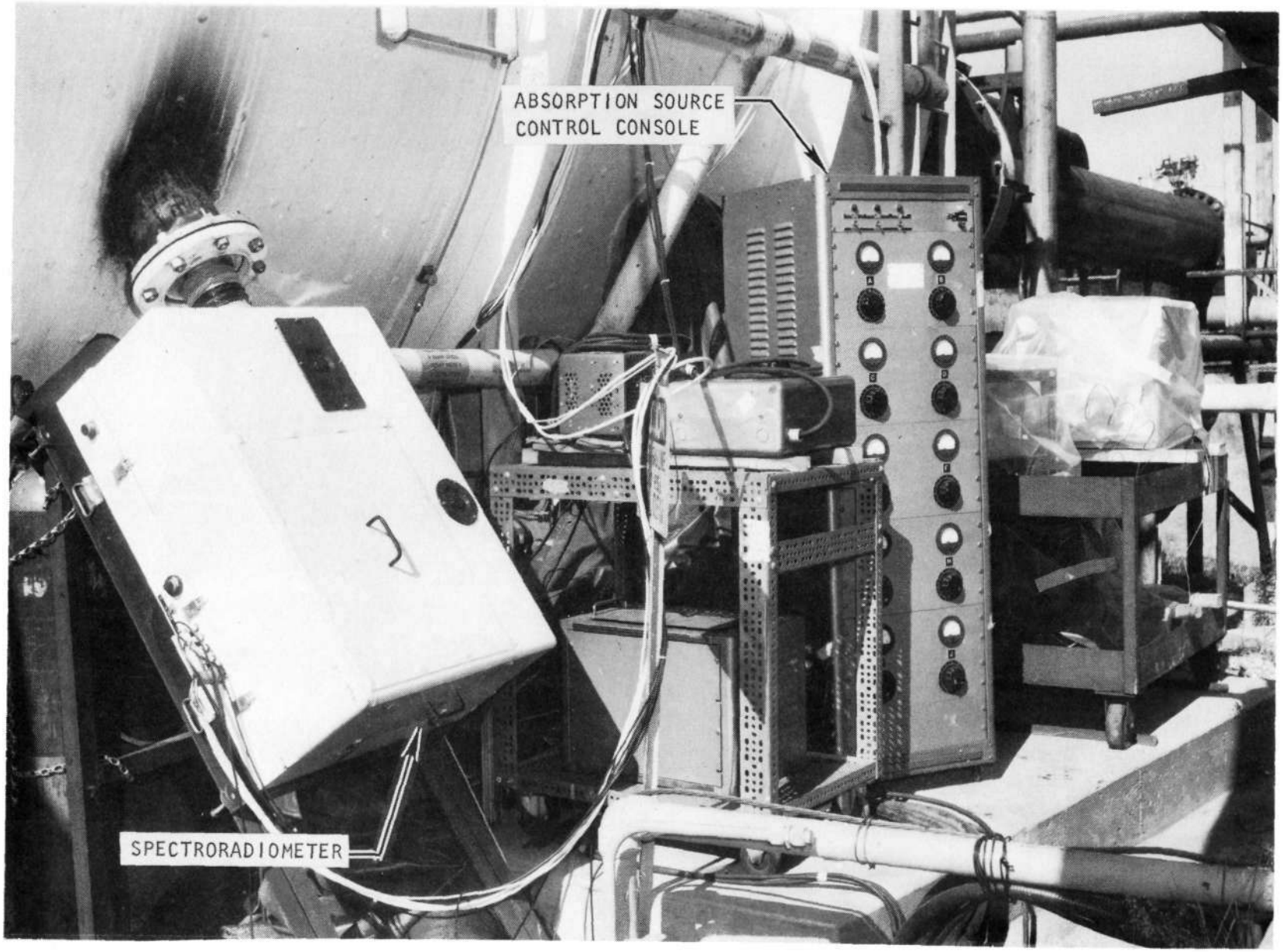

1XX13-10/29/71-S1B

Figure 27. External Radiometer Installation

operated at a nominal chamber pressure of 1.72×10^6 newton/m^2 (250 psi) and developed a nominal 35,550 newtons (8000 pounds) of thrust.

The altitude simulation system maintained an altitude in excess of 22,800 meters (75,000 feet) for 800 seconds, the maximum duration of any hyperflow. During this period, a series of individual engine firings was made at various mixture ratios and film-cooling conditions. Hot-fire run durations were on the order of 2 seconds with approximately 120 seconds between successive tests.

RESULTS AND DISCUSSION

DATA COLLECTION

The absorption sources were set to the desired intensity and allowed to stabilize for 3600 seconds before a test series, and the spatial scan mirror was activated and instrument controls were set at desired values. For a period from approximately 5 seconds before startup to cutoff, the absorption source and scan mirror shutters were opened and the tape recorder activated. The emission from the absorption sources was scanned and recorded continuously at 2.5×10^{-6} meter (2.5 micron) throughout this interval. The attenuated emission from the sources and exhaust emission were scanned (spatially) as described in Phase I.

Wavelength calibration was obtained by recording the absorption spectra of atmospheric water vapor. The emission from the absorption source lamps, which was recorded between individual tests of a series, served as the background measurement for absorption determination. The absorption sources were also used for intensity calibration, with each tungsten lamp having been calibrated with an optical pyrometer.

Hyperflow No. 2, Test Series 542 to 544 (3 November 1971)

Three hot-firing tests were conducted during this hyperflow. Optical data were obtained for the first test firing; however, no detectable background signal was

observed after engine cutoff; therefore, no meaningful data were acquired for tests 543 and 544. Posttest inspection of the mirrors inside the vacuum chamber showed them to be covered with condensed water vapor. A check of mirror alignment after the mirrors were cleaned and dried indicated that no misalignment from engine vibrations had occurred. The loss of background signal was attributable to mirror contamination. Therefore, a gaseous nitrogen purge was directed toward the mirrors in an attempt to keep the mirrors dry, or at least dry them off between tests.

Hyperflow No. 3, Test Series 545 to 552
(3 November 1971)

Eight hot-firing tests were conducted during this hyperflow. Optical data were obtained only for the first test firing. Posttest inspection of the mirrors did not indicate the presence of any condensed water vapor but a new contamination problem. A white deposit was observed on a number of the mirrors. The apparent source of this deposit was attributed to outgassing from insulation and tape used on various components in the engine assembly. The heaviest deposits were observed near the gaseous nitrogen purge which probably assisted, by recirculation, the observed contamination. A check could not be made of the mirror alignment due to difficulties experienced in cleaning the contaminated mirrors.

DATA REDUCTION

The output signal, recorded on magnetic tape for the two runs where optical data were obtained, was time reduced and transferred to an oscillogram prior to calculating plume temperature and water vapor partial pressure. Inspection of the oscillogram revealed that the quality and quantity of the data were insufficient for further meaningful data reduction. Diffuser blowback during the ignition and initial mainstage interval reduced the time available for optical data acquisition to slightly greater than 1 second. This meaningful portion of the run was further reduced by approximately 500 milliseconds by a period of relatively high emission that initially saturated the output signal. The available run time remaining was

insufficient for one complete scan. In addition, the data obtained during this interval portrayed some anomalous behavior indicative of a large quantity of scattered background radiation or the onset of mirror contamination. Although the data cannot be utilized for the calculation of plume properties, it was helpful for directing redesign efforts and component modification for Phase V.

PHASE V

SYNOPSIS

Phase V, conducted from January 1972 to February 1973, was directed toward further monitoring of the exhaust plumes from the H_2/O_2 rocket engine being tested under Contract NASw-2106, and possible improvements to the data reduction procedures.

The DCS system utilized during Phase IV was improved somewhat. Improvements included: (1) addition of a GN_2-filled light guide between the scanning mechanism and collector mirror; and (2) reworking the scanning mechanism assembly to increase the scanning rate, seal the assembly against leakage, improve the scanning wheel code, and reduce the mirror size. The installation of the DCS system was substantially equivalent to that used during Phase IV, with the exception of the light guide and relocation of the absorption source and scanning mechanism for the 4:1 nozzle tests. Gross alignment of the DCS system was successfully accomplished; however, variations in the alignment for each line of sight (measured by variations in recorded intensity for a constant input intensity) could not be eliminated entirely. Therefore, a compromise alignment, which minimized the alignment variations, was utilized for the measurements.

All of the test firings conducted at the CTL-4, cell 29, test site under Contract NASw-2106 were monitored. Eight 25:1 expansion ratio nozzle tests were made at a simulated altitude of approximately 23,000 meters (75,000 feet) on 18 August 1972. Emission and absorption data were obtained from the initial hot firing during hyperflow operation. However, a hard shutdown occurred at the end of the first test, which destroyed the alignment of the relay and collector mirrors and precluded useful measurements for the remaining seven tests. Eight 4:1 expansion ratio nozzle tests were made at sea level conditions on 8 September 1972. Emission and absorption data were recorded successfully on seven of the eight tests. The data obtained from four of the seven tests were of sufficient quality to permit analysis.

Hard starts, which induced some misalignment of the optical system, were experienced on all of the sea level tests. However, periodic realignment after one to two tests allowed a strong signal to be obtained for four of the tests. Apparent movement of the spectrometer toward the end of the test series reduced signal strength to an insufficient level for meaningful data reduction. No data were obtained from the first test because the scanning mechanism relay was jarred loose during the start transient.

The effort directed toward improving data reduction procedures was primarily concerned with obtaining "better" values for the absorption coefficients, refinements to the computer program in the areas of the line-of-sight determinations, and improvements in the method of utilizing the calibration data.

Time-reduced oscillograms were made from the data. These records were read manually and converted to the form needed in the data reduction computer program. In many cases, the signal strength was greater than anticipated, resulting in saturation (overranging) of the tape record. Saturation of the spectroradiometer electronics did not occur.

When the data were analyzed to calculate the plume properties, physically unrealistic results were obtained and the results were found to be very sensitive to the smoothness of the input data. This observed sensitivity led to a review of the data obtained and the calculation procedure. It was determined that the uncertainty in the data was not within the limit required by the data reduction scheme, which precluded valid data interpretation.

MEASUREMENTS

DCS SYSTEM

The DCS system utilized for the Phase V efforts was virtually identical to that of the Phase IV program. The basic system is described in earlier sections of this report; therefore, only modifications to the system will be described in this section.

Only minor modifications were made to the DCS system for this phase. These were: (1) a GN_2-filled 10.18-cm (4-inch)-ID tubular light guide between the scanning mechanism and collector mirror, Fig. 28 and 29; and (2) reworking the scanning mechanism assembly to increase the scanning rate to approximately 2 scans/second, seal the assembly against leakage, improve the scanning wheel code, and reduce the mirror size. Housing the majority of the optical components in a positively pressurized 6.89×10^2 newton/m^2 (0.1 psig) inert atmosphere to ensure that an optimum environment existed for the relatively long path from the scanning mechanism to the spectrometer precluded the entry of stray absorbing gases in the optical path, and circumvented deposition and condensation on the mirrors. The scanning apparatus was sealed by replacing the shutter with an aluminum plate which housed a quartz (optical quality) window and sealing all joints with cork gaskets. The windowed adapter plate is shown in Fig. 30.

The higher scanning rate increased the number of scans obtained during the approximately 3-second run durations (increased by 1 second for the Phase V tests) and was within the response rate of the DCS system electronics. The improved scanning wheel code greatly facilitated line-of-sight data interpretation by positively identifying the scanning mirror location on the tape record. The reduced scanning mirror size decreased the possibility of stray radiation entering the optical path. The allowable size reduction was determined by masking the surface until the recorded intensity of the transmitted light source was affected.

The installation description given in Phase IV is directly applicable for the 25:1 nozzle tests with the addition of the light guide described above. For the 4:1

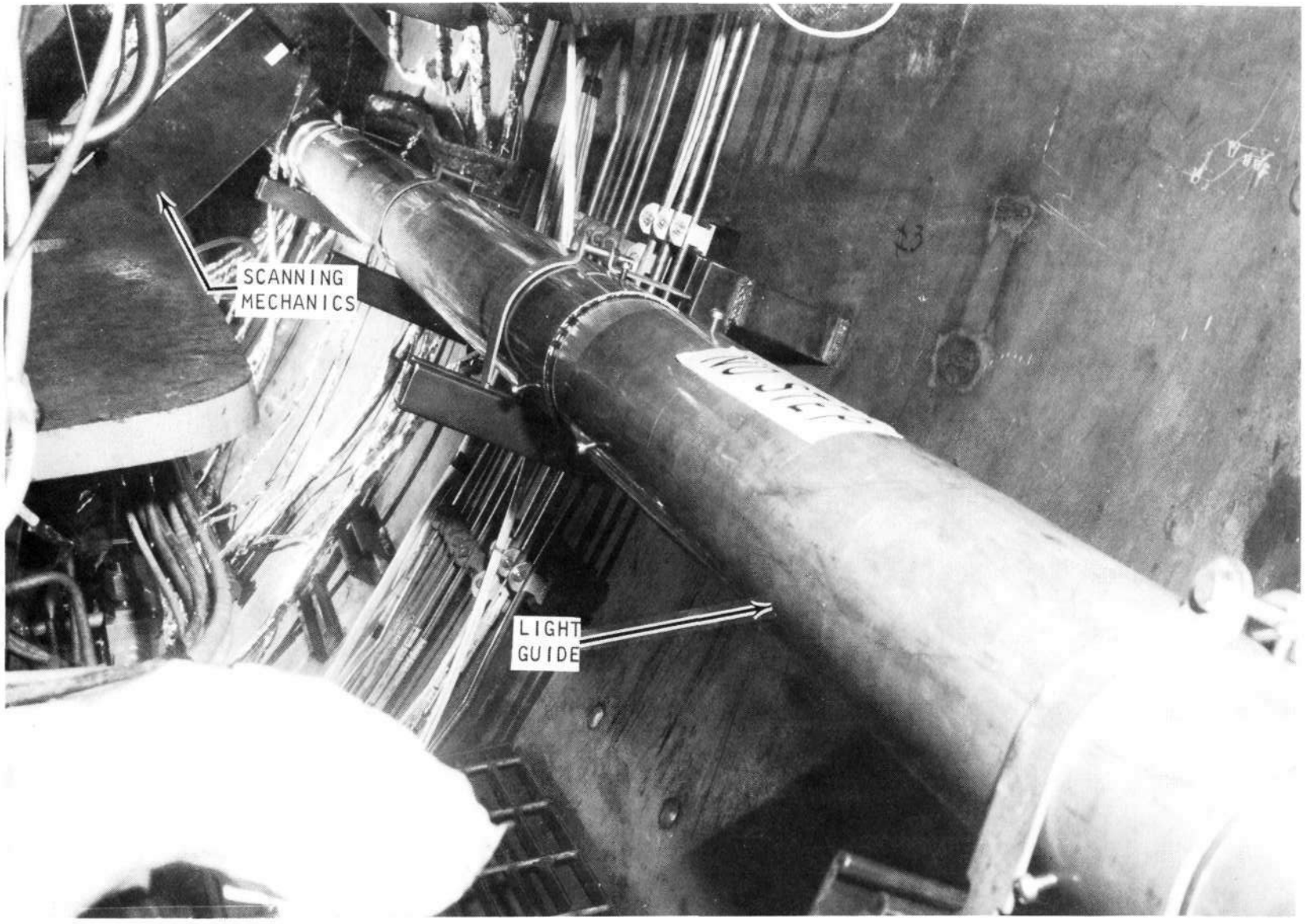

5AH24-8/18/72-S1D

Figure 28. Light Guide

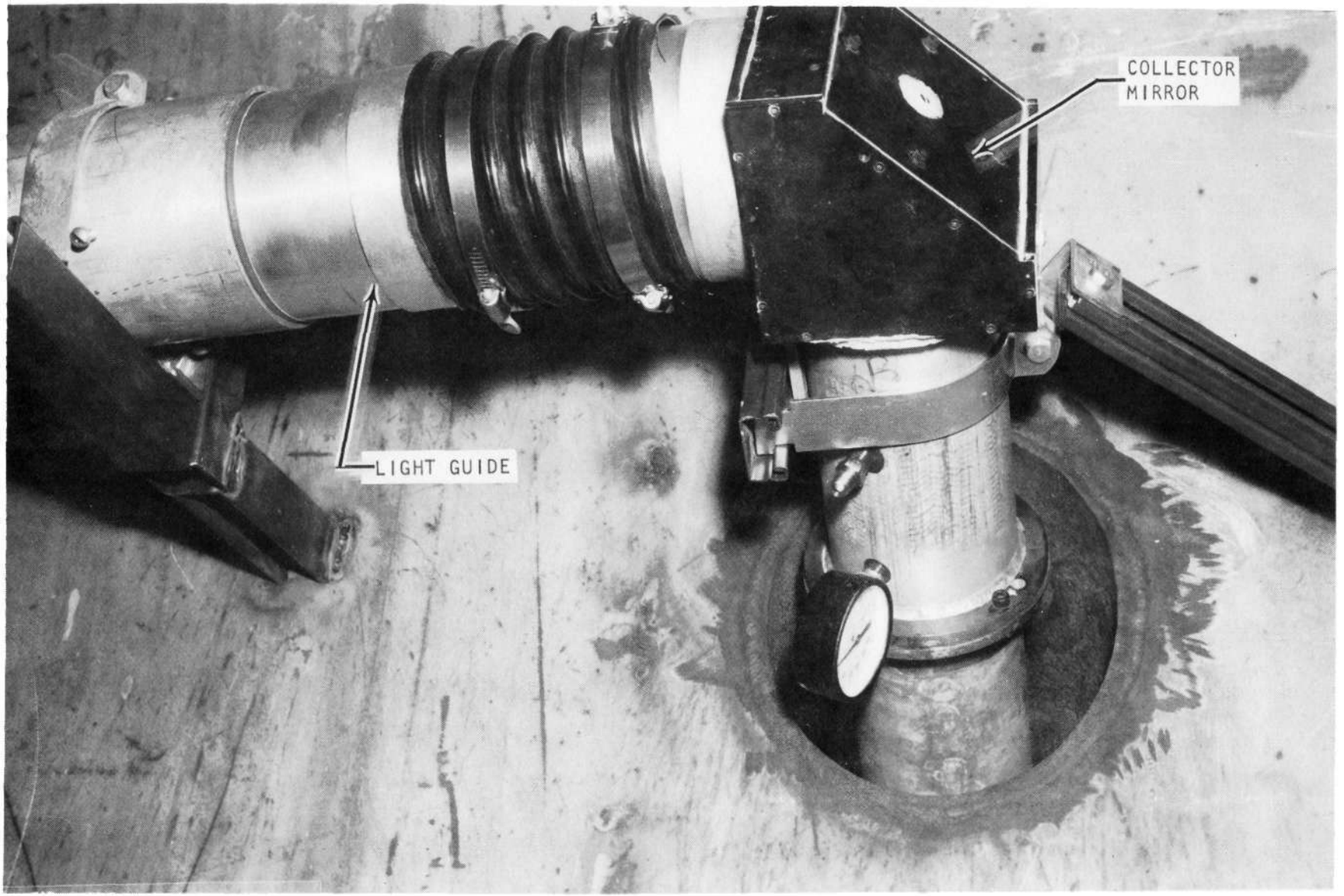

5AH24-8/18/72-S1A

Figure 29. Light Guide Connected to Collector Mirror

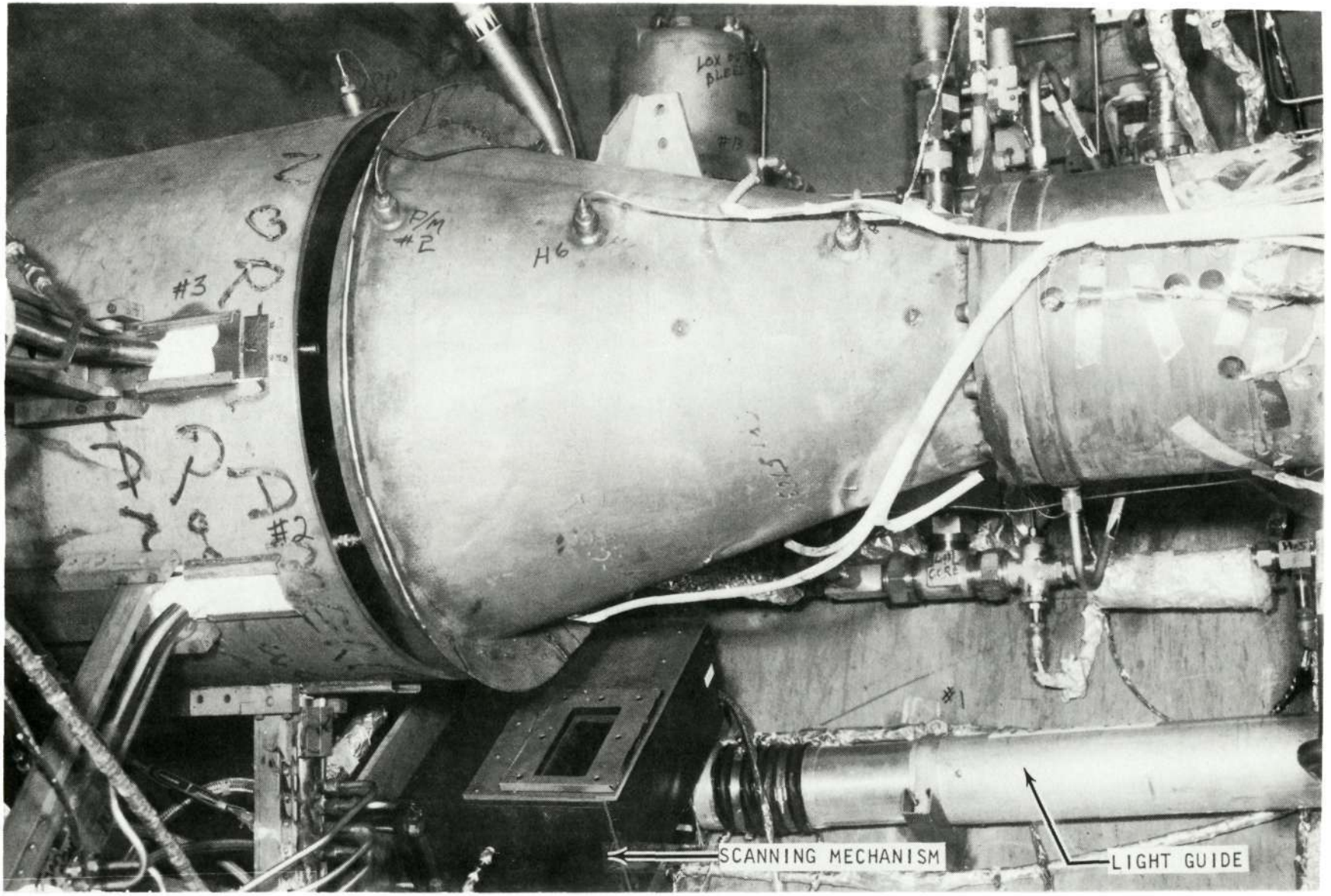

5AH24-8/18/72-S1C

Figure 30. Windowed Adapter Plate

nozzle tests, the absorption sources and the scanning mechanism were relocated to accommodate the shorter nozzle and its smaller exhaust diameter. A new scanning mechanism mounting bracket was welded to the test cell wall to permit an identical installation to that utilized for the 25:1 nozzle tests, but in a plane parallel and approximately 61.0 cm (24 inches) closer to the nozzle throat plane. In Fig. 31, the scanning mechanism is shown in place for the tests.

The absorption source installation for the 4:1 nozzle tests is shown in Fig. 32. In this figure, the absorption sources are pointing in the direction of the thrust chamber; whereas, in the 25:1 installation, they pointed in the direction of the diffuser. To avoid overlapping, only seven light sources could be used in the 4:1 installation. The seven absorption sources were mounted on an aluminum plate which, in turn, was bolted to the opposite side of the steel channel stringers utilized for mounting the absorption source mounting plate for the 25:1 installation. This mounting arrangement provided the necessary translation required between the 25:1 and 4:1 installations.

Alignment of the DCS system was a tedious and arduous task. In all cases, gross alignment could be achieved only by performing all operations in darkness. This situation was further aggravated by the space limitations within the test module. For a given field installation, fitting the DCS system to the test cell invariably adds mirrors to the system, thereby complicating system alignment. Further, the placement of these mirrors cannot always be made readily accessible due to physical constraints of the test cell.

Gross alignment of the DCS system was successfully accomplished; however, variations in alignment for each line of sight could not be eliminated entirely. Variations in alignment were observed by monitoring the lamp intensity delivered to the spectrometer for the various lines of sight, with all lamps set to the same brightness temperature. Fine tuning of the alignment reduced the variations of intensity between different lines of sight, but all variations could not be eliminated. By elimination, the principal source of the variation appeared to be the scanning mirror itself. The observed behavior could be explained if the axis of rotation was actually on the shaft rather than on the mirror surface; or, if the shaft

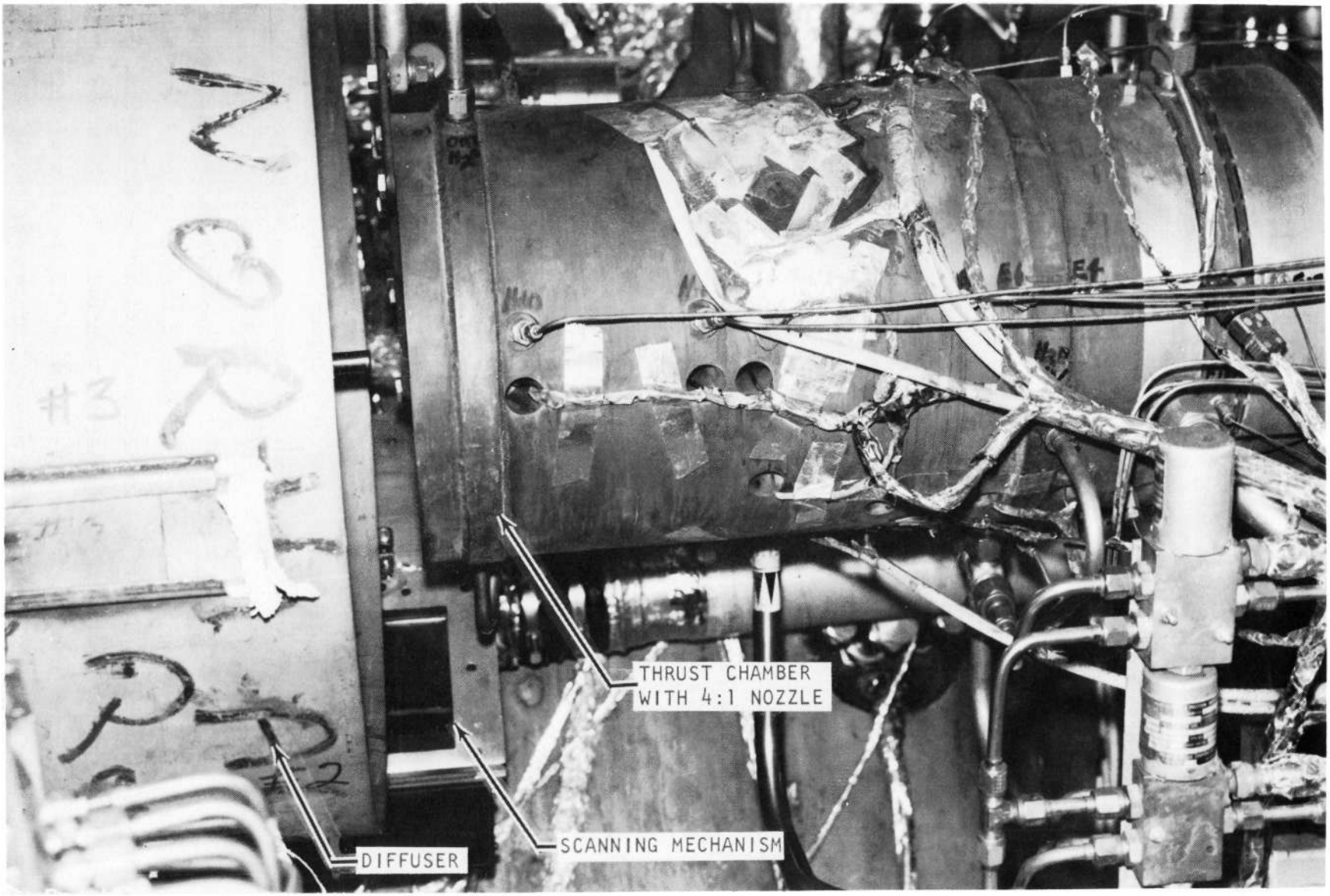

5AJ11-8/25/72-S1B

Figure 31. Scanning Mechanism Installed for 4:1 Nozzle Tests

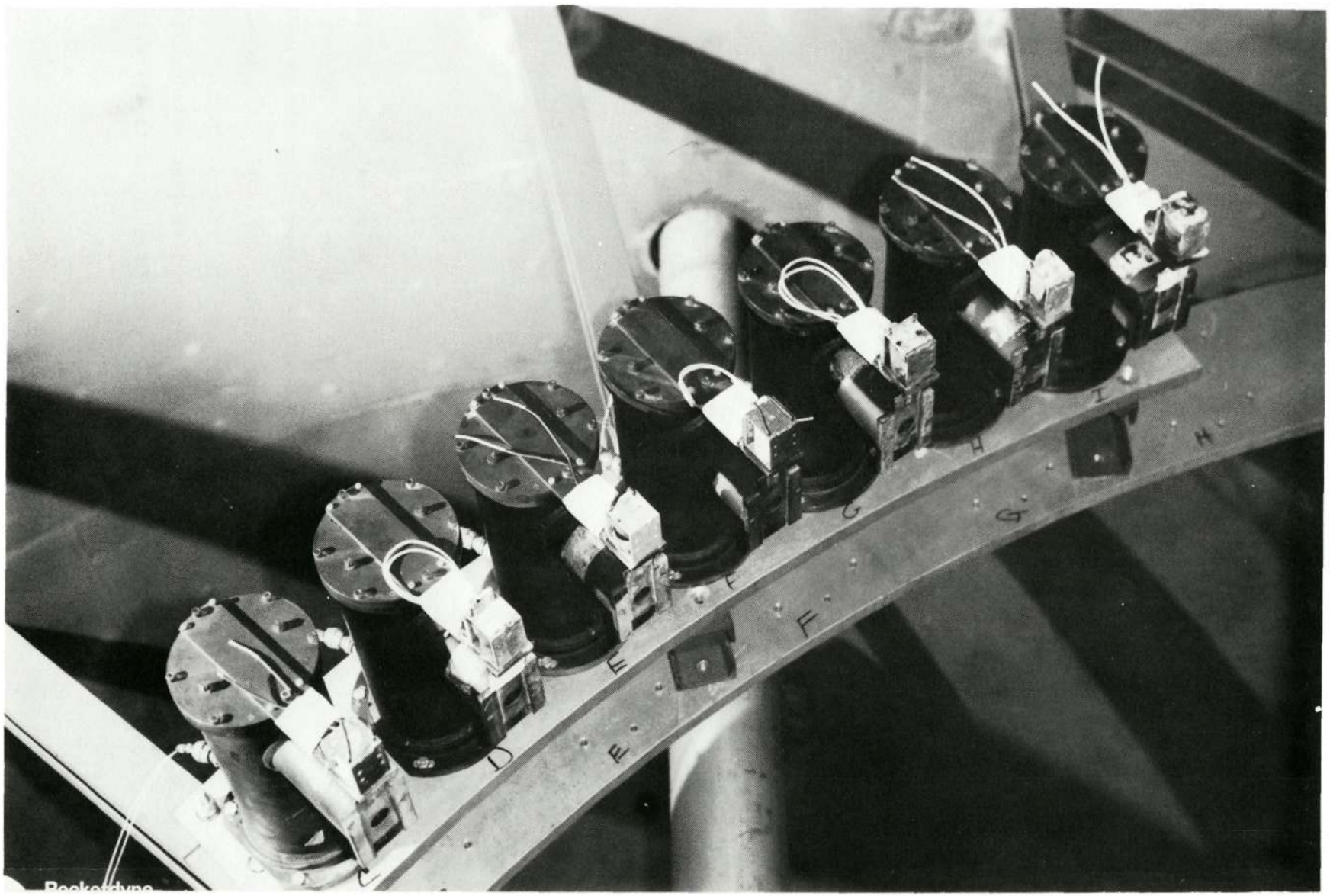

5AK11-8/25/72-S1A

Figure 32. Absorption Sources for 4:1 Nozzle Tests

rotation was eccentric. However, this was difficult to determine. A compromise alignment (the alignment that minimized the alignment variations) was utilized for test measurements.

DATA COLLECTION

All the test firings conducted under Contract NASw-2106 were monitored. The details of the test engine and associated hardware are described in Ref. 11 and are only outlined here. The engine had an 0.262-radian (15-degree) conical nozzle expansion terminating at an exit diameter of 24.35 cm (9.564 inches) and a 4:1 expansion ratio. A conical nozzle skirt attachment, exit diameter 60.7 cm (23.911 inches), was added for tests at an expansion ratio of 25:1. The engine was operated at a nominal chamber pressure of 1.72×10^6 newton/m^2 (250 psi), and developed a nominal 35,550 newtons (8000 pounds) of thrust.

Altitude simulation in excess of 23,000 meters (75,000 feet) was provided by a diffuser and ejector system (hyperflow), which could be operated for up to 3000 seconds. During this period of operation, a series of individual engine firings at various mixture ratios and film-cooling conditions was made. Hot-fire run durations were on the order of 3 seconds, with approximately 300 seconds between tests. For sea level tests (4:1 nozzle), the hyperflow system was not utilized and the engine products were exhausted through the diffuser.

Test Series 238-245, 25:1 Expansion Ratio Nozzle

These tests were made on 18 August 1972. Emission and absorption data were obtained for the initial hot firing during hyperflow operation. However, a hard shutdown occurred at the end of the first test, which destroyed the alignment of the relay and collector mirrors and precluded the recording of useful data during the remaining seven tests. Review of the motion picture records of the test firings indicated that the initial 35 percent of the test duration was required to reach steady state; therefore, only optical data recorded after that time were used for data interpretation and analysis.

Test Series 246-253, 4:1 Expansion Ratio Nozzle

These tests were made on 8 September 1972. Eight tests were made at sea level exhaust conditions. Emission and absorption data were recorded successfully on seven of the eight tests. However, the data obtained from only four of the seven tests were of sufficient intensity for data reduction purposes.

Hard starts occurred on all of the sea level tests, which degraded the alignment of the optical system. However, periodic realignment after one or two tests enabled acquisition of a strong signal for four of the tests. Apparent movement of the spectrometer toward the end of the test series reduced signal strength to inadequate levels. Data from the first test were lost because the scanning mechanism relay was jarred loose during the start transient.

Review of the motion picture records for these firings indicated that less run time was required to complete engine/facility startup transients and reach steady state. For these tests, the last 80 percent of the test firing was available for data interpretation purposes.

Data Acquisition

Wavelength calibration was verified by recording the absorption spectra of atmospheric water vapor. No calibration shift was noted and the grating was fixed in position corresponding to a wavelength of 2.5×10^{-6} meter (2.5 microns).

Intensity calibrations were obtained by recording the emission from the absorption source lamps at three lamp currents (0.7, 0.8, and 0.9 amperes) several thousand seconds prior to each test series. The three lamp currents corresponded to those used for optical pyrometer calibrations.

Operation of the DCS system was identical for both series of tests. Instrument controls were set to the desired values, and the absorption sources (shutters fixed in an open position) were set to the desired intensity and allowed to stabilize for approximately 3600 seconds before a test series and, subsequently, the spatial

scan mirror was activated. For a period from approximately 10 seconds before startup to 5 seconds after cutoff, the tape recorder was activated and data were recorded continuously at 2.5×10^{-6} meter (2.5 microns) throughout this interval at output signal amplifications of 1:1, 5:1, and 10:1. The attenuated emission from the sources and exhaust emission were scanned (spatially) as described in previous sections. The slit width and lamp current for the 25:1 nozzle tests were 1×10^{-4} meter (100 microns) and 0.9 ampere, respectively; whereas, for the 4:1 nozzle tests, the corresponding values were 1.3×10^{-4} meter (130 microns) and 0.098 ampere.

The emission from the absorption source lamps, which was recorded immediately prior to individual tests of a series, served as the background measurement for absorption determinations. Also, variations in the background intensity level, prerun and postrun in addition to run-to-run, served as a measure of alignment shifts.

DATA ANALYSIS

The Phase V data analysis was divided into three tasks: improvements, data reduction, and correlation.

IMPROVEMENTS

Improvements in the data reduction procedures were directly primarily toward: (1) obtaining "better" values for the absorption coefficients, (2) refinements to the data analysis computer program in the areas of line-of-sight determinations, and (3) improvements in the method of utilizing the calibration data.

An empirical, rather than statistical, approach was selected as the technique for improved absorption coefficient determinations. Copies of NASA computer data tapes of water vapor absorption data were obtained and listed; however, the data on a number of the tapes were found to be incomplete due to truncation of the duplicated data tables. The truncation resulted in reducing the applicable water vapor absorption data by approximately 65 percent and was discovered too late to request complete copies. Therefore, significantly less water vapor absorption data were

available for "improved" absorption coefficient determinations. Since the limited data severely compromised determination of an empirical absorption coefficient, this effort was suspended pending the outcome of subsequent data analysis. For calculation purposes, the absorption coefficient data were taken from Ref. 10.

Refinements in the computer program were directed toward generalizing the line-of-sight determinations and improving the method of utilizing the calibration data.

The original computer program was written for a fixed-geometry plume, a prescribed number of absorption sources, and a single absorption source calibration curve. Because two different nozzle plumes were monitored during Phase V, and because on-site DCS system calibrations yielded different calibration curves for each line-of-sight, the computer program was revised to handle the more complicated system. A generalized line-of-sight determination section was added, which calculated the path length for equalled space absorption sources as functions of the number of sources and the plume diameter. (Equal spacing of the absorption sources was designed into the facility installation.) Additionally, the calculational procedure was modified to permit incorporation of intensity calibration curves for each line of sight.

The computer programs utilized for calculation of plume properties for the 25:1 and 4:1 nozzles are given in Tables 2 and 3, respectively. Except for physical and intensity calibration differences between the 25:1 and 4:1 installations, the codes are basically the same. A slightly different method of calculating plume radiance was used for the 25:1 data, but it did not significantly alter the calculated plume properties. In general, the computer program comprises data input, radial position calculations, calculation of the PK product, local radiance calculations, a subroutine that contains the required calibration and physical data, and, finally, partial pressure and temperature calculations.

TABLE 2. COMPUTER CODE ZRRED

```
50C
60C      PRØGRAM "ZRRED"
70C
100      DIMENSIØN RAD(5),RS(5),Y(5,5),T(5),TO(5),TT(5),
101&               PK(5),PR(5),R(5),P(5)
118C
119C    INPUT I0
120C
125      DATA TO/1.4,1.4,1.4,1.4,1.4/
126C
127C    INPUT INTENSITY DATA
128C
129      DATA TT/4.01,4.11,4.81,5.91,9.31/
130C
131C    INPUT EMMISSIØN DATA
132C
135      DATA PR/2.7,2.8,3.5,4.6,8./
140C
141C     INPUT NØ ØF DATA PØINTS
142      N=5
143C
144C     INPUT PLUME DIAMETER
145      PD=25.991
146C
150 2    FØRMAT(3E18.9)
160 3    FØRMAT(I3,5F10.3)
170 4    FØRMAT(2X,"I",7X,"R",9X,"N",9X,"PK",8X,"T",9X,"P",/)
200C
210      DØ5I=1,N
220 5    T(I)=(TT(I)-PR(I))/TO(I)
230C
300C    CØMPUTE RADIAL PØSITIØNS
310C
315      DØ10I=1,N
320      X=(31.1667-I*5.6667)*3.1416/180.
325      RAD(I)=26.56*SIN(X)
330      RS(I)=RAD(I)*RAD(I)
335 10   CØNTINUE
340      RØS=PD*PD/4.
345      DØ20L=1,N
350      J=N-L+1
355      DØ30K=1,N
360      I=N-K+1
365      IF(I.GT.J) GØ TØ 30
370      IF(I-1.NE.0) XI=RS(I-1)
375      IF(I-1.EQ.0) XI=RØS
380      Y(I,J)=SQRT(XI-RS(J))
385      MM=I+1
386      JJ=J+1
390      DØ15M=MM,JJ
395      IF(M.GT.J) GØ TØ 15
400      Y(I,J)=Y(I,J)-Y(M,J)
```

TABLE 2. (Continued)

```
405 15   CONTINUE
410 30   CONTINUE
412      IF(I.EQ.J) Y(I,J)=2.*Y(I,J)
415 20   CONTINUE
420C
425C    COMPUTE PK PRODUCT
430C
435      DO 100 I=1,N
440      X=-ALOG(T(I))
445      K=I-1
450      DO200J=1,K
455      IF(I.EQ.1) GO TO 200
460      X=X+2.*PK(J)*Y(J,I)
465 200  CONTINUE
470      PK(I)=X/Y(I,I)
480 100  CONTINUE
485      PRINT4
490C
495C    COMPUTE LOCAL RADIANCE
500C
505      DO300I=1,N
510      ANUM=0.
515      X=ALOG(T(I))
520      K=2*I-1
525      DO400M=1,K
530      IF(M.EQ.I) GO TO 350
535      IF(M.LT.I) J=M
540      IF(M.GT.I) J=K-M+1
545      ANUM=ANUM+R(J)*((EXP(PK(I)*Y(J,I))-1.)/PK(I))*EXP(X)
550      X=X+PK(J)*Y(J,I)
555 350  IF(M.EQ.I) X=X+PK(I)*Y(I,I)
560 400  CONTINUE
565      X=0.
566      LL=I
570      DO500M=1,LL
575      X=X-PK(M)*Y(M,I)
580 500  CONTINUE
585      DEN=((EXP(PK(I)*Y(I,I))-1.)/PK(I))*EXP(X)
590      R(I)=(PR(I)-ANUM)/DEN
592   PRINT2,PR(I),ANUM,DEN
595C
600C CALCULATE PRESSURE AND TEMPERATURE
605C
610      RI=R(I)
615      PKI=PK(I)
616       M=I
620       CALL COEF(RI,PKI,TEM,AK,M)
625      P(I)=PKI/AK
630      PRINT3,I,RAD(I),R(I),PK(I),TEM,P(I)
635 300  CONTINUE
640      END
```

TABLE 2. (Concluded)

```
800       SUBROUTINE COEF(RI,RKI,TEM,AK,M)
810       REAL CR(12,5),TEMP(12),AK0(12)
830       DATA CR/.01,.01,.01,.01,.01,.01,.55,1.25,2.3,4.55,6.78,11.25
831&,.01,.01,.01,.01,.01,.01,.8,1.67,3.05,5.85,8.65,14.15
832&,.01,.01,.01,.01,.01,.01,1.2,2.05,3.55,6.5,9.5,15.4
833&,.01,.01,.01,.01,.01,.01,.5,1.05,2.15,4.25,6.35,10.5
834&,.01,.01,.01,.01,.01,.01,.65,1.4,2.6,5.1,7.55,12.5/
840       DATA TEMP/300.,750.,850.,1000.,1200.,1350.,1600.,1750.
841&,2000.,2500.,3000.,4000./
850       DATA AK0/0.,.33,.381,.406,.406,.396,.342,.322,.318,.33
851&,.356,.411/
855       DO 10 I=2,12
860       J=I
870        IF(RI.LT.CR(I,M)) GO TO 20
880 10    CONTINUE
885 20     CONTINUE
890       TEM=TEMP(J-1)+(RI-CR(J-1,M))*(TEMP(J)-TEMP(J-1))/(CR(J,M)
891&-CR(J-1,M))
900       AK=AK0(J-1)+(AK0(J)-AK0(J-1))*(TEM-TEMP(J-1))/
910&       (TEMP(J)-TEMP(J-1))
914       IF(TEM.LT.0.0) TEM=300.
916       IF(AK.LT.0.0)  AK=0.0
920       RETURN
930       END
```

TABLE 3. COMPUTER CODE ZRRED 4

```
50C
60C      PRØGRAM "ZRRFD"
70C
100       DIMFNSIØN RAD(4),RS(4),Y(4,4),T(4),TO(4),TT(4),
101&                    PK(4),PR(4),R(4),P(4)
118C
119C    INPUT IØ
120C
125       DATA TO/.3,.6,1.1,1.6/
126C
127C    INPUT INTENSITY DATA
128C
129       DATA TT/7.,16.2,22.7,24.4/
130C
131C    INPUT EMMISSIØN DATA
132C
135       DATA PR/6.,14.8,21.1,22.8/
140C
141C     INPUT NØ ØF DATA PØINTS
142       N=4
143C
144C     INPUT PLUME DIAMETER
145       PD=9.564
146C
150 2     FØRMAT(3E18.9)
160 3     FØRMAT(I3,5F10.3)
170 4     FØRMAT(2X,"I",7X,"R",9X,"N",9X,"PK",8X,"T",9X,"P",/)
200C
210       DØ5I=1,N
220 5     T(I)=(TT(I)-PR(I))/TO(I)
230C
300C    CØMPUTE RADIAL PØSITIØNS
310C
315       DØ10I=1,N
320        X=(12.86-I*2.86)*3.1416/180.
325       RAD(I)=26.56*SIN(X)
330       RS(I)=RAD(I)*RAD(I)
335 10    CØNTINUE
340       RØS=PD*PD/4.
345       DØ20L=1,N
350       J=N-L+1
355       DØ30K=1,N
360       I=N-K+1
365       IF(I.GT.J) GØ TØ 30
370       IF(I-1.NE.0) XI=RS(I-1)
375       IF(I-1.EQ.0) XI=RØS
380       Y(I,J)=SQRT(XI-RS(J))
385       MM=I+1
386       JJ=J+1
390       DØ15M=MM,JJ
395       IF(M.GT.J) GØ TØ 15
400       Y(I,J)=Y(I,J)-Y(M,J)
```

TABLE 3. (Continued)

```
405  15  CONTINUE
410  30  CONTINUE
412      IF(I.EQ.J) Y(I,J)=2.*Y(I,J)
415  20  CONTINUE
420C
425C    COMPUTE PK PRODUCT
430C
435      DO 100 I=1,N
440      X=-ALOG(T(I))
445      K=I-1
450      DO200J=1,K
455      IF(I.EQ.1) GO TO 200
460      X=X+2.*PK(J)*Y(J,I)
465  200 CONTINUE
470      PK(I)=X/Y(I,I)
480  100 CONTINUE
485      PRINT4
490C
495C    COMPUTE LOCAL RADIANCE
500C
505      DO300I=1,N
510      ANUM=0.
515      X=ALOG(T(I))
520      K=2*I-1
525      DO 400M=1,K
530      IF(M.EQ.I) GO TO 350
535      IF(M.LT.I) J=M
540      IF(M.GT.I) J=K-M+1
545      ANUM=ANUM+R(J)*Y(J,I)*EXP(X)
550      X=X+PK(J)*Y(J,I)
555  350 IF(M.EQ.I) X=X+PK(I)*Y(I,I)
560  400 CONTINUE
565      X=0.
566      LL=I
570      DO500M=1,LL
575      X=X-PK(M)*Y(M,I)
580  500 CONTINUE
585      DEN=Y(I,I)*EXP(X)
590      R(I)=(PR(I)-ANUM)/DEN
592   PRINT2,PR(I),ANUM,DEN
595C
600C CALCULATE PRESSURE AND TEMPERATURE
605C
610      RI=R(I)
615      PKI=PK(I)
616       M=I
620       CALL COEF(RI,PKI,TEM,AK,M)
625      P(I)=PKI/AK
630      PRINT3,I,RAD(I),R(I),PK(I),TEM,P(I)
635  300 CONTINUE
640      END
```

TABLE 3. (Concluded)

```
800       SUBROUTINE COEF(RI,PKI,TEM,AK,M)
810       REAL CR(4,12),TEMP(12),AK0(12)
830       DATA CR/.2,.2,.2,.2,.2,.2,.2,.2,.2,.2,.2,.2
831&,.3,.3,.3,.3,.3,.3,.3,.3,.3,.3,.3,.3
832&,.3,.3,.3,.3,.3,.3,.48,.7,1.25,2.7,4.38,7.5
833&,.3,.3,.3,.3,.5,.6,.95,1.32,2.3,5.4,8.85,15.7/
840       DATA TEMP/300.,750.,850.,1000.,1200.,1350.,1600.,1750.
841&,2000.,2500.,3000.,4000./
850       DATA AK0/0.,.33,.381,.406,.406,.396,.342,.322,.318,.32
851&,.356,.411/
855      DO10I=1,20
860      J=I
870       IF(RI.LT.CR(I,M)) GO TO 20
880 10   CONTINUE
885 20    CONTINUE
890       TEM=TEMP(J-1)+(RI-CR(J-1,M))*(TEMP(J)-TEMP(J-1))/(CR(J,M)
891&-CR(J-1,M))
900      AK=AK0(J-1)+(AK0(J)-AK0(J-1))*(TEM-TEMP(J-1))/
910&      (TEMP(J)-TEMP(J-1))
920      RETURN
930      END
```

DATA REDUCTION

Time-reduced oscillograms were made from all of the optical data. These records were read manually and converted to the form needed in the data reduction computer program. Figure 33 shows a typical section of the Brush record oscillogram for Run 238 with the 5:1 gain, 1:1 gain, scanner code, and chopper signal channels.

The relative location of the absorption sources may be obtained from the scanner code. Inspection of the figure reveals that the transmittance from absorption sources located at the plume boundaries (lamps A and J) is high and falls off for sources located toward the center of the plume. This characteristic induced some uncertainty into the raw data reduction. The multiple peaks in the vicinity of Lamp B were attributed to vibration of the scanning mirror during the dwell of the drive mechanism as the scan direction was being reversed.

For the 4:1 nozzle tests, the signal strength was greater than anticipated. This resulted in saturation (overranging) of the tape record in a number of cases as shown in Fig. 34, a portion of the Brush record for Run 247. However, the spectroradiometer electronics were not saturated. The lack of a clear destination between the plume emission alone and the plume emission when augmented with lamp radiation made measuring the relative intensity through the plume difficult. It could not have been done without a well-defined scanner code.

The background intensities and run data for the 25:1 nozzle tests are summarized in Fig. 35 through 40. Similar results for the 4:1 nozzle tests are shown in Fig. 41 through 55. The apparent brightness temperature was maintained at a nearly constant level during the tests by accurately controlling the lamp current; this temperature is indicated on the figures containing background data.

Several general comments about the data may be made. The data for the 25:1 nozzle tests (Fig. 39 and 40) suggest a degradation of the alignment as the run proceeded. Misalignment during the run did not occur for the 4:1 nozzle tests, as shown in Fig. 45, 46, 48, 49, 51, 52, 54, and 55; however, an alignment shift from run to run was observed. Inconsistencies between prerun and postrun background intensities

Page intentionally left blank

FOLDOUT FRAME 1

FOLDOUT FRAME 2

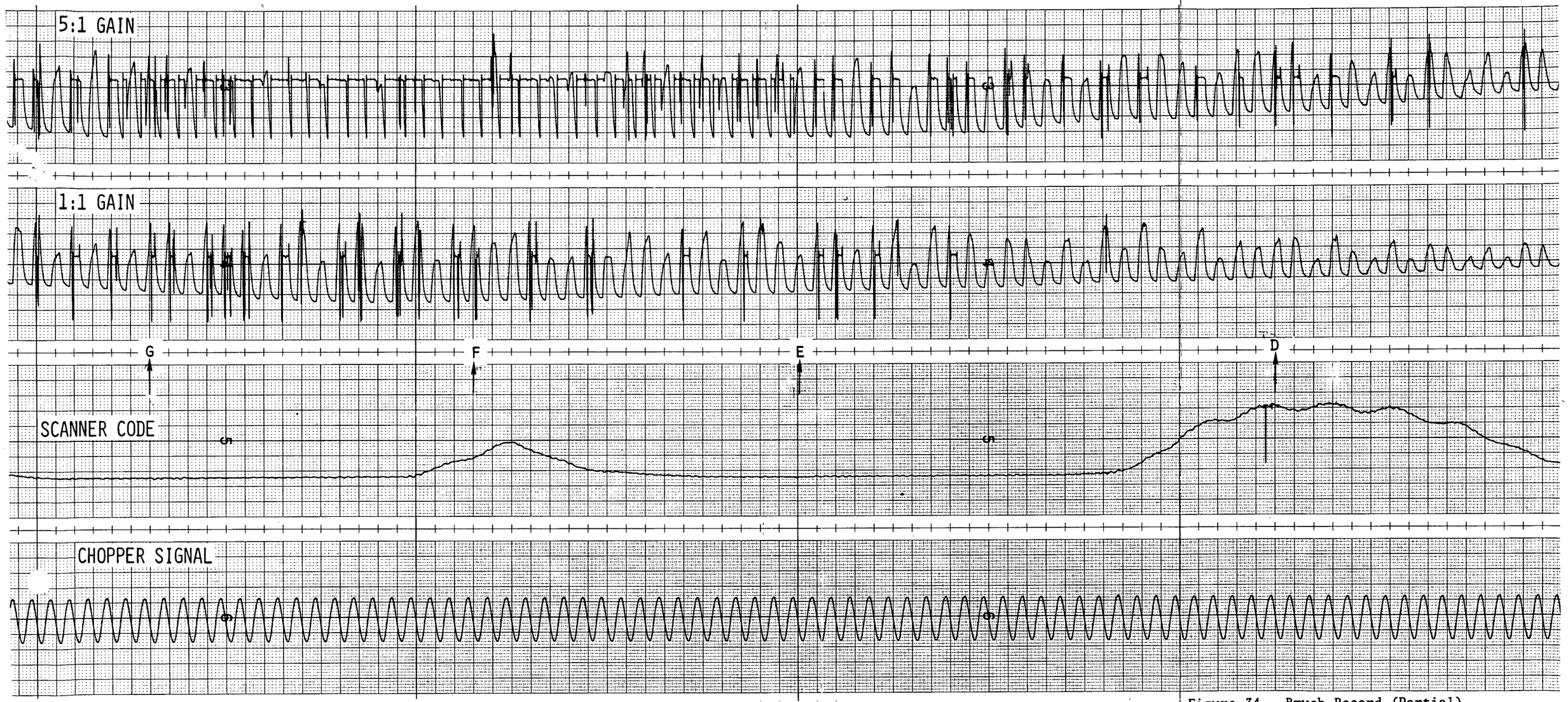

Figure 34. Brush Record (Partial), Run 247

Figure 35. Ambient Background, Lamp Current 0.8 Ampere

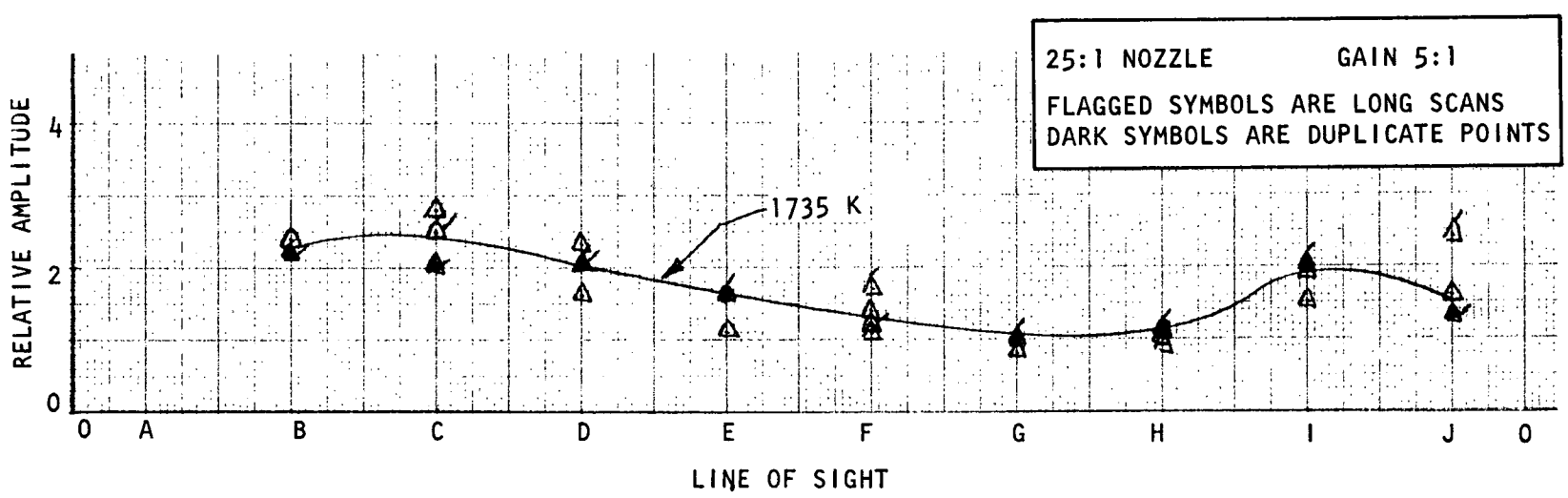

Figure 36. Ambient Background, Lamp Current 0.9 Ampere

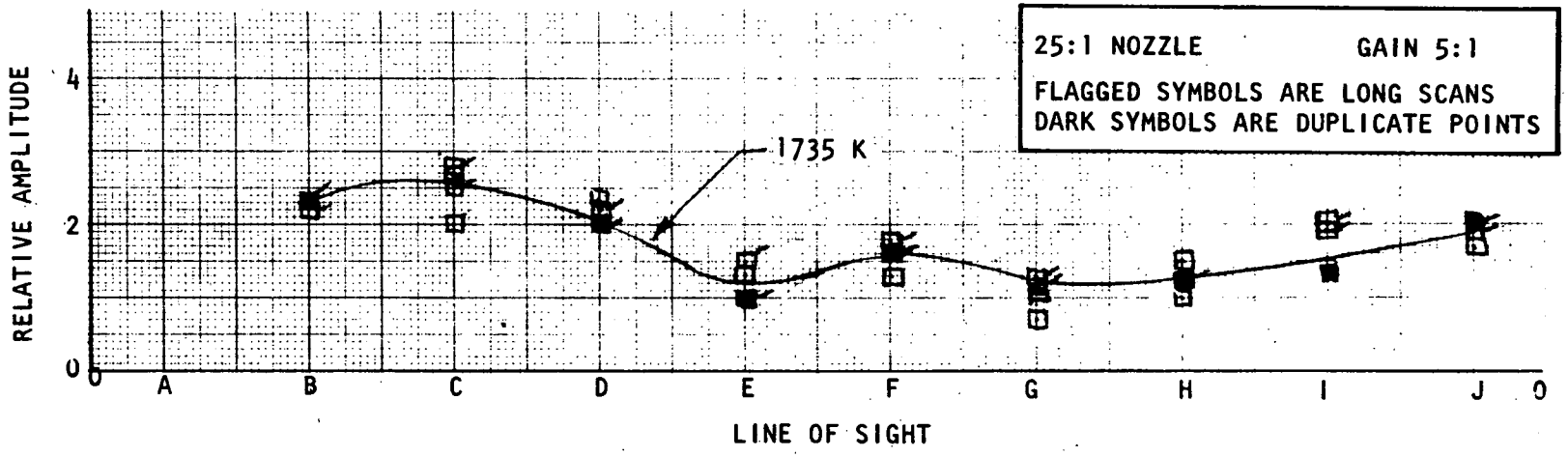

Figure 37. Altitude Background, Lamp Current 0.9 Ampere

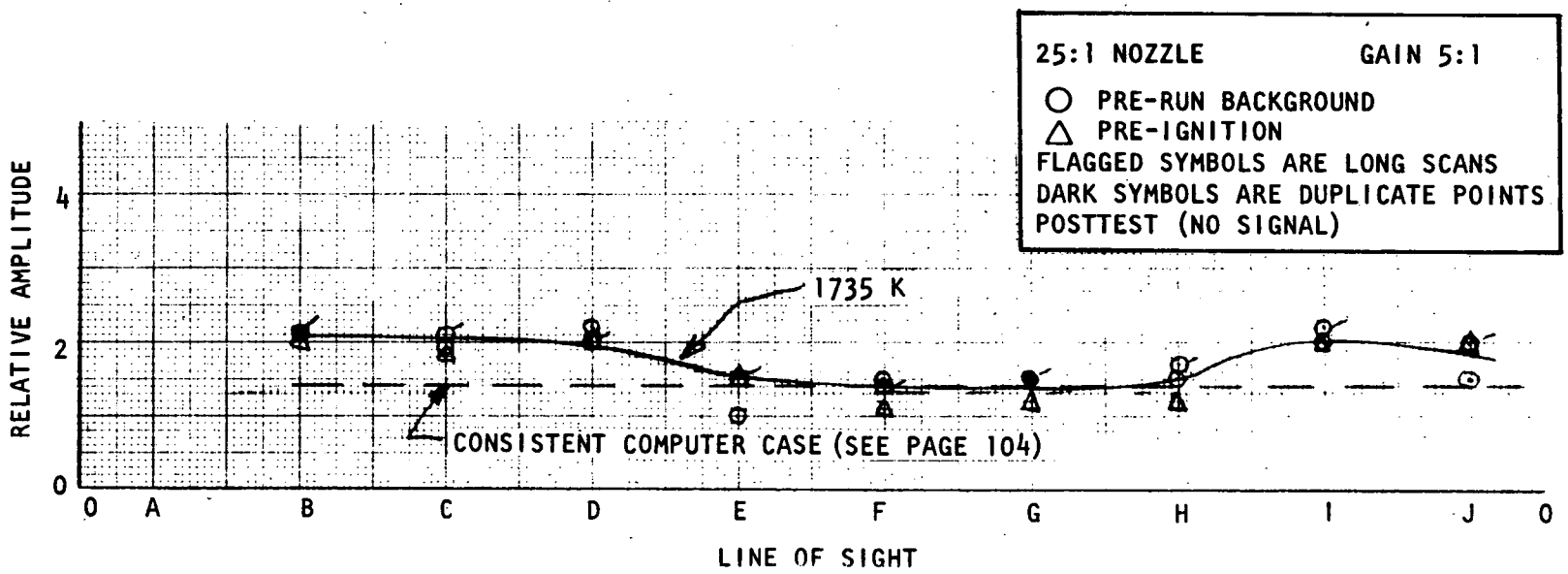

Figure 38. Prerun Background, Lamp Current 0.9 Ampere, Run 238

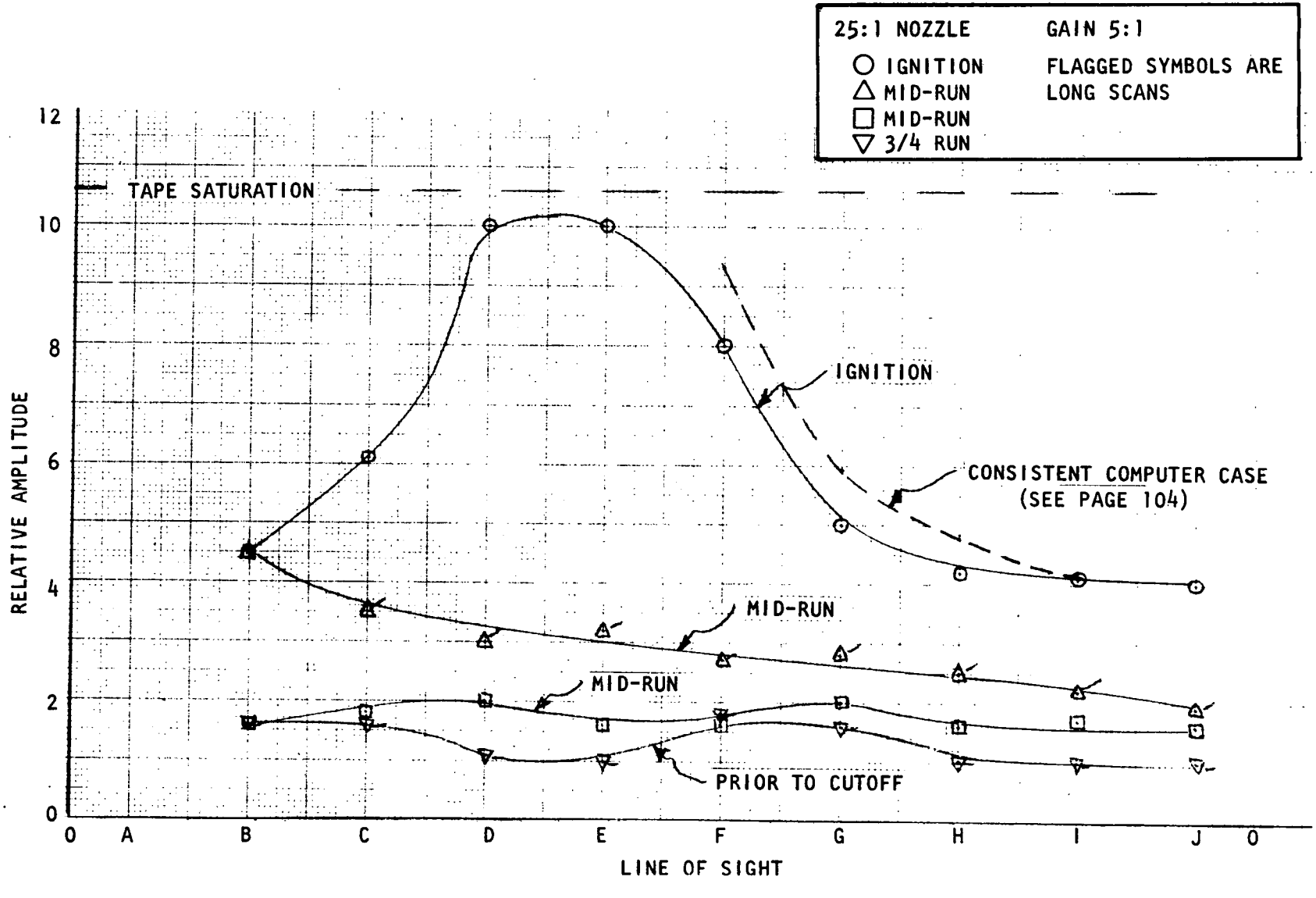

Figure 39. Emission Plus Lamp Radiation, Run 238

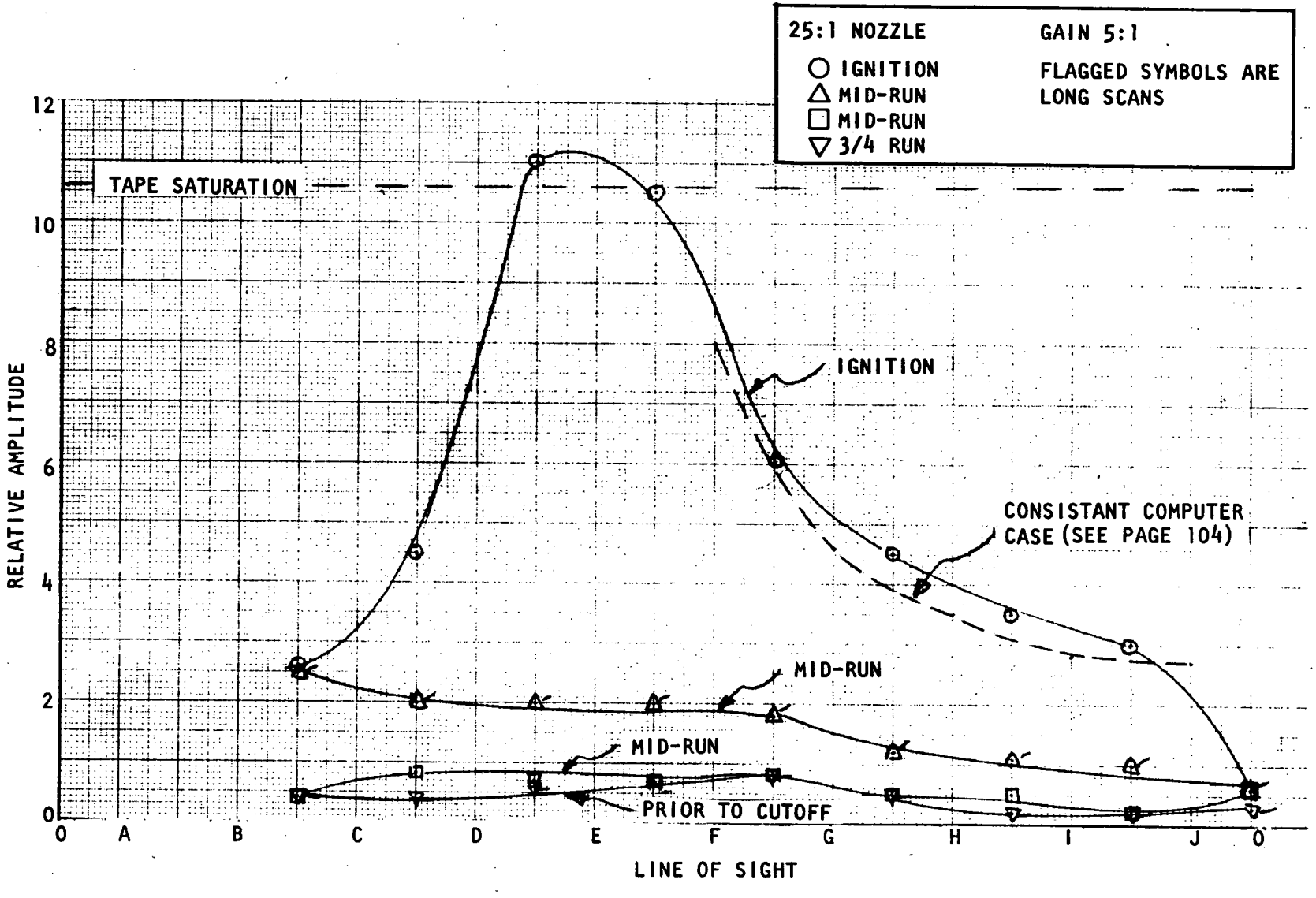

Figure 40. Emission Only, Run 238

C-2

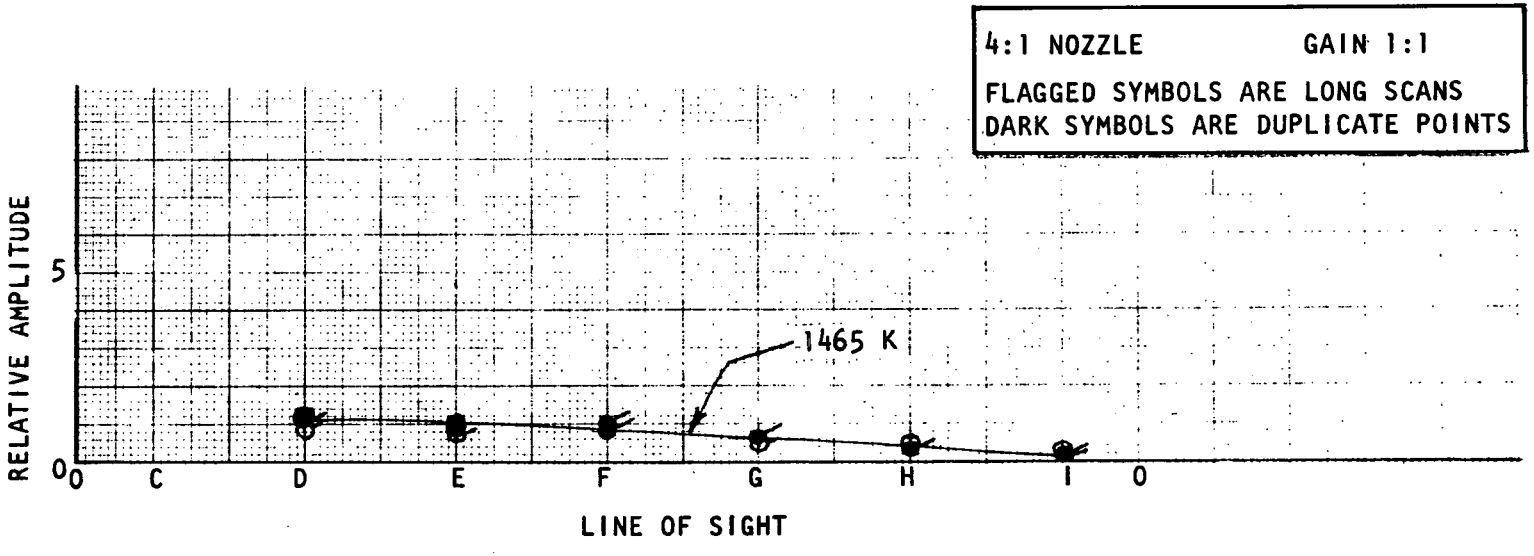

Figure 41. Ambient Background, Lamp Current 0.7 Ampere

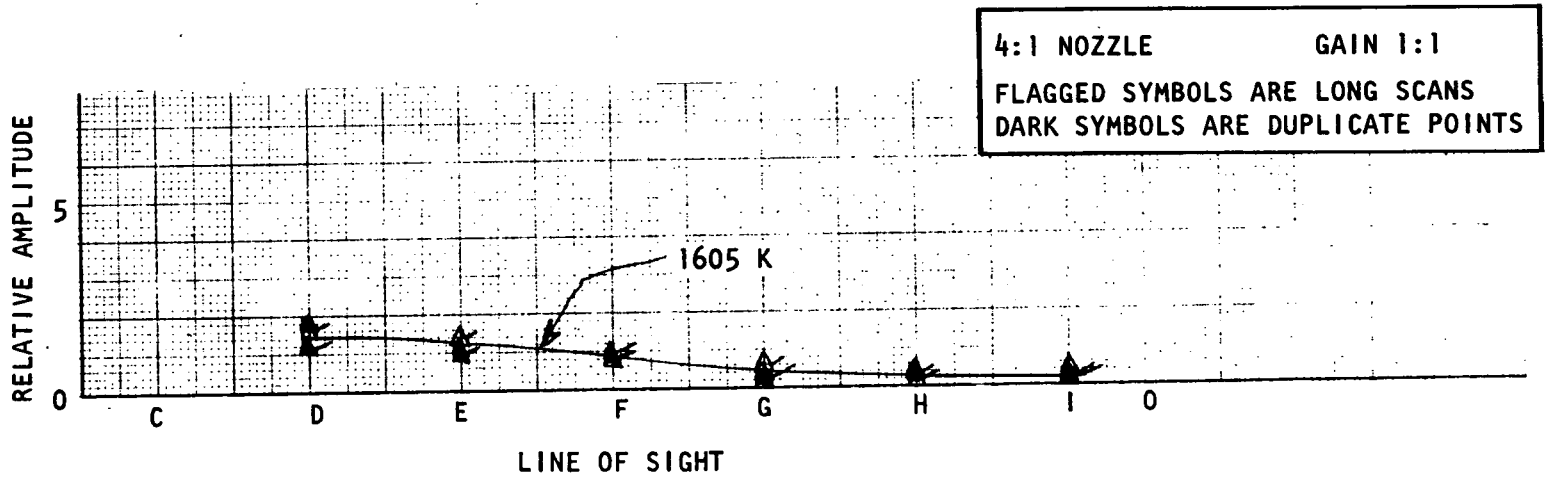

Figure 42. Ambient Background, Lamp Current 0.8 Ampere

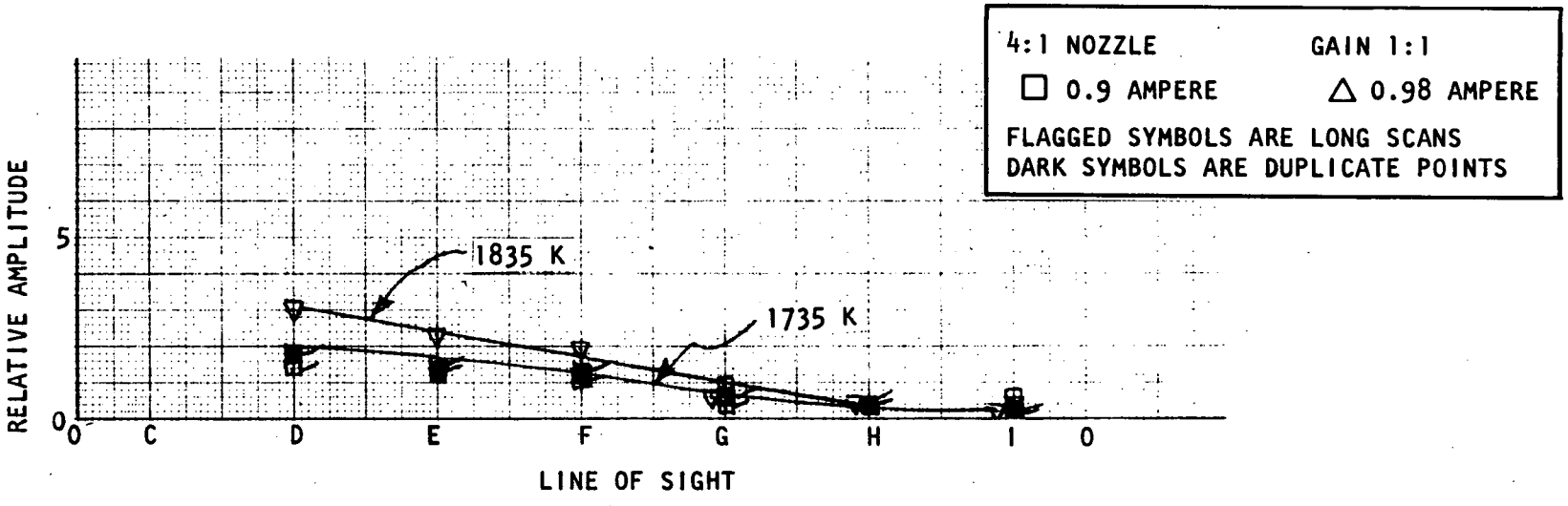

Figure 43. Ambient Background, Lamp Current 0.9 and 0.98 Ampere

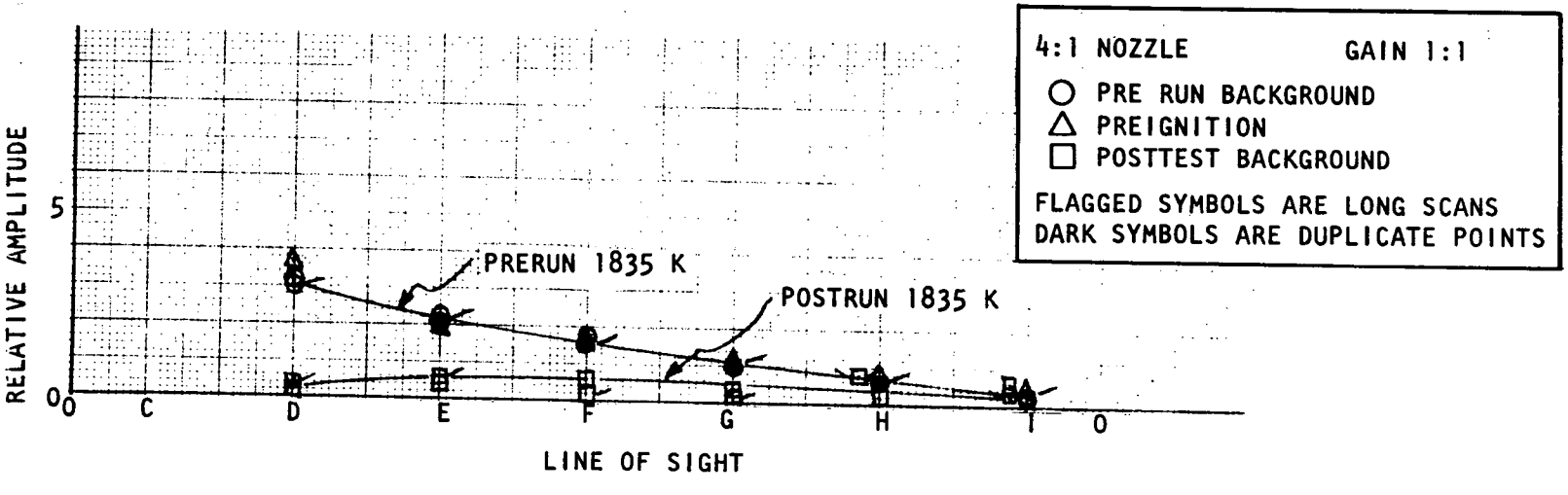

Figure 44. Prerun and Postrun Background, Lamp Current 0.98 Ampere, Run 247

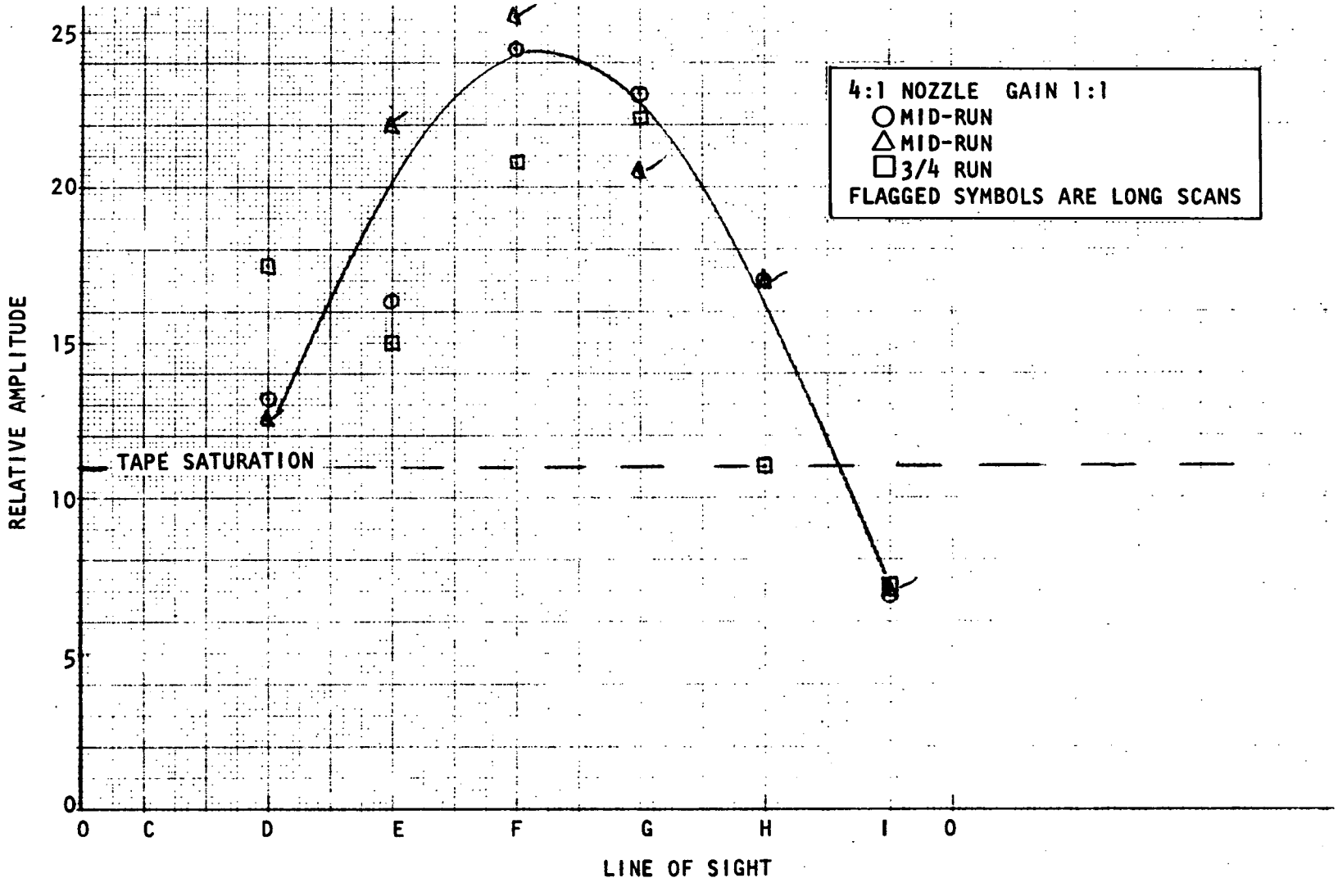

Figure 45. Emission Plus Lamp Radiation, Run 247

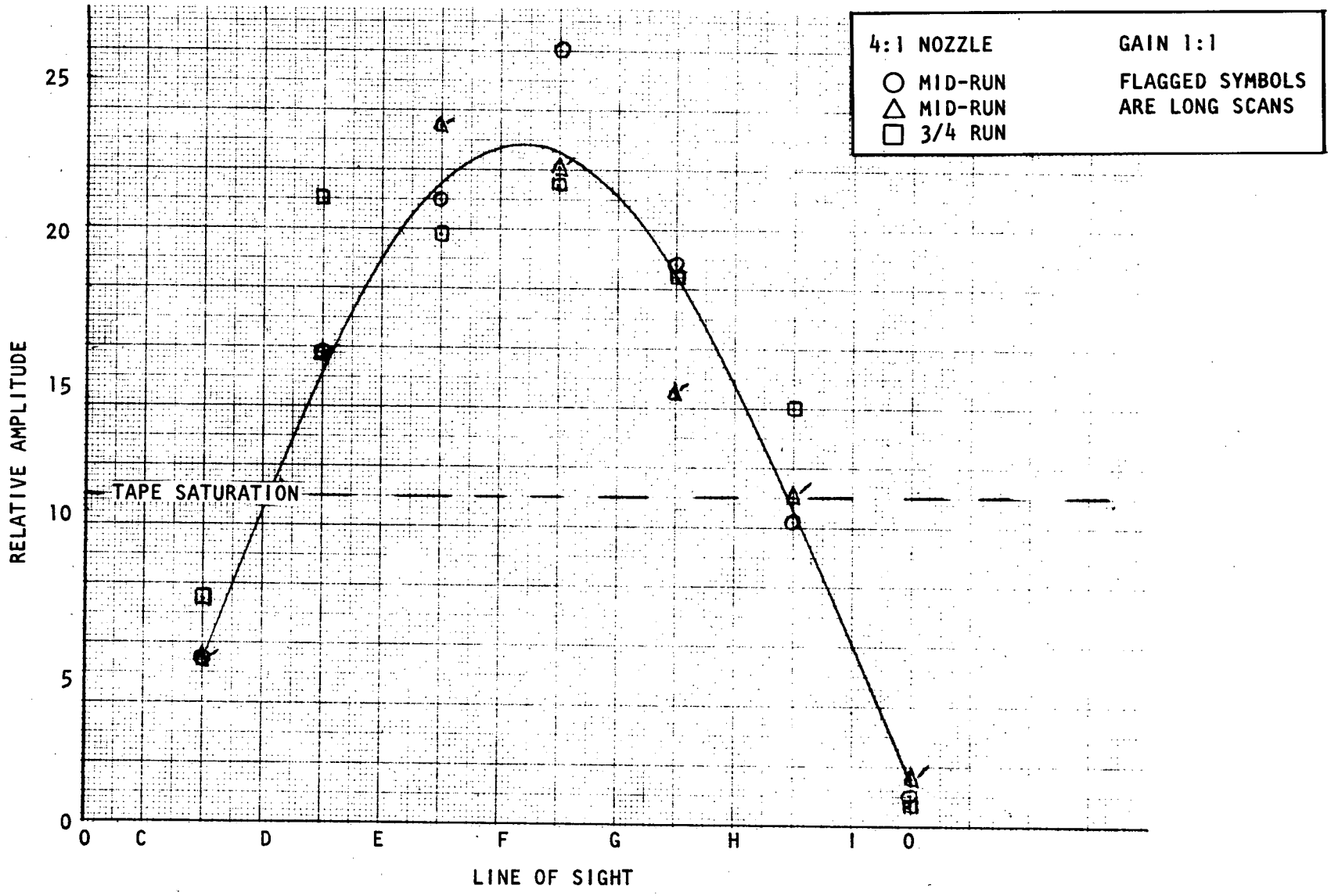

Figure 46. Emission Only, Run 247

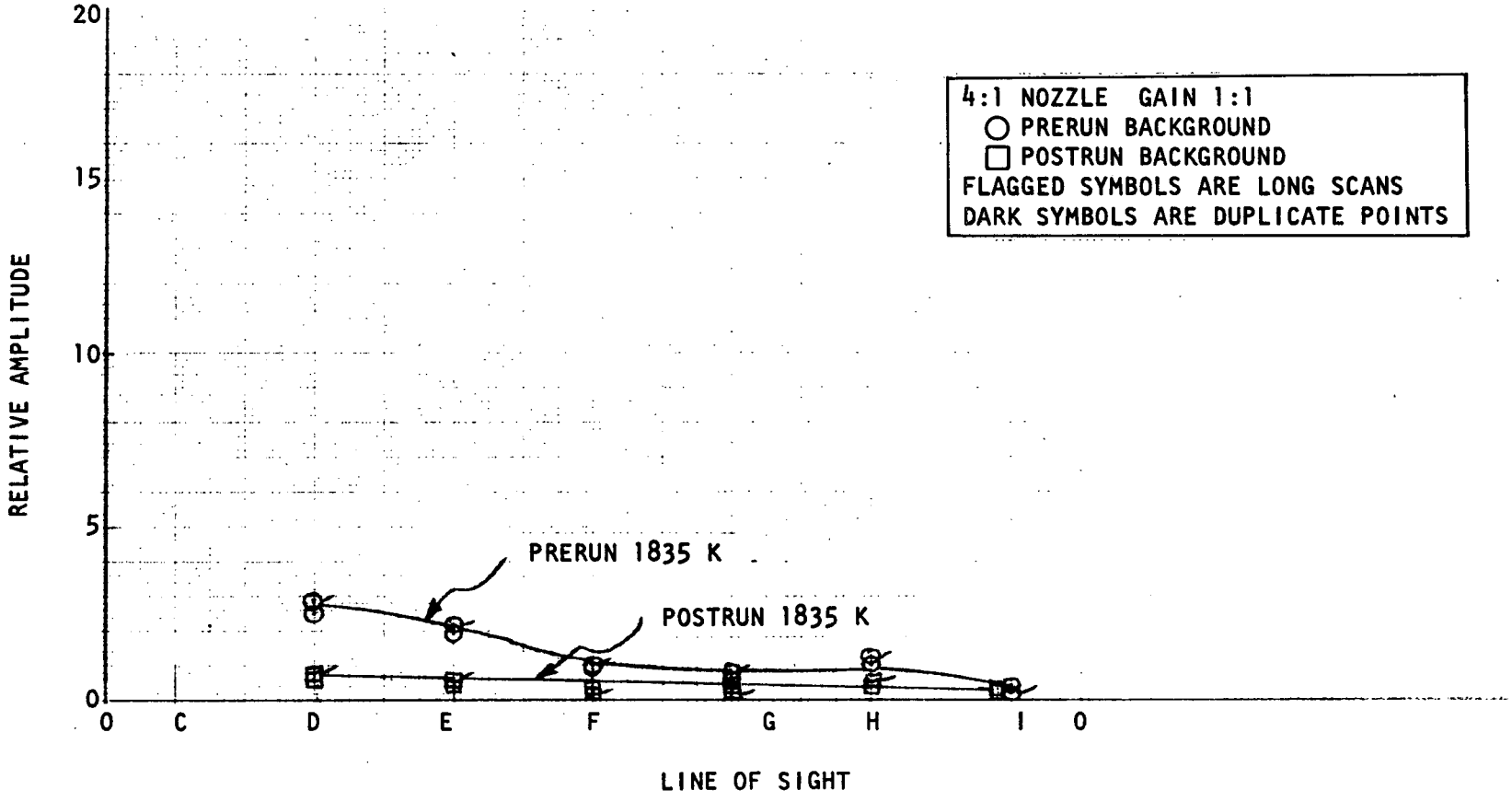

Figure 47. Prerun and Postrun Background, Lamp Current 0.98 Ampere, Run 248

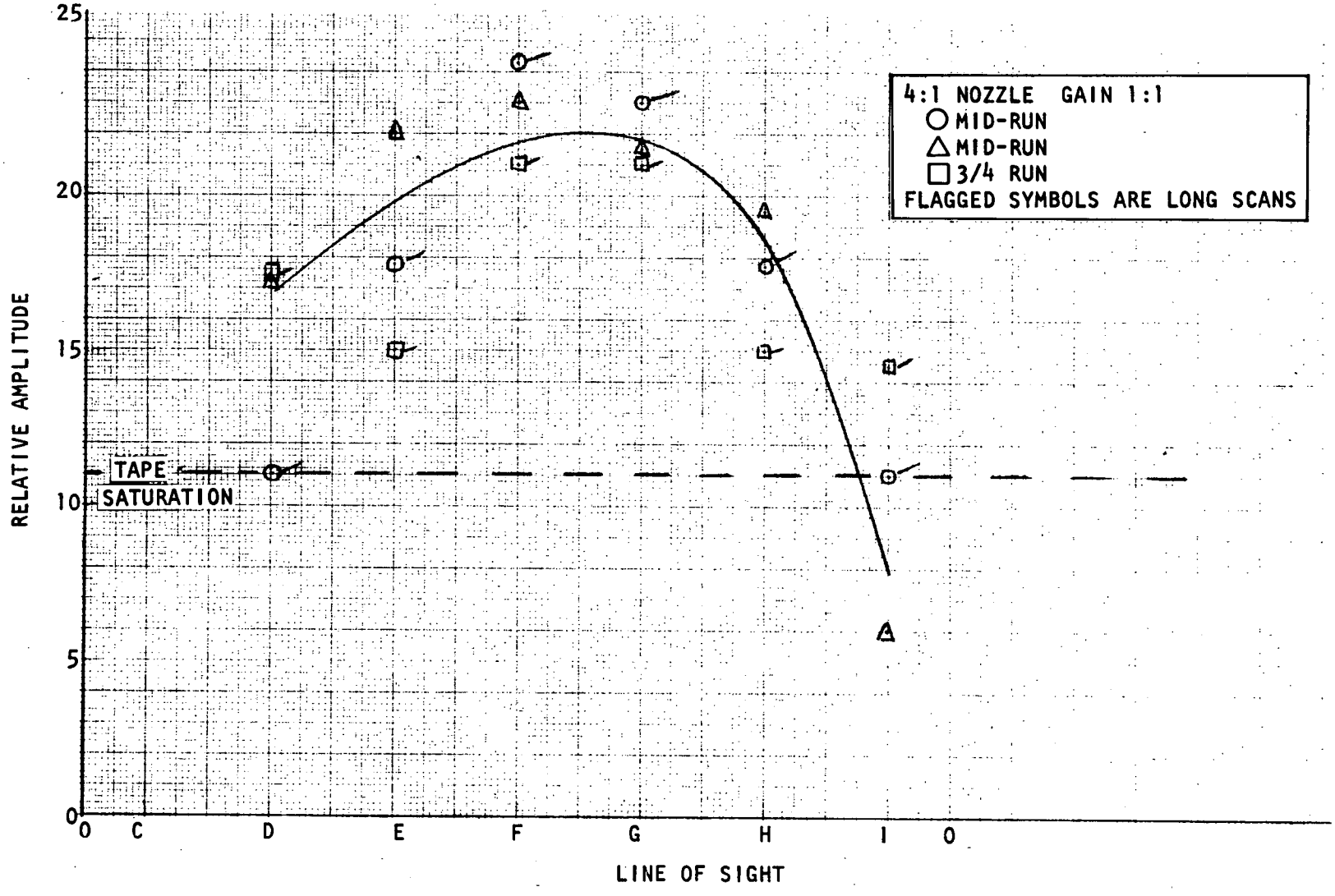

Figure 48. Emission Plus Lamp Radiation, Run 248

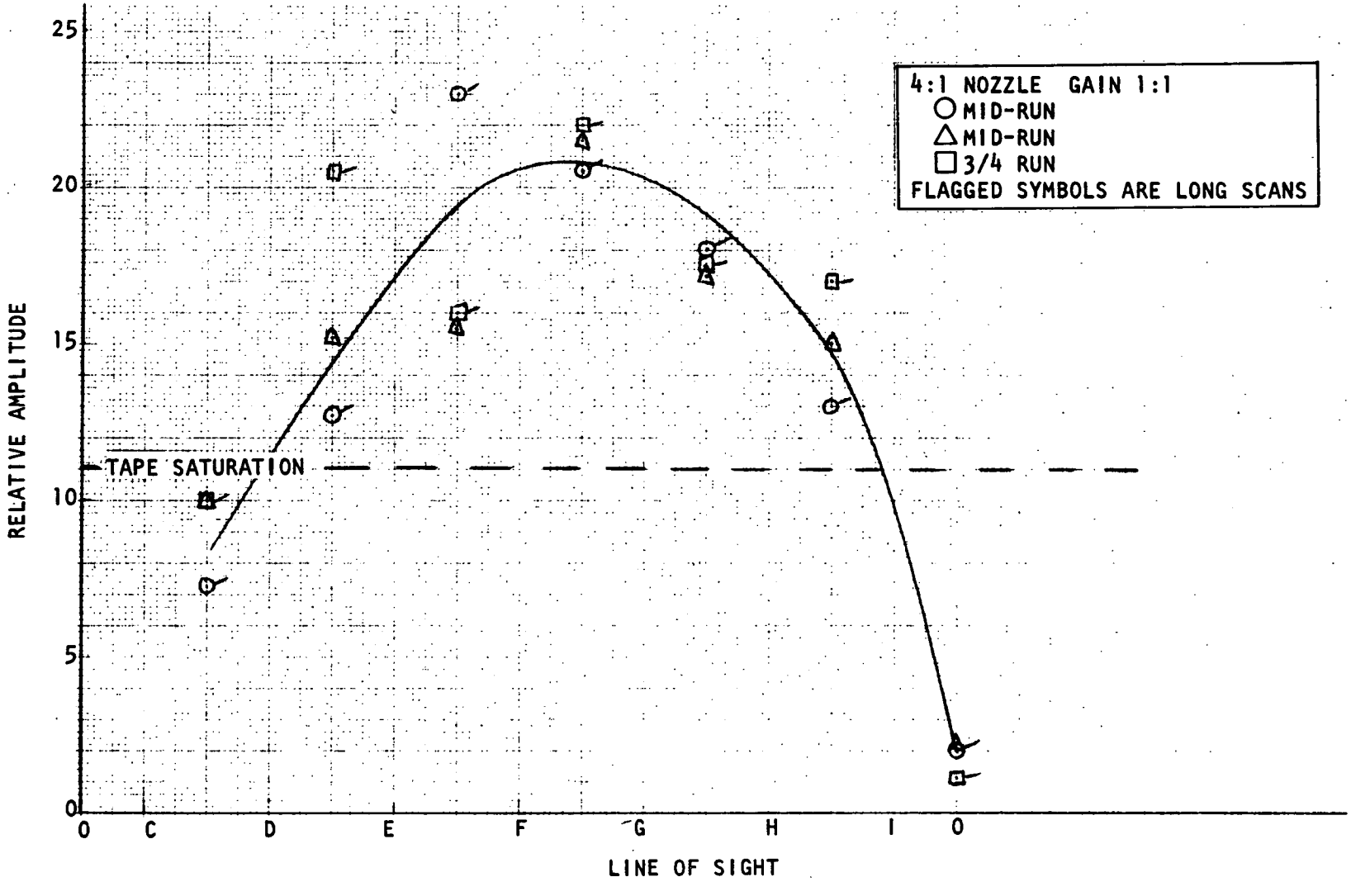

Figure 49. Emission Only, Run 248

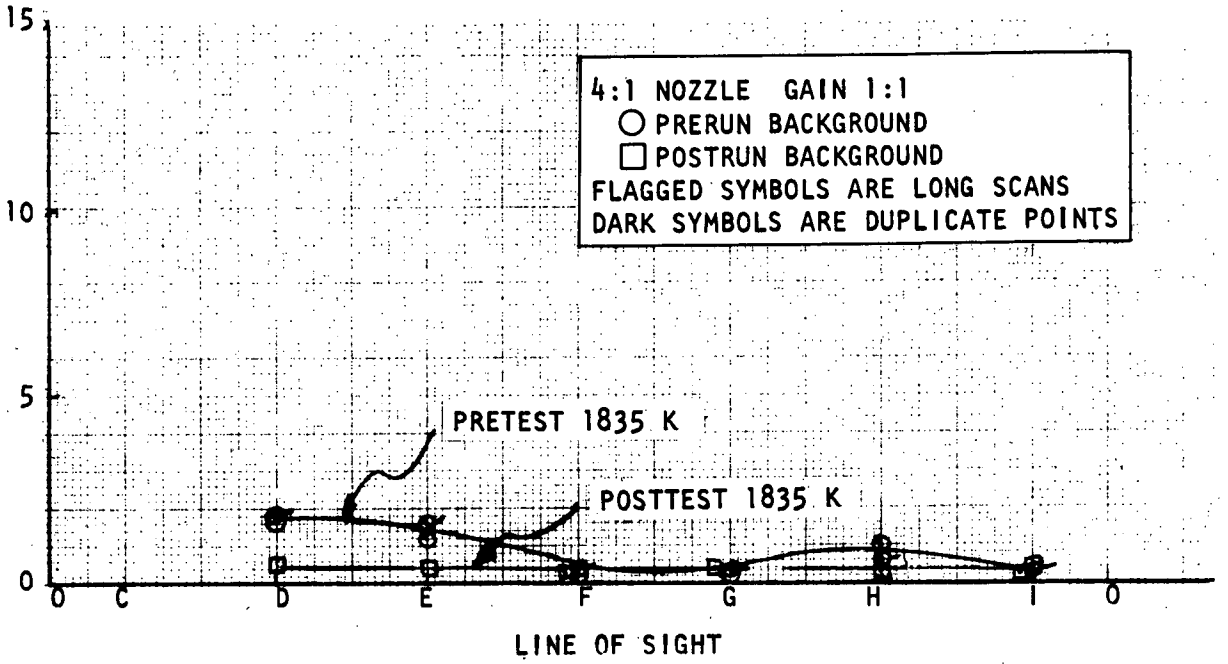

Figure 50. Prerun and Postrun Background, Lamp Current 0.98 Ampere, Run 249

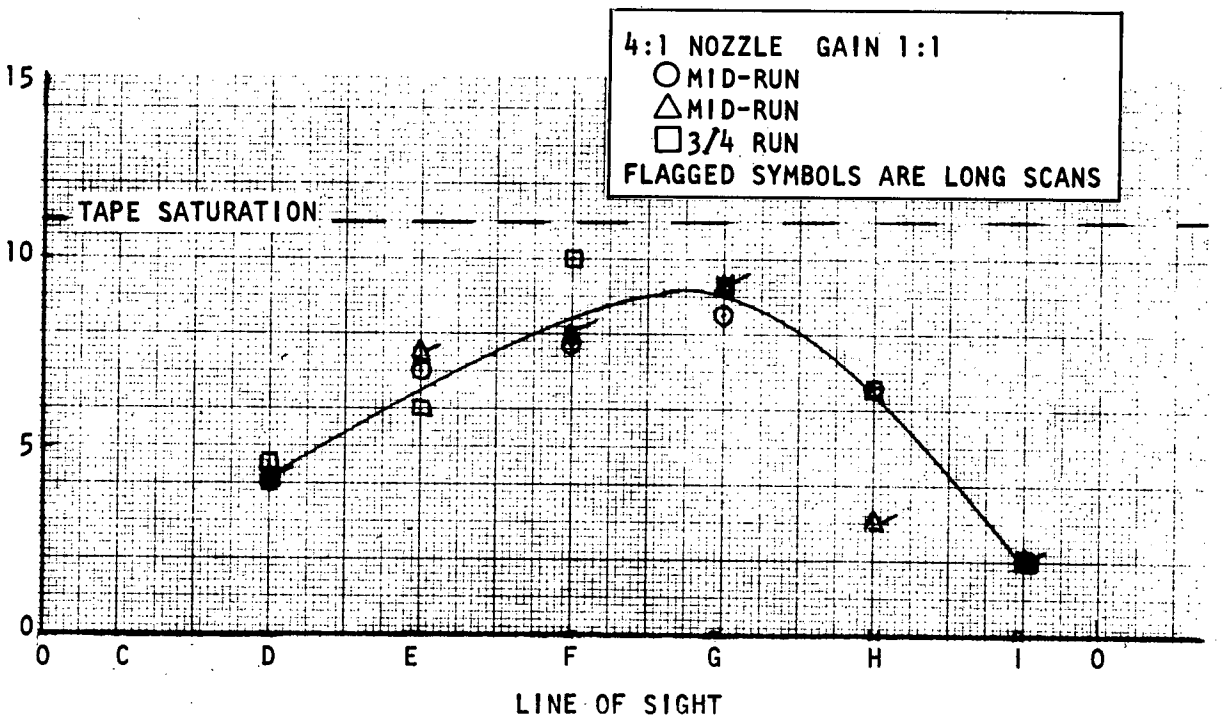

Figure 51. Emission Plus Lamp Radiation, Run 249

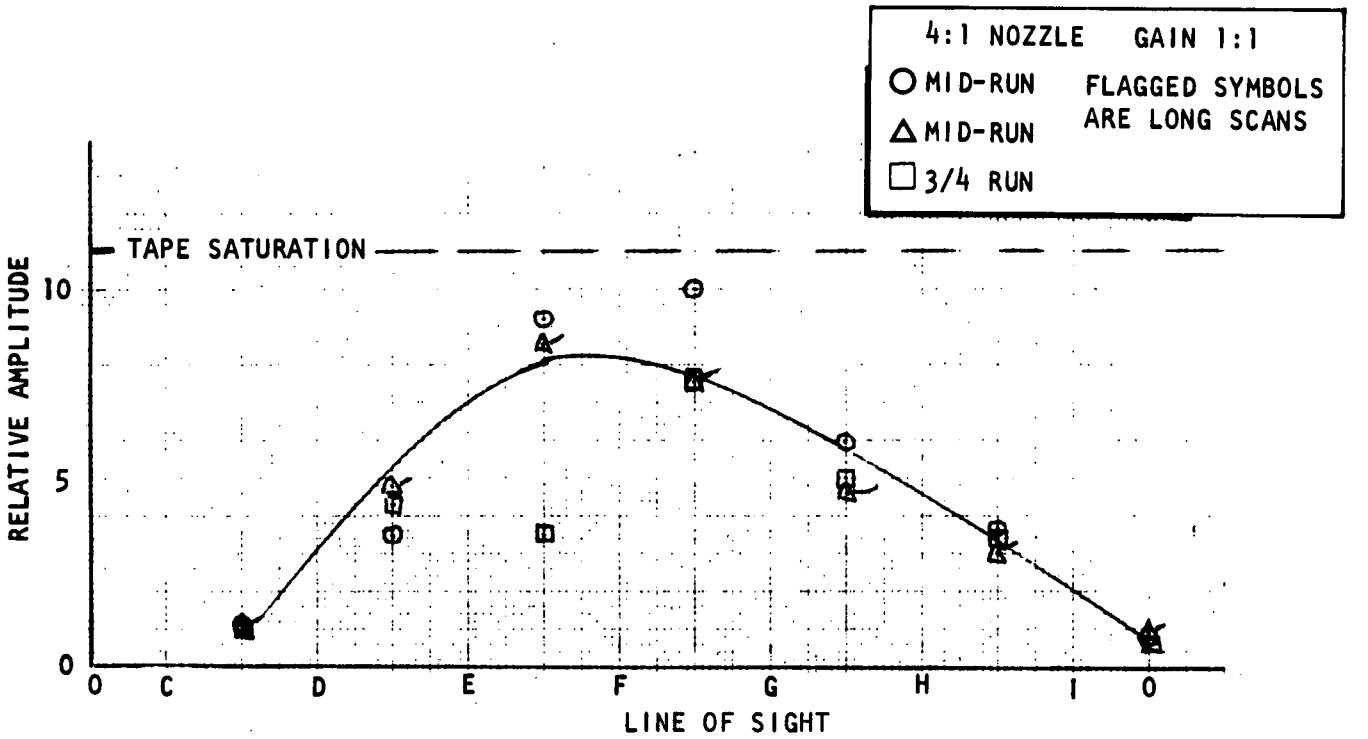

Figure 52. Emission Only, Run 249

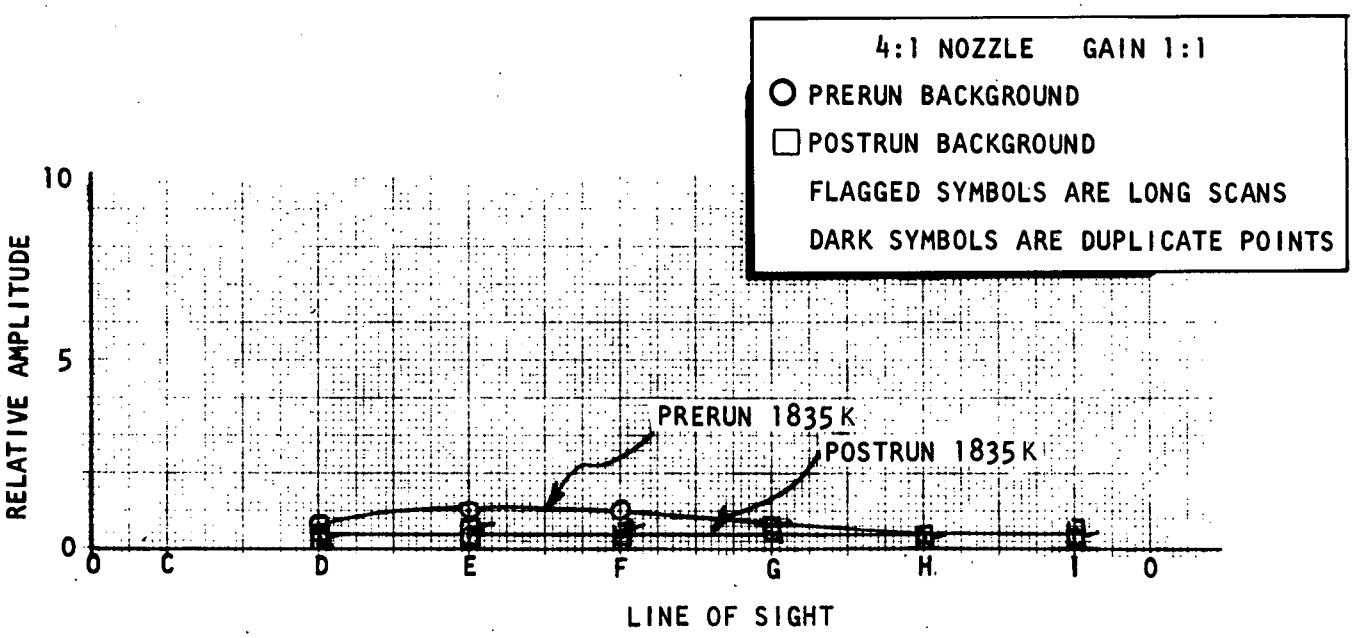

Figure 53. Prerun and Postrun Background, Lamp Current 0.98 Amperes, Run 250

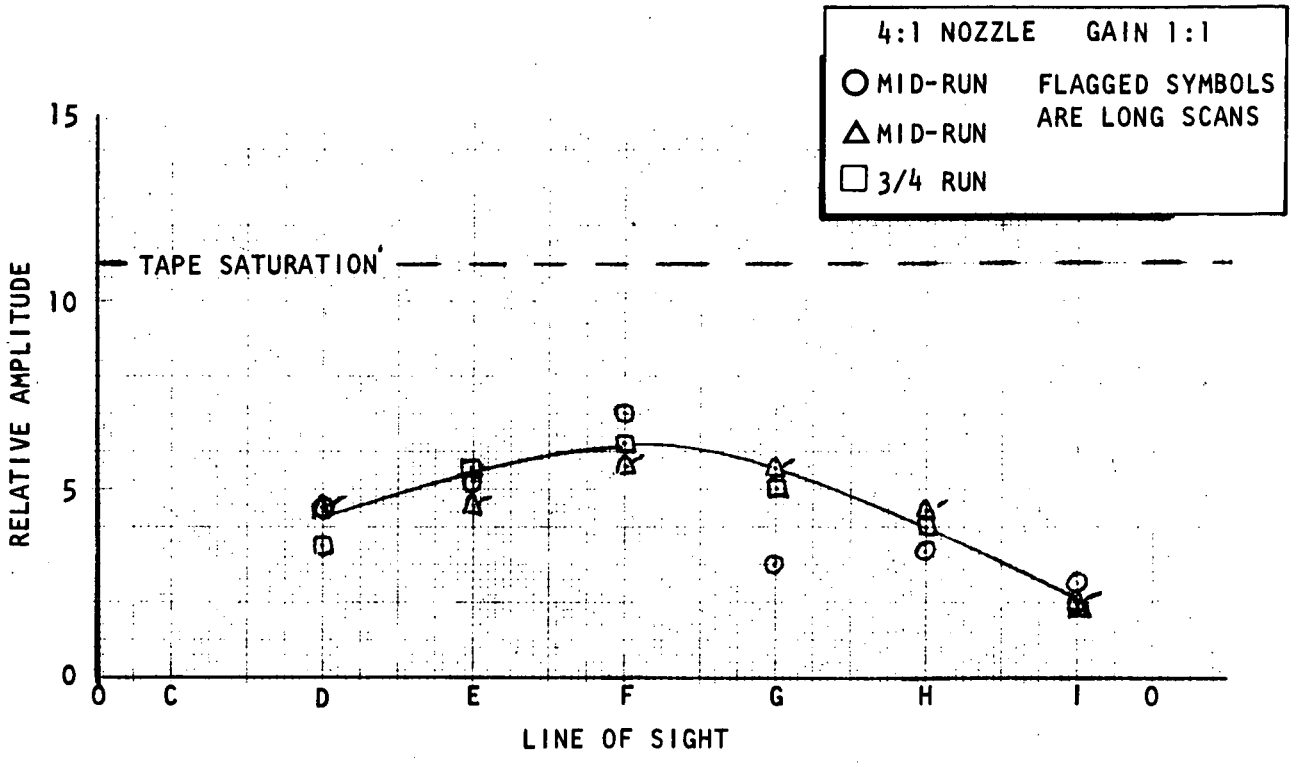

Figure 54. Emission Plus Lamp Radiation, Run 250

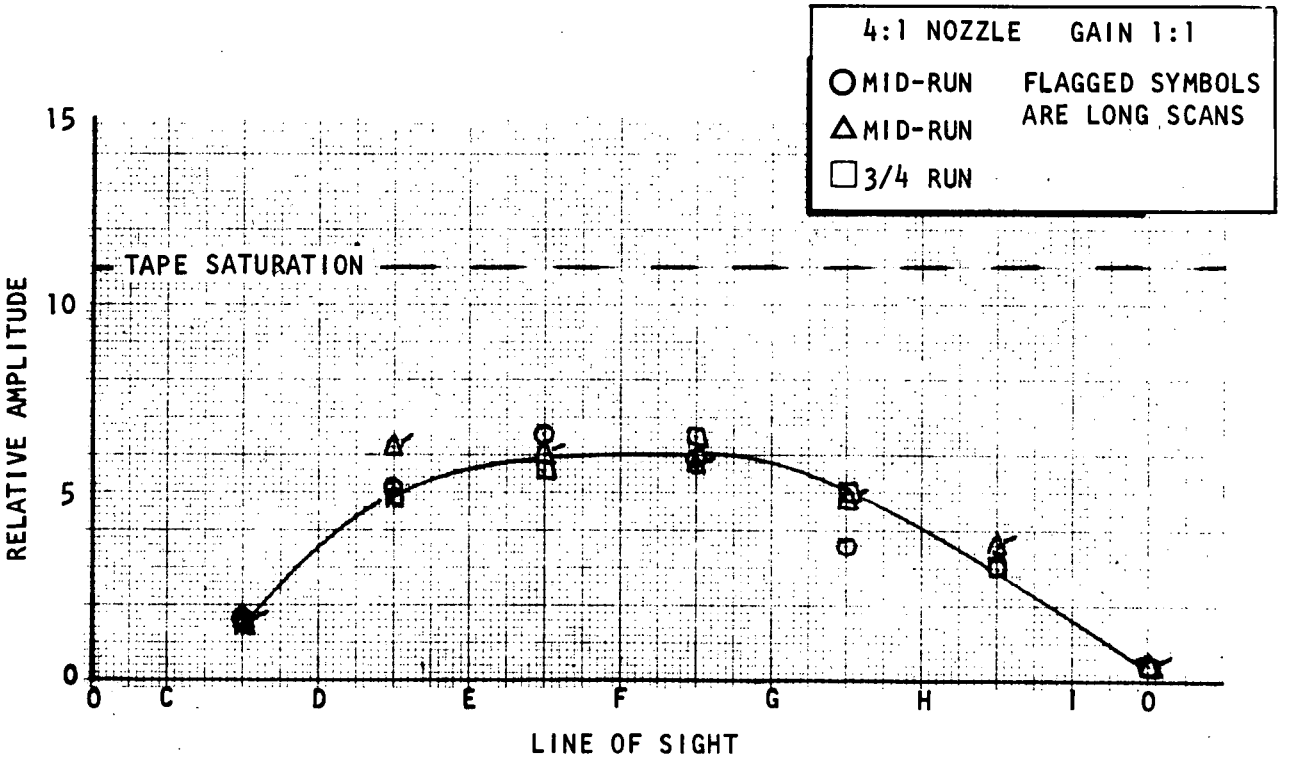

Figure 55. Emission Only, Run 250

are most probably caused by events occurring during the engine shutdown sequence coupled with a gradual change in the instrumentation system alignment, because a detectable signal, that was somewhat reduced in strength, returned after relatively long periods of time.

For the 1:1 gain channel, the data from Runs 247 and 248 indicated that the signal was of sufficient magnitude to overdrive the tape recorder. Although this invalidates these data, the relative trend of the data is similar to data gathered under conditions where tape recorder saturation did not occur.

CORRELATION

The data correlation effort consisted of structuring all of the gathered data in a format suitable for the calculation of plume properties and then comparing these calculated values to other measurements and analytic predictions. The run data were taken directly from the smoothed data curves presented above; however, further manipulation of the background data was required.

The absorption source lamp calibration data are shown in Fig. 56 and 57. The brightness temperature was measured with an optical pyrometer that was located at the monochromator entrance slit in a simulated zone radiometer installation. In general, brightness temperature is linearly dependent on lamp current (with a non-zero intercept) for currents greater than 0.7 ampere. The same calibration curve applies to all lamps; however, due to the alignment variations, separate calibration curves for each line of sight were generated (Fig. 58 through 60). These curves were derived by plotting, for each lamp, the relative amplitude (intensity) versus the apparent brightness temperature corresponding to the applied lamp current. Large extrapolations of the curves were made to match the temperature range of the absorption source data. Theoretical plume temperatures were within the range of the background data; therefore, the extrapolations had no effect on physically realistic plume property calculations.

The calculation of plume properties utilizing the reduced optical data met with great difficulty. The data were apparently inconsistent because, for every set of

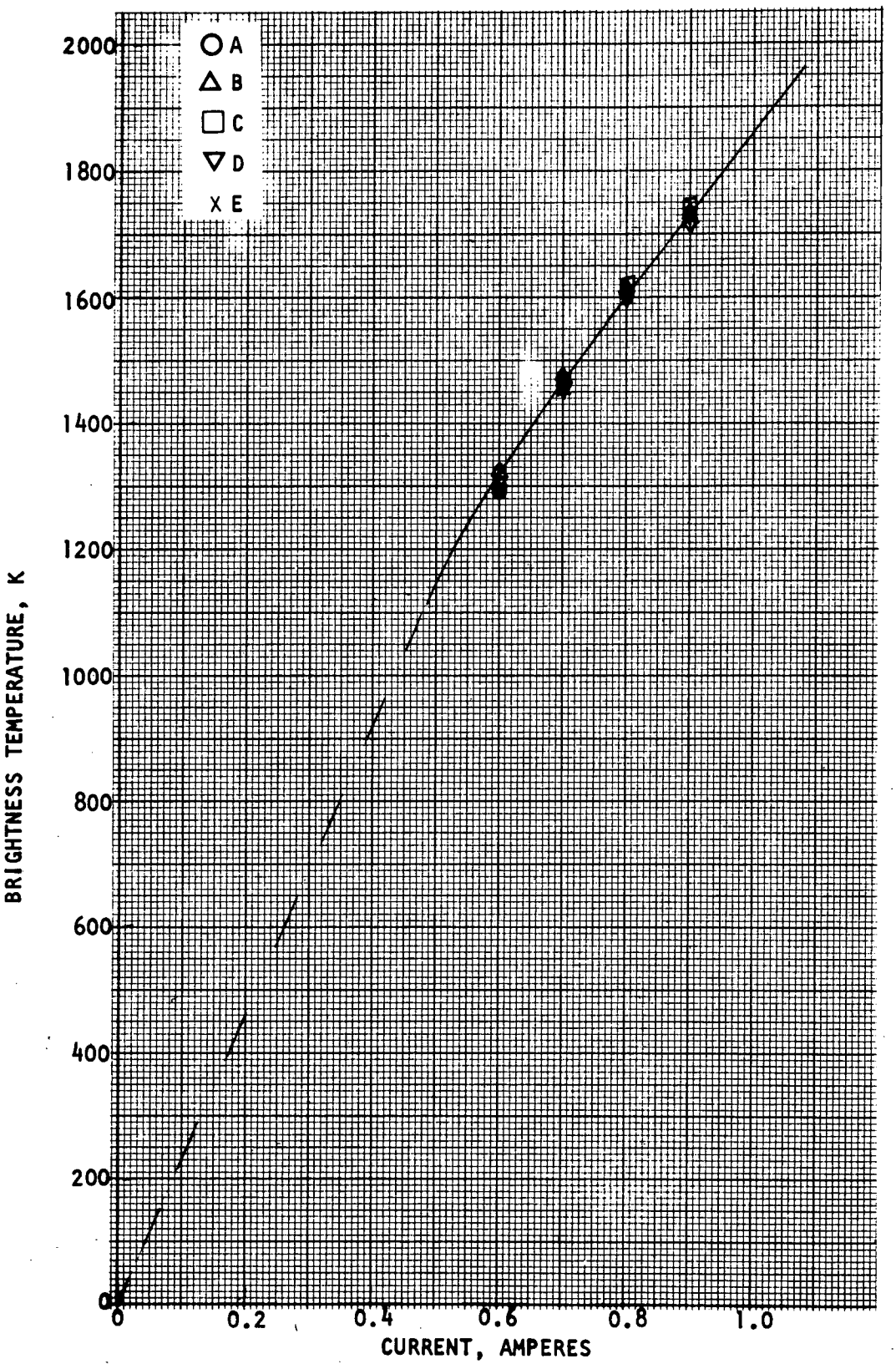

Figure 56. Brightness Temperature vs Lamp Current, Lamps A, B, C, D, and E

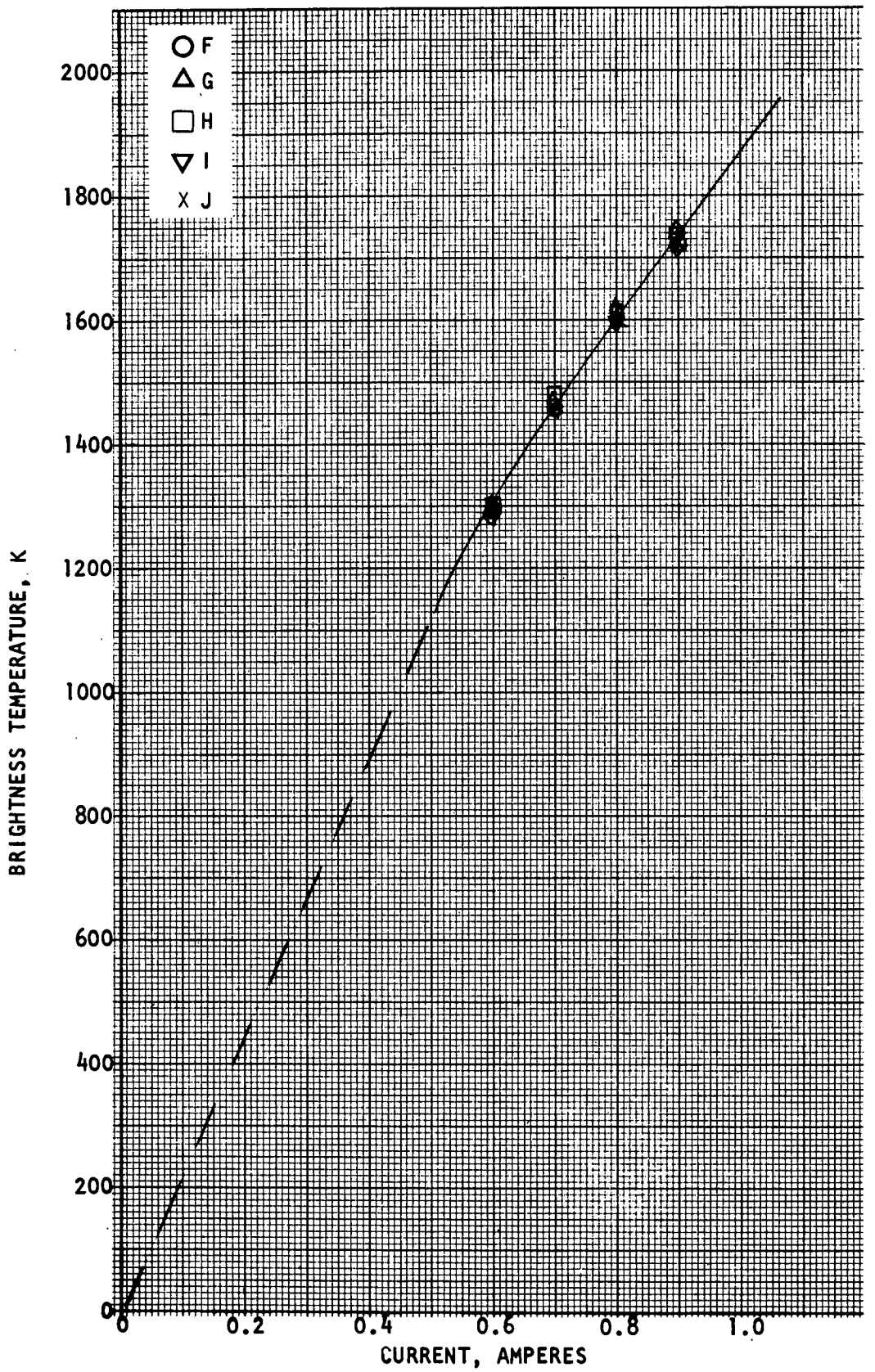

Figure 57. Brightness Temperature vs Lamp Current, Lamps F, G, H, I, and J

R-9183

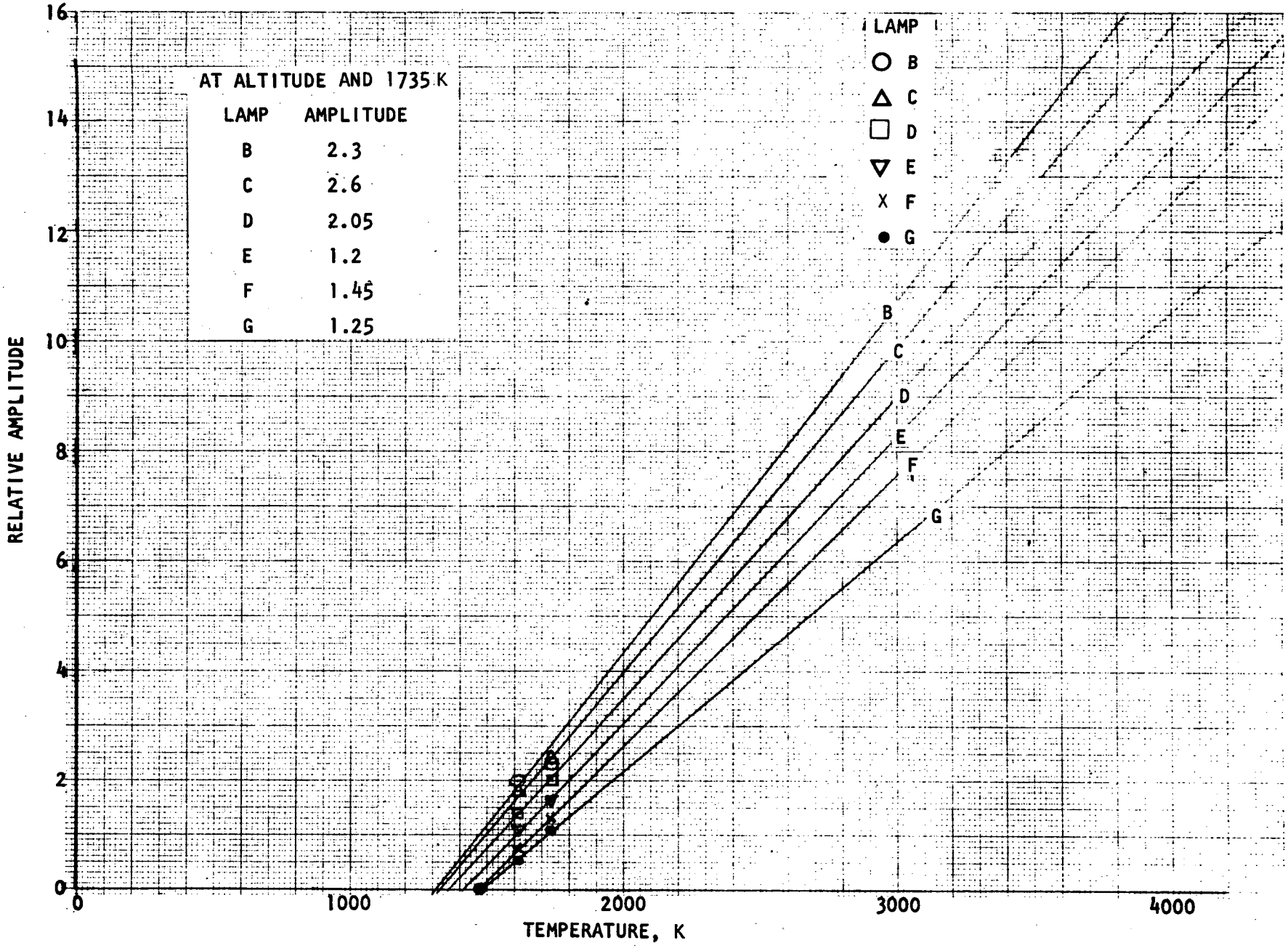

Figure 58. Individual Lamp Calibration Curves, Lamps B, C,D, E, F, and G, 25:1 Nozzle

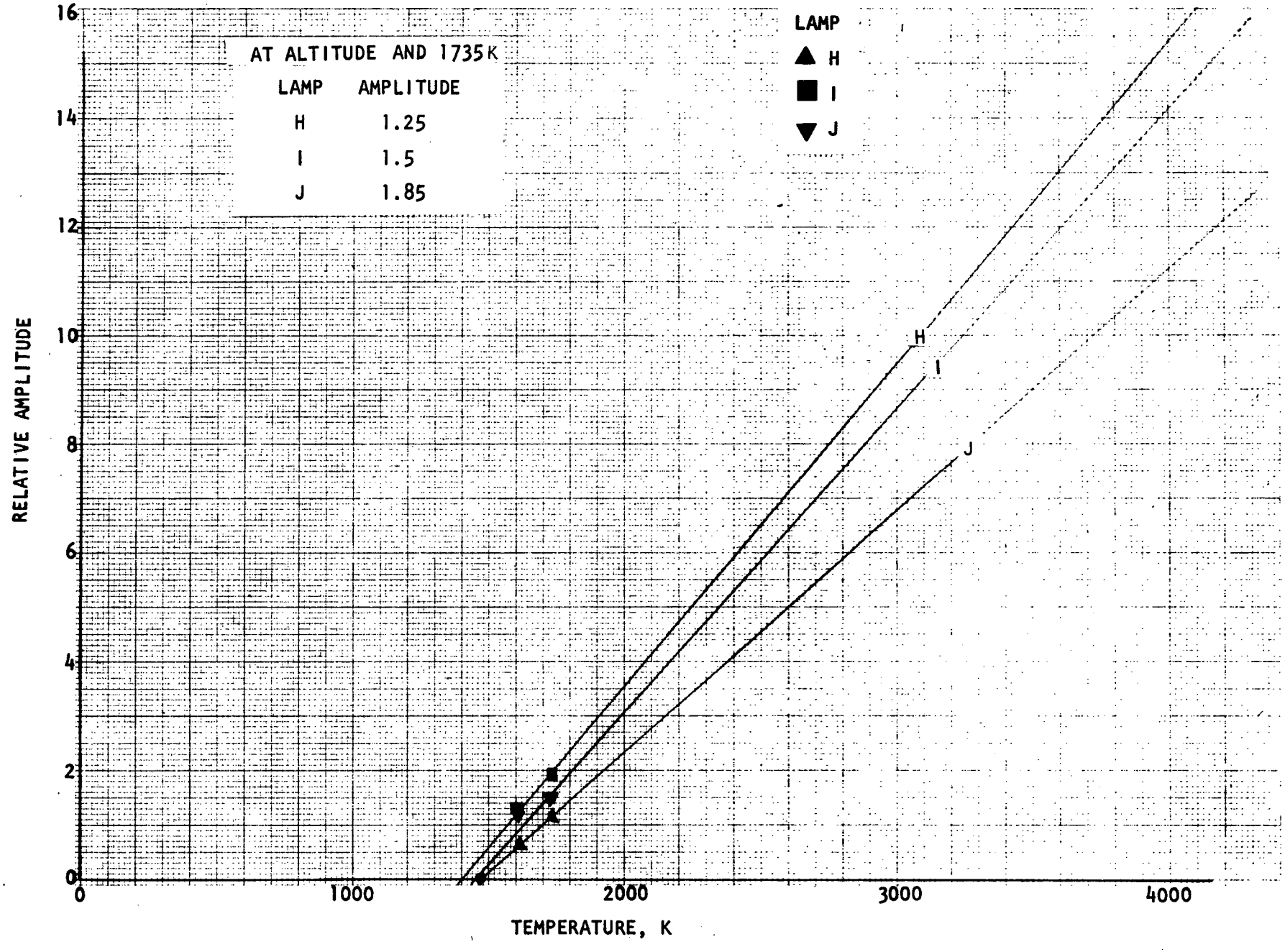

Figure 59. Individual Lamp Calibration Curves, Lamps H, I, and J, 25:1 Nozzle

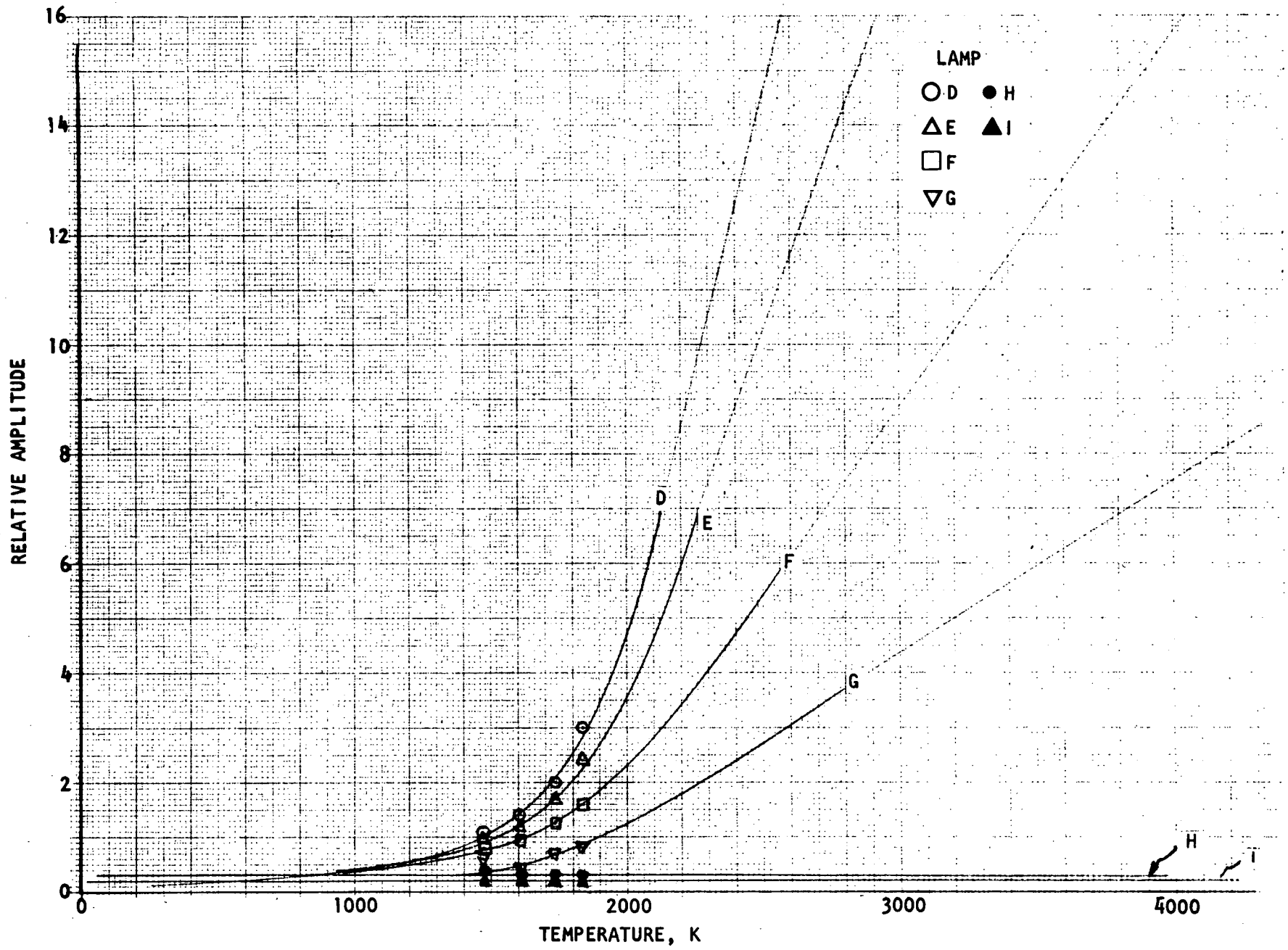

Figure 60. Individual Lamp Calibration Curves, Lamps D, E, F, G, H, and I, 4:1 Nozzle

input data, the calculated values, as the program stepped from the edge to the center plume, became either physically unrealistic or the calculation scheme blew up.

Considerable difficulty was encountered in attempting to analyze the optical data to calculate the plume properties. The analysis procedure is based on simultaneous solution of a set of linear equations. Because the matrix of equations can be written in triangular form, the solutions can be obtained by successive substitutions. Unfortunately, the matrix appears to be ill-conditioned and the solutions are highly sensitive to small variations in the numerical values of the coefficients. Consequently, when the analysis procedure was used with the optical plume data, the calculated plume properties were either unrealistic or the calculation was terminated by the computer. This sensitivity of the calculation was not evident until actual data were used in the calculation rather than hypothetical checkout cases.

After difficulties were encountered, the calculation scheme was examined thoroughly and found to be physically correct, but the results were extremely sensitive to data uncertainty at the beginning of the calculation. Uncertainty on the order of ±3 percent was acceptable at the beginning of calculation, whereas deviations as large as ±50 percent were acceptable at the end of calculation. Changing the computer program to start the calculation at the center of the plume did not alter the limitations on acceptable data uncertainty. Thus, the data were concluded to be inconsistent at least with respect to this analysis scheme. Alternate mathematical techniques, such as modified finite-difference methods, could be used to circumvent these difficulties; however, available funding did not permit examination of this alternative.

To explore this problem and define the allowable uncertainties, an artificial input data set was developed that permitted computer calculation of fairly realistic plume properties. Comparisons were made between these values and data obtained experimentally. The "consistent data set" was derived by trial and error adjustment to input data for Run 238; it is overlayed on Fig. 38, 39, and 40. The general trend approximates the experimental data, but it appears that the calculation scheme required the transmittance (emission plus lamp radiation) to be somewhat higher, the emission-only data to be somewhat lower, and the background data to be very uniform.

The alignment difficulties discussed previously precluded a uniform background. The nonuniformity of the background in some cases exceeded 50 percent. If consideration was given to the possibility that the system alignment could change between firing and nonfiring conditions (e.g., due to transmission of engine vibrations to the components of the DCS system), then a data uncertainty as great as the background nonuniformity could occur. This possibility alone could account for all the difficulties experienced with the data analysis. The lack of correlation of prerun and postrun backgrounds supports this argument.

The requirement for decreasing the emission curve can be attributed to stray radiation entering the optical path. Stray radiation would cause the level of the experimentally obtained emission curve to be above the actual value. The need for an ever increasing reduction of the emission curve as the calculation steps toward the center of the plume, where the probability for capture of stray radiation increases, is supporting evidence for the hypothesis.

Requiring an increase in transmittance implies either that plume absorption was higher than anticipated or that the difference between the transmittance measurement and the emission measurement had to be increased to create a physically realistic situation. The first case could result from excessive blowback from the diffuser during engine operation. Although this was not apparent from the test-firing motion pictures, these pictures represent only visible light. The second case implies that stray radiation was not adequately handled by lowering the emission curve, and that additional adjustments were necessary.

Funding limitations precluded a more comprehensive analysis of all the data and resolution of the difficulties encountered. Thorough analysis of the experimental data, which is probably the best yet obtained with a DCS system, should enable a well-defined assessment of zone radiometric experimental methods and data handling procedures.

The calculated plume properties obtained from the consistent data set are compared with theoretical calculations for Run 238, which operated at an overall mixture ratio of 5 (Table 4). The starting poing in the calculation was line-of-sight (LOS) J and the diametrical zone was LOS F.

TABLE 4. CALCULATED DATA COMPARISON

LOS	Temperature, K	P_{H_2O}, newton/m^2 x 10^5	P_{H_2O}, atm
F (diametrical)	1358	0.419	0.414
G	1431	0.160	0.158
H	1377	0.070	0.069
I	1430	0.0344	0.034
J (outer zone)	1450	0.0142	0.014
Theoretical*	1386.8	0.0506	0.05

*MR = 5, 25:1 Expansion, P_c = 2.062 x 10^6 newtons/m^2 (300 psia)

In general, the calculated temperatures are within 5 percent of theoretical values but the calculated water vapor partial pressures are greater than theoretically possible. The divergence of the calculated partial pressures can be attributed partially to inaccurate absorption coefficients used in the calculation; however, the trend in the calculated values indicates further data inconsistencies.

The agreement between the temperatures is somewhat encouraging, especially at the diametrical line of sight where correlation is within 2 percent and should be most representative of the overall mixture ratio. The calculated temperatures being in excess of the theoretical values near the plume boundary may be indicative of afterburning with residual oxygen in the test chamber.

The results from these experiments and analysis lead to the conclusion that a great deal more effort will be required before field use of a zone radiometry system for large-diameter engines becomes practical and, further, a number of basic questions concerned with the data acquisition and analytical approach must be answered before the intended use of the DCS system can be realized.

CONCLUSIONS AND RECOMMENDATIONS

An instrumentation system was assembled to measure (using zone radiometry) the optical properties of the exhaust plumes of "large" rocket engines. The system was used in the field with varying degrees of success to monitor engine plumes for a wide variety of propellant combinations. All components of the system performed as designed, and feasibility of the basic approach was demonstrated. However, the ultimate goal (the acquisition of high-quality data for comparison with existing plume models and alternate measurement techniques) was never realized. The relatively small number of tests monitored was a significant factor in non-attainment of this goal. Additionally, field installation difficulties and the relatively small data uncertainties required by the data reduction scheme were contributing factors of major proportions.

It is recommended that field application of the DCS system be curtailed until greater understanding of zone radiometry principles are gained under well-controlled laboratory conditions. These small-scale experiments, modeling an actual field installation for large-diameter plumes, should include a large number of experiments to characterize all possible parameters (e.g., the ratio of background intensity to plume intensity, alignment tolerance, stray radiation, scanning rate, absorption source quality and spacing, path length environment, and spectrometer functions. This experimental study should be supplemented with a thoroughgoing analytical investigation.

REFERENCES

1. R-7296, Study of Dual-Channel Infrared Spectroradiometer Systems, Interim Report, NAS8-21144, Rocketdyne, a division of North American Rockwell Corporation, Canoga Park, California, December 1967.

2. R-7733, Study of Dual-Channel Infrared Spectroradiometer Systems, Interim Report: Phase II, NAS8-21144, Rocketdyne, a division of North American Rockwell Corporation, Canoga Park, California, December 1968.

3. R-8838, Study of Dual-Channel Infrared Spectroradiometer Systems, Interim Report: Phase III and IV, NAS8-21144, Rocketdyne, a division of North American Rockwell Corporation, Canoga Park, California, December 1971.

4. R-6288, An Instrumentation System to Study Rocket Exhaust Plume Radiative Processes: Final Report, Contract No. NAS8-11261, Rocketdyne, a division of North American Rockwell Corporation, Canoga Park, California, 27 August 1965.

5. R-6742, Radiative and Structural Characteristics of Rocket Engine Exhaust Plumes, Rocketdyne, a division of North American Rockwell Corporation, Canoga Park, California, 29 September 1966.

6. R-8140, A Compendium of Zone Radiometry Measurements of Exhaust Plumes, NAS8-18734-A, Rocketdyne, a division of North American Rockwell Corporation, Canoga Park, California, February 1970.

7. R-6636-2, F_2/H_2 Performance Evaluation Phase I, Part II NASA CR-72038, Final Report, NASw-1299, Rocketdyne, a division of North American Rockwell Corporation, Canoga Park, California, April 1967.

8. R-15068-7, F_2/H_2 Performance Evaluation for the Period Ending 26 June 1968, Quarterly Progress Report, NASw-1299, Rocketdyne, a division of North American Rockwell Corporation, Canoga Park, California.

9. R-15068-8, F_2/H_2 Performance Evaluation for the Period Ending 26 September 1968, Quarterly Progress Report, NASw-1299, Rocketdyne, a division of North American Rockwell Corporation, Canoga Park, California.

10. R-8390, Performance Analysis of Propulsion Systems; Final Report, NAS8-24568, Rocketdyne a division of North American Rockwell Corporation, Canoga Park, California, November 1970.

11. R-8903, Experimental Investigation of Combustor Effects on Rocket Thrust Chamber Performance: Interim Report, NASw-2106, Rocketdyne, a division of North American Rockwell Corporation, Canoga Park, California June 1972.